

**Role of Ame1, a central component of
the *Saccharomyces cerevisiae* kinetochore,
in kinetochore function and structure**

Dissertation

submitted to the

Combined Faculties for the Natural Sciences and for Mathematics

of the Ruperto-Carola University of Heidelberg, Germany

for the degree of

Doctor of Natural Science

Presented by

Astrid Schäfer

*The beginning of knowledge
is the discovery of something
we do not understand.*

Frank Herbert

**Role of Ame1, a central component of
the *Saccharomyces cerevisiae* kinetochore,
in kinetochore function and structure**

Dissertation

submitted to the

Combined Faculties for the Natural Sciences and for Mathematics
of the Ruperto-Carola University of Heidelberg, Germany

for the degree of

Doctor of Natural Science

Presented by

Diplom-Biochemist

Astrid Schäfer

Referees:

Prof. Dr. Felix Wieland
PD Dr. Johannes Lechner

Date of oral examination:

18.10.2006

	Table of contents	I-IV
	Abbreviations	V
<hr/>		
SUMMARY		1
ZUSAMMENFASSUNG		3
1. INTRODUCTION		5
1.1 The <i>S. cerevisiae</i> cell cycle – getting in and out of mitosis		6
1.2 The kinetochore - an adaptor between chromosome and microtubule		10
1.2.1 Specifying kinetochore location		10
1.2.2 Components of an active kinetochore		10
1.2.3 Kinetochore architecture		13
1.3 Microtubules – the machinery involved in kinetochore capture and chromosome movement		15
1.3.1 Microtubule structure		15
1.3.2 Initial encounter and bipolar attachment of kinetochores and microtubules		16
1.3.3 Spindle positioning and chromosome movement		17
1.3.4 Anaphase spindle stability		18
1.4 Faithful chromosome segregation is monitored by checkpoints		19
1.4.1 The spindle assembly checkpoint		19
1.4.1.1 Attachment versus tension		20
1.4.1.2 A single unattached kinetochore can induce the spindle assembly checkpoint		21
1.4.2 The spindle positioning checkpoint		22
1.4.3 Cdc14 early anaphase release - FEAR		23
1.4.4 Mitotic exit network - MEN		24
1.4.5 The role of the Cdc14 phosphatase		25
1.5 Goal of the present work		27
2. RESULTS		28
2.1 Functional analysis of <i>ame1-2</i> temperature-sensitive mutants		28
2.1.1 Generation of an <i>ame1-2</i> temperature-sensitive mutant		28
2.1.2 Analysis of kinetochore –microtubule attachments in <i>ame1-2</i>		29
2.1.2.1 Tension between sister chromatids is not maintained in <i>ame1-2</i>		29
2.1.2.2 <i>ame1-2</i> mutants show defects in the distribution of sister chromatids		30

2.1.3 Checkpoint analysis in <i>ame1-2</i> mutant cells	32
2.1.3.1 The occupancy checkpoint is active in <i>ame1-2</i>	32
2.1.3.2 <i>ame1-2</i> shows a delay in Pds1 degradation and arrests with a 2N DNA content	34
2.1.3.3 The delay in Pds1 degradation in <i>ame1-2</i> is conform with an induction of the tension checkpoint	36
2.1.4 <i>ame1-2</i> mutants are unable to perform cytokinesis despite a functional MEN	37
2.1.5 <i>ame1-2</i> exhibits a spindle defect	39
2.1.5.1 <i>ame1-2</i> interferes with anaphase spindle formation	39
2.1.5.2 Ame1 is not a microtubule-associated protein (MAP)	41
2.1.5.3 Investigating the cause of the <i>ame1-2</i> spindle defect	42
2.1.5.3.1 The <i>ame1-2</i> mutant interferes with a nucleolar Cdc14 release in early anaphase (FEAR)	42
2.1.5.3.2 Tension-like activation of the spindle assembly checkpoint prevents FEAR induction	44
2.1.5.3.3 Cdc14 overexpression does not rescue anaphase spindles formation in <i>ame1-2</i>	45
2.1.5.3.4 Inactivation of checkpoint protein Mad2 partially rescues the spindle defect of <i>ame1-2</i>	46
2.1.5.3.5 Overexpression of Esp1 in <i>ame1-2</i> allows for a partial rescue of anaphase spindles	48
2.1.5.3.6 The spindle defect in <i>ame1-2</i> cannot be attributed to lacking Esp1 activity	49
2.1.5.3.7 The <i>ame1-2</i> spindle defect already occurs when spindle poles separation resembles a metaphase	50
2.1.5.3.8 Establishment of bipolar attachments prior to the induction of <i>ame1-2</i> leads to the formation of stable anaphase spindles, despite defective kinetochores	51
2.1.5.3.9 Kinetochores preformed in absence of tension still cause a spindle defect	55
2.1.5.3.10 An <i>ame1-2ndc80-1</i> double mutant shows intact anaphase spindles	56
2.1.6 Influence of the <i>ame1-2</i> allele on kinetochore structure	57
2.1.6.1 Influence of <i>ame1-2</i> on the centromere-binding of integral kinetochore proteins	57
2.1.6.2 Influence of <i>ame1-2</i> on centromere-binding of kinetochore associated proteins	59
2.1.6.3 Establishment of bipolar attachments prior to the induction of <i>ame1-2</i> leads to a less compromised kinetochore structure	60
2.1.6.4 Structural damages of the <i>ame1-2</i> kinetochore are not caused by tension and do not require kinetochore assembly during S-phase	62
2.2 Biochemical analysis of interactions between individual kinetochore complexes of the central and outer layer	63
2.2.1 The Okp1 complex interacts with the Mtw1 complex	64
2.2.2 Dephosphorylation of Okp1 and Mtw1 complexes has no influence on their interaction	64
2.2.3 Testing for further interaction partners of the Okp1 and Mtw1 complexes	65
2.2.4 Mtw1 and Ndc80 complexes interact with the Spc105 complex	67
2.2.5 The Okp1, Mtw1 or Ndc80 complexes also do not interact with the DDD complex under dephosphorylating conditions	67

3. DISCUSSION	69
3.1 Functional analysis of <i>ame1-2</i> ts mutants	69
3.1.1 The monopolar segregation defect in <i>ame1-2</i> is caused by the breaking of one kinetochore-microtubule attachment	69
3.1.2 Ame1 and the spindle attachment checkpoint	70
3.1.3 The <i>ame1-2</i> defect interferes with the Cdc14 release from the nucleolus in early anaphase (FEAR)	72
3.1.4 <i>ame1-2</i> prevents the formation of a stable mitotic spindle	72
3.1.5 Establishment of bipolar attachments rescues the <i>ame1-2</i> spindle defect	74
3.1.6 Cytokinesis is impaired in the <i>ame1-2</i> mutant	75
3.1.7 A comprehensive model of the Ame1 kinetochore functions	76
3.2 Refined structural model of the <i>S.cerevisiae</i> kinetochore	77
4. METHODS	80
4.1 Culturing condition	80
4.1.1 <i>E. coli</i>	80
4.1.2 <i>S. cerevisiae</i>	80
4.2 Molecular biology techniques	81
4.2.1 Standard methods	81
4.2.1.1 PCR amplifications	81
4.2.1.2 Cloning of PCR product	81
4.2.1.3 Restriction analysis	81
4.2.1.4 Agarose gel electrophoreses	81
4.2.1.5 Isolation of DNA from agarose gels	81
4.2.1.6 Klenow reaction	81
4.2.1.7 T4 polymerase reaction	81
4.2.1.8 CIAP	81
4.2.1.9 Phenol/Chloroform extraction	82
4.2.1.10 DNA precipitation	82
4.2.1.11 Ligation	82
4.2.1.12 Transformations of <i>E. coli</i>	82
4.2.1.13 <i>E. coli</i> colony PCR	82
4.2.1.14 Isolation of plasmids from <i>E. coli</i>	83
4.2.2 Working with yeast (general techniques)	83
4.2.2.1 Yeast transformation	83
4.2.2.2 Isolation of genomic DNA	83

4.2.2.3 Yeast colony PCR	83
4.2.2.4 Mating	83
4.2.2.5 Sporulation, tetrad dissection	83
4.3 Biochemical techniques (general methods)	84
4.3.1 Yeast protein extracts	84
4.3.2 Bradford	84
4.3.3 SDS-PAGE	84
4.3.4 Western blotting	84
4.4 Special methods	85
4.4.1 Construction of <i>ame1 ts</i> mutants (adapted from Janke et al., 2001)	85
4.4.1.1 Cloning of a temperature sensitive <i>ame1</i> parental strain	85
4.4.1.2 Construction of <i>ame1-2</i> strains for functional analysis	85
4.4.2 Epitope tagging of genes	86
4.4.3 Cell synchronization	86
4.4.4 Microscopy	86
4.4.5 Quantification of Pds1-levels	87
4.4.6 FACS analysis	87
4.4.7 Chromatin immunoprecipitation - ChIP (adapted from Hecht et al., 1998)	87
4.4.8 Quantifications of ChIP-experiments by real time PCR	88
4.4.9 TAP purification (adapted from Puig et al., 1999)	88
4.4.10 Complex binding assays	88
5. MATERIALS	89
5.1 Plasmids, strains and oligonucleotides	89
5.1.1 Plasmids	89
5.1.2 <i>S. cerevisiae</i> strains	90
5.1.3 Oligonucleotides	92
5.2 Chemicals and enzymes	93
5.3 Instruments	94
6. REFERENCES	95

Abbreviations

ade	adenine
amp	ampicillin
bp	base pair
CEN	centromere
ChIP	chromatin immunoprecipitation
Chr	chromosome
DMSO	dimethyl sulfoxide
DNA	deoxyribonucleic acid
dNTP	deoxynucleosid 5'-triphosphate
DOC	deoxycholate
DTT	dithiothreitol
<i>E. coli</i>	<i>Escherichia coli</i>
EDTA	Ethylenediaminetetraacetic acid
EtOH	ethanol
FACS	fluorescence assisted cell sorting
FOA	5'-fluoroorotic acid
GFP	Green Fluorescent Protein
h	hour
his	histidine
IP	immunoprecipitation
k	1000
kb	kilo base
leu	leucine
LiAc	lithium acetate
lys	lysine
min	minute
MT	microtubule
NZ	nocodazole
o/n	over night
OD ₅₈₇	optical density at 587 nm
ON	oligonucleotide
ORF	open reading frame
p	plasmid
PAGE	polyacrylamide gel electrophoresis
PCR	polymerase chain reaction
PEG	polyethyleneimine
PMSF	phenylmetanosulfonylfluoride
ProA	protein A
PVDF	polyvinylidendifluoride
rpm	rotations per min
RT	room temperature
<i>S. cerevisiae</i>	<i>Saccharomyces cerevisiae</i>
SDS	sodium dodecyl sulfate
sec	second
SPB	spindle pole body
TAP	tandem affinity purification
trp	tryptophane
ts	temperature sensitive
U	unit
ura	uracil
Y	yeast strain

SUMMARY

The present work provides an analysis of kinetochore function and structure with respect to Ame1, a central component of the yeast *Saccharomyces cerevisiae* kinetochore. Applying mutant analyses (*ame1-2*) and biochemical binding assays the following results were obtained:

1. Classical kinetochore functions, chromosome attachment, chromosome segregation, and the supervision of these events by the spindle assembly checkpoint were analyzed in the *ame1-2* mutant:
 - The Ame1 protein is needed for the establishment of bipolar attachments to microtubules emanating from opposing poles. Under tension one of the attachments is lost due to a structural weakening of the kinetochore, which results in monopolar segregation of sister chromatides.
 - Checkpoint analysis revealed that checkpoint functions are not impaired in the mutant, as judged by the inducement of the occupancy checkpoint and the ability of *ame1-2* cells to sense their own attachment / tension defect.
 2. *ame1-2*, as also other kinetochore mutants, causes a severe defect in the stability of interpolar microtubules (mitotic spindle). This effect is somewhat surprising, since kinetochores and interpolar microtubules do not interact with each other. Failure in spindle formation caused by kinetochore defects can be explained in two alternative ways: First, kinetochore proteins can also function as spindle stabilizing MAPs (microtubule associated proteins). Second, spindle defects are also observed if a separation of spindle poles occurs in absence of Esp1 and Cdc14 activity. Following experimental evidence suggests that the spindle defect in *ame1-2* is not due to the above mentioned causes, but rather results from an alternative function of the kinetochore that is compromised in the mutant in a cell cycle dependent manner:
 - Ame1 does not locate to the mitotic spindle and thus is not a MAP.
 - As mentioned above, the *ame1-2* mutant fails to achieve a stable bipolar attachment leading to the separation of spindle poles. In parallel the mutant senses this defect and maintains an active spindle assembly checkpoint which inhibits Esp1 and Cdc14 activation. As described (Higuchi and Uhlmann, 2005), such a spindle defect can be rescued by overexpression of Esp1 or Cdc14. The main cause for the spindle defect in *ame1-2* however, is not a spindle pole separation in presence of low Esp1 or Cdc14 activity:
 - i) Overexpression of Cdc14 in *ame1-2* does not rescue the spindle defect of the mutant.
 - ii) Overexpression of Esp1 in *ame1-2* does only allow for a partial rescue of the spindle defect.
 - iii) Inactivation of the spindle assembly checkpoint by Mad2 depletion also leads to only a partial rescue of the spindle defect.
 - iv) A considerable number of cells separate their spindle pole bodies in presence of active Esp1, but nevertheless display a spindle defect.
 - v) Most spindle defects occur at spindle pole distances that are characteristic of metaphase, when spindle stability is independent of the presence and activity of Esp1.
-

-
- The *ame1-2* kinetochore defect is more severe (particularly the kinetochore localization of the Mtw1 complex) when the mutation is induced prior to an establishment of bipolar attachment than after. This differentially compromised kinetochore structure in *ame1-2* is apparently reflective of derived kinetochore functions. Similar kinetochore defects (monopolar segregation, failure in Cdc14 release) are observed, no matter if the mutation is induced before or after bipolar attachment. However, only the latter situation allows for the assembly of wild type metaphase and anaphase spindles. Thus, a certain kinetochore structure (including the Mtw1 complex) may be involved in generating a spindle stabilizing factor.
3. The present structural model of the *S. cerevisiae* kinetochore has been refined in the current work by the following findings:
- A direct protein interaction network between the Okp1 / Mtw1 / Spc105 / Ndc80 kinetochore complexes could be established by *in vitro* binding assays performed with isolated protein complexes.
 - These data together with those derived from ChIP analyses of the *ame1-2* mutant show a clear dependency of the centromeric association of all other central and outer kinetochore complexes on the Okp1 complex and are thus placing this complex in close proximity to the DNA binding CBF3 complex.
 - However, when bipolar attachments are achieved prior to the induction of *ame1-2*, the localization of the Mtw1 complex becomes independent of the presence of the Okp1 complex.

The functional characterization of Ame1 in combination with the biochemical mapping of intra-kinetochore interactions allowed for a structural refinement of the present-state kinetochore model. Moreover, a direct influence of the kinetochore on spindle stability has been uncovered, which may be attributed to the presence of the Mtw1 complex.

ZUSAMMENFASSUNG

Die vorliegende Arbeit liefert eine Funktions- und Strukturanalyse des Kinetochors unter Berücksichtigung von Ame1, einer zentralen Kinetochorkomponente in der Hefe *Saccharomyces cerevisiae*. Mit Hilfe von Mutantenanalysen (*ame1-2*) und biochemischen Bindungsexperimenten wurden folgenden Ergebnisse erzielt:

1. Klassische Kinetochorfunktionen, Chromosomenanheftung, Chromosomenverteilung und die Überwachung dieser Ereignisse durch den Spindel-Checkpoint, wurden in der *ame1-2* Mutanten analysiert:
 - Das Ame1 Protein wird für eine bipolaren Anheftungen an Microtubuli benötigt, die von gegenüberliegenden Polen ausgehen. Unter Spannung geht eine dieser Anheftungen aufgrund einer strukturellen Schwächung des Kinetochores verloren, was zu einer monopolen Verteilung von Schwesterchromatiden führt.
 - Checkpoint Analysen zeigten, dass die Funktionalität des Spindel-Checkpoints in der Mutanten nicht beeinträchtigt ist, soweit man die Induzierbarkeit des Besetzungs-Checkpoints und die Fähigkeit von *ame1-2* den eigenen Anheftungs- / Spannungsdefekt zu erkennen, beurteilt.
 2. *ame1-2*, wie auch andere Kinetochormutanten, verursacht einen schweren Defekt in der Stabilität der interpolaren Microtubuli (mitotische Spindel). Dieser Effekt ist insofern überraschend, als Kinetochore und interpolare Microtubuli nicht miteinander wechselwirken. Fehler in der Spindelausbildung, die auf Kinetochordefekte zurückgehen, können auf zwei verschiedene Arten erklärt werden: Erstens können Kinetochorproteine auch als spindelstabilisierende MAPs (Microtubuli assoziierte Proteine) wirken. Zweitens treten Spindeldefekte auch dann auf, wenn eine Trennung der Spindelpole in Abwesenheit von Esp1 und Cdc14 Aktivität erfolgt. Folgende experimentelle Befunde weisen darauf hin, dass der Spindeldefekt in *ame1-2* nicht auf die genannten Ursachen zurückzuführen ist, sondern vielmehr auf eine alternative Funktion des Kinetochors, die in der Mutanten in einer zellzyklusabhängigen Weise beeinträchtigt ist:
 - Ame1 befindet sich nicht an der mitotischen Spindel und ist folglich kein MAP.
 - Wie bereits erwähnt, ist die *ame1-2* Mutante nicht in der Lage eine stabile bipolare Anheftung zu erreichen, was zu einer Trennung der Spindelkörper führt. Gleichzeitig erkennt die Mutante diesen Defekt und hält einen aktiven Spindel-Checkpoint aufrecht, der eine Aktivierung von Esp1 und Cdc14 verhindert. Wie beschrieben (Higuchi and Uhlmann, 2005), können diese Art von Spindeldefekten durch Überexpression von Esp1 oder Cdc14 aufgehoben werden. Die Hauptursache für den Spindeldefekt in *ame1-2* ist jedoch nicht die Trennung von Spindelkörpern in Anwesenheit von geringer Esp1 und Cdc14 Aktivität:
 - i) Eine Überexpression von Cdc14 in *ame1-2* rettet den Spindeldefekt der Mutanten nicht.
 - ii) Eine Überexpression von Esp1 in *ame1-2* führt nur zu einer teilweisen Rettung des Spindeldefektes.
-

-
- iii) Auch eine Inaktivierung des Spindel-Checkpoints durch Depletion von Mad2 führt nur zu einer teilweisen Rettung des Spindeldefektes.
 - iv) Eine beträchtliche Anzahl von Zellen trennt ihre Spindelpolkörper in Anwesenheit von aktivem Esp1; weist aber dennoch einen Spindeldefekt auf.
 - v) Die meisten Spindeldefekte treten bei einer Entfernung zwischen den Spindelpolen auf, die charakteristisch für eine Metaphase ist. Zu diesem Zeitpunkt ist die Spindelstabilität jedoch unabhängig von der Anwesenheit und Aktivität von Esp1.
- Der *ame1-2* Kinetochordefekt ist stärker ausgeprägt (besonders im Hinblick auf die Kinetochorlokalisierung des Mtw1 Komplexes), wenn die Mutation vor der Ausbildung einer bipolar Anhaftung induziert wird, als bei einer nachträglichen Induktion. Diese unterschiedliche Beeinträchtigung der Kinetochorstruktur in *ame1-2* spiegelt sich anscheinend in den abgeleiteten Kinetochorefunktionen wider. Ähnliche Kinetochordefekte (monopolare Segregation, Aufhebung der Freisetzung von Cdc14) werden unabhängig davon beobachtet, ob die Mutation vor oder nach einer bipolaren Anheftung induziert wird. Jedoch tritt nur im letzteren Fall ein mit dem Wildtyp vergleichbarer Zusammenbau von Meta- und Anaphasespindeln auf. Folglich könnte eine bestimmte Kinetochorstruktur (die den Mtw1 Komplex mit einschließt) an der Erzeugung eines spindelstabilisierenden Faktors beteiligt sein.
3. Gegenwärtige Vorstellungen zur Struktur des *S. cerevisiae* Kinetochors wurden in der vorliegenden Arbeit wie folgt erweitert:
- Ein direktes Interaktionsnetzwerk zwischen den Okp1 / Mtw1 / Spc105 / Ndc80 Kinetochorkomplexen konnte durch *in vitro* Bindungsexperimente mit isolierten Proteinkomplexen identifiziert werden.
 - In Zusammenhang mit ChIP-Analysen der *ame1-2* Mutante belegen diese Daten eine Abhängigkeit der Centromer-Assoziation aller anderen zentralen und äußeren Kinetochorkomplexen vom Okp1 Komplex und ordnen diesen Komplex folglich in die unmittelbare Nachbarschaft des DNA-bindenden CBF3 Komplexes ein.
 - Wenn bipolare Anheftungen jedoch vor der Induktion von *ame1-2* erreicht werden, ist die Lokalisierung des Mtw1 Komplexes unabhängig von der Anwesenheit des Okp1 Komplexes.

Die funktionelle Charakterisierung von Ame1 in Verbindung mit der biochemischen Bestimmung von Intra-Kinetochorwechselwirkungen ermöglichte somit eine Optimierung des gegenwärtigen Kinetochormodells. Außerdem wurde ein direkter Einfluss des Kinetochores auf die Spindelstabilität aufgezeigt, welcher vermutlich der Gegenwart des Mtw1 Komplexes zugeschrieben werden kann.

1. INTRODUCTION

“*Omnis cellula e cellula*”, one cell stems from another cell. This sentence from Rudolf Virchow in 1858 emphasizes the central role that cell division plays for life. No matter how complicated the organism its basic unit is the cell. Cells have one of the most fascinating abilities, self duplication. In unicellular organisms each division leads the formation of two independent cells. It thus is of extreme importance that the genetic information is steadily passed on from mother to daughter. To ensure this, many different surveillance mechanisms have evolved during evolution. They all take care that none of the information is lost and that the new cell maintains the ability of reproduction and development. During DNA synthesis chromosomes have to be exactly replicated and during the subsequent mitosis the resulting sister chromatides are accurately distributed between mother and daughter. DNA segregation depends on microtubules, filamentous elements that attach to a defined structure on chromosomes, the so called kinetochore. The kinetochore assembles on centromeric DNA, a special area within chromosomes. This region is of major importance during mitosis and meiosis.

Chromosome segregation is a complex and complicated process with many control instances, the so called cell cycle checkpoints. Even though these control mechanisms work very precisely, there are still once in a while mistakes occurring. These are usually resulting in death, malformation or cancer. One of the best known examples is the down-syndrome or trisomy 21, where the homologues chromosomes XXI are not segregated correctly in meiosis I. Chromosome non-disjunction and chromosome loss result in aneuploidy, a state with profound consequences (Hassold and Hunt, 2001). Chromosome instability has been shown to play an important role in the formation many solid and colon tumours (Cahill et al., 1999; Lengauer et al., 1997; 1998; Kinzler and Vogelstein, 1996).

Developing new therapeutics for cancer involves understanding the way cancer emerges. This requires knowledge about how cell cycle processes take place and how they are regulated and controlled. A lot of information about the mechanisms of cell division can be retrieved from unicellular organisms like the eukaryotic yeast *Saccharomyces cerevisiae*. Although it has comparatively simple kinetochore and centromere structures, several of their components have been conserved through evolution (Kitagawa and Hieter, 2001; Cheeseman et al., 2002b; Biggins and Walczak, 2003; Cleveland et al., 2003). The knowledge we gain from yeast can thus lead us to deeper insights into the structures and processes of cell division in mammalian cells.

1.1 The *S. cerevisiae* cell cycle - getting in and out of mitosis

The cell cycle is a sequence of events that leads to the growth of a cell and finally to its division into two daughter cells, each containing a full copy of the genetic information of the progenitor. In eukaryotes the cell cycle can be divided into four distinct stages: two functional ones – S and M phase and two preparing ones – G1 and G2 phase (Figure 1). The progression of these stages is highly conserved and coordinated.

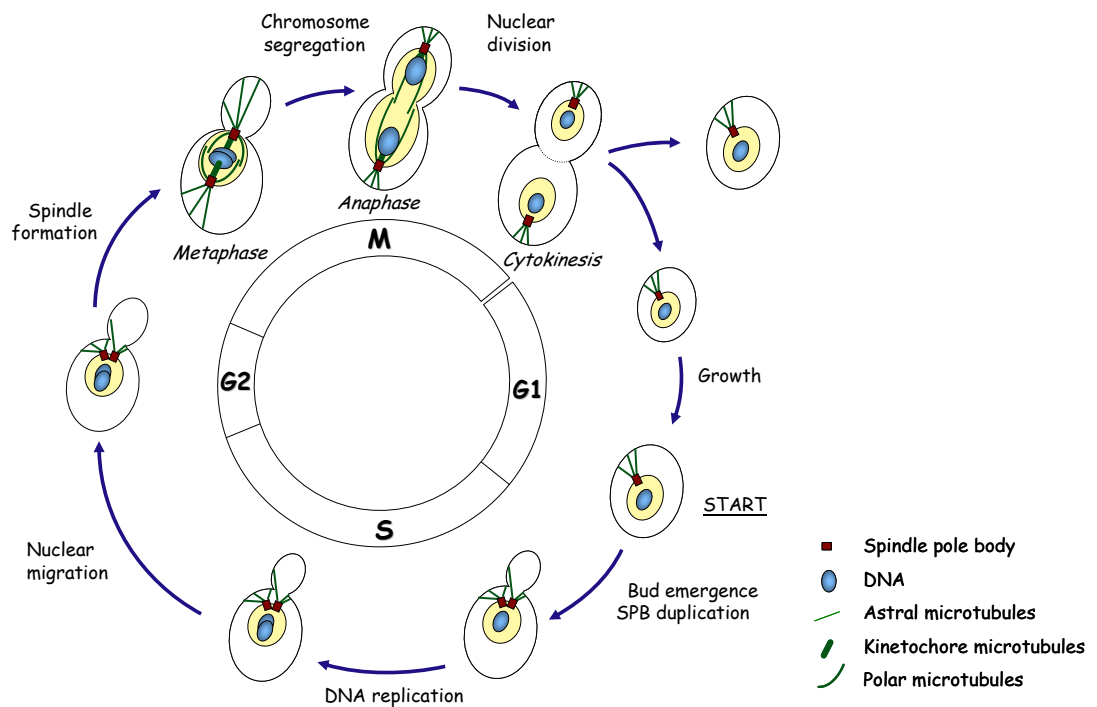


Figure 1. The *S. cerevisiae* cell cycle.

G1 – rest and get ready

The G1 phase is the interval (gap) between mitosis and the initiation of DNA replication. In this phase the unbudded cell has one DNA mass and one spindle pole body (SPB). Cells can be arrested in this phase by lack of nutrients or by the presence of mating hormones. The latter is experimentally used for synchronization of growing yeast cultures. The progression from G1 to S-phase, the entry into the cell cycle, is controlled at a regulatory point called START. The transition is induced by external signals like availability of nutrients as well as cell size. Once that cyclin kinase activity has reached a critical level, cells can enter S-phase (reviewed in Nasmyth, 1993). The major kinase involved in this processes is Cdc28, whose activity depends on associated G1 cyclins (Cln1, Cln2, Cln3). START represents a decision point. Once this line has been passed cells are committed to S-phase entry and one cell division cycle.

S-phase – duplicate everything

S-phase is characterized by three major events: bud emergence, spindle pole body (SPB) duplication, and DNA replication. The SPB is a multilayered cylindrical structure embedded in the nuclear envelope. Its duplication starts in late G1 and depends on the activity of two kinases Mps1 and Cdc28 and on the phosphorylation of the SPB component Spc42 (Jaspersen et al., 2004). Duplication follows a conservative mechanism, meaning that the old SPB serves as platform for the formation of the new one (Pereira et al., 2001). It begins with the development of a satellite adjacent to the existing SPB. Both structures stay connected by a so called bridge. After Cln-Cdc28 activation the satellite expands to a duplication plaque which is inserted into the nuclear envelope. Both SPBs are found next to each other until M-phase, when they are separated by the mitotic spindle (reviewed in Jaspersen and Winey, 2004).

After SPB duplication DNA replication is initiated at so called origins (Bell and Dutta, 2002; Blow and Dutta, 2005). Although a preinitiation complex already associates during G1, DNA replication only starts once Cdc28 is activated (Diffley, 2004). Regulatory protein Cdc6 controls that each origin of replication fires only once per cell cycle (Mailand and Diffley, 2005). In its unphosphorylated form it is part of the preinitiation complex. Upon phosphorylation Cdc6 is prone to degradation.

During DNA replication sister chromatids are generated and held together by the cohesion complex (Michaelis et al., 1997; Guacci et al., 1997; Uhlmann and Nasmyth et al., 1998). This complex consists of the Scc1-4 and the Smc1-2 proteins. They form a ring-like structure that surrounds both sister chromatids. Cleavage of Scc1 at the transition from metaphase to anaphase leads to the liberation of the two sisters chromatids. In parallel to chromosome duplication also new kinetochores have to be formed. The mechanism of this process is currently unknown. Kinetochores are the attachment points of microtubules that play a major role in chromosome segregation.

G2 – almost there

This phase is almost nonexistent in budding yeast. It serves for the final maturation of SPBs. During G2 phase a γ -tubulin ring complex associates at the nuclear side of each SPB (Vinh et al., 2002; reviewed in Schiebel, 2000). This leads to an increase in their microtubule nucleating activity. Also the separation of the two SPBs occurs in G2 and requires the activity of different kinases and kinesin related proteins (Byers and Goetsch, 1974; Fitch et al., 1992; Mathias et al., 1996; Jacobs et al., 1988; Roof et al., 1992). During the following mitosis, the SPBs serve as microtubules organization centres. They form the mitotic spindle apparatus required for the separation of sister chromatids (see 1.2 for details).

M-phase – separate and divide

Mitosis is the most dramatic period of the cell cycle leading to the reorganization of many components. This fundamental process controls the faithful segregation of sister chromatids and is highly conserved from yeast to higher eukaryotes. The transition from G2 to M-phase is achieved by the activation of the Cdc28/cyclinB complex, leading to the phosphorylation and activation of further downstream kinases (Hartwell et al., 1970; Hartwell, 1971; Hartwell et al., 1974). Phosphorylation by the *wee1* kinase inactivates Cdc28 and dephosphorylation by Cdc25 stimulates its activity (Russell and Nurse, 1986/1987; Gould et al., 1991).

The basic events in mitosis comprise the formation of a mitotic spindle, the attachment of chromosomes via kinetochores, and the separation of sister chromatids. Their migration to opposing poles, followed by cytokinesis leads to the formation of two separated cells. Mitosis can be divided into four different steps: prophase, metaphase, anaphase and telophase. One major difference between *S. cerevisiae* and higher eukaryotes is the persistence of the nuclear envelope throughout the cell cycle (closed mitosis).

During *prophase* the chromatin of higher eukaryotes condenses. However, chromosome condensation is less pronounced in yeast. Due to this absent condensation a direct visualization of single yeast chromosomes by light microscopy is not possible. Instead the tet-repressor/tet-operator system is used to label desired regions on chromosome arms or the centromere with GFP (He et al., 2000; Michaelis et al., 1997; Straight et al., 1997).

Metaphase is reached when all chromosomes are bipolarly connected to microtubules emanating from opposing poles. The attachment point is formed by the kinetochore, a multi-subunit complex assembled on the centromeric region of the chromosome (see 1.2 for details; reviewed in McAnish et al., 2003). Correct bipolar attachment is monitored by the spindle assembly checkpoint (see 1.4.1 for details). In higher eukaryotes all chromosomes congress in the so called equatorial plate, but this has not been shown for *S. cerevisiae* so far.

Between the two SPBs a short metaphase spindle of about 2 μm is formed and each yeast kinetochore is attached to one single microtubule. The number of microtubules can vary up to 24 in higher eukaryotes (McEwen, 1997). The bipolar attachment of microtubules emerging from opposing sides of the cell creates tension on each cohesed pair of sister chromatids, leading to their separation in the centromeric region (Goshima and Yanagida 2000; He et al., 2000). Split by up to 1 μm for a time of up to 10 minutes, metaphase kinetochores can be resolved as two distinct dots by fluorescent microscopy. However, centromeric regions also re-associate demonstrating the dynamics of MT polymerization and chromatin stretching (Gardner et al., 2005). This process is called “chromosome breathing” (Goshima and Yanagida, 2000; He et al., 2000).

Anaphase comprises the activation of the anaphase promoting complex (APC), the separation of sister chromatides by the cleavage of cohesions, and their movement to opposing poles. The progression from metaphase to anaphase is triggered by ubiquitin-mediated proteolysis of key regulatory proteins. The ubiquitin ligase APC (Murray et al., 1995; Zahariae et al., 1998; Townsley and Ruderman, 1998; Hwang et al., 1998) is activated once the spindle assembly checkpoint signals that all kinetochores are properly bipolarly attached (see 1.4.1 for details). One major substrate of the APC is Pds1, whose poly-ubiquitinated form is prone to proteolytic destruction (Cohen-Fix et al., 1996; Zachariae and Nasmyth, 1999). Its degradation leads to the liberation of active Esp1. This protease is involved in the cleavage of the cohesion protein Scc1 and thereby leads to the separation of sister chromatides (Nasmyth, 2002; Uhlmann et al., 2000). Only upon cohesion cleavage sister chromatides are moved apart by the force applied on them via microtubules. This is a biphasic process. During anaphase A kinetochore microtubules are shortened resulting in a poleward movement of chromatides. In anaphase B the overall distance between the two poles is increased by an elongation of the mitotic spindle. In *S. cerevisiae* these phases occur concomitantly with the major contribution to the separation coming from anaphase B. The anaphase spindle length is increasing from 2 to 8 μm , whereas the distance between the kinetochore and the SPB is only shortened from 0.4 to 0.2 μm (Winey and O'Toole, 2001). During this phase spindle stabilizing proteins are translocating to the spindle midzone, the overlap region between polar microtubules (see 1.3.4 for details).

During *telophase* SPBs are further separated eventually reaching the ends of mother and daughter cell. In this phase an activation of the mitotic exit network (MEN) takes place (see 1.4.4 for details; Bardin et al., 2000, Pereira et al., 2000). A phosphatase, Cdc14 is released from the nucleolus into the cytoplasm and mediates degradation of mitotic cyclins by the APC (Bardin and Amon, 2001; Juang et al., 1997; Jaspersen, 1998). Moreover, the APC is also involved in the degradation of spindle stabilizing proteins whose removal causes spindle breakdown (Juang et al., 1997). Subsequent cytokinesis leads to the formation of two separated cells, ready for the next cell cycle round.

1.2 The kinetochore - an adaptor between chromosome and microtubule

Chromosome movement in mitosis depends on two structures: the kinetochore and the microtubule. Kinetochores associate at the interface of chromosomes and microtubules. The kinetochore mediates the attachment of chromosomes to the spindle and is also involved in the surveillance of this interaction. Additionally it provides a platform for chromosome movement during mitosis. The kinetochore is a multi-subunit complex assembled at special sites at chromosomes, the centromeric region. The length of this region can vary dramatically from 125 bp in *S. cerevisiae*, over 450 kbp in *D. melanogaster*, up to 3 Mbp in humans. It serves as basis for the formation of the kinetochore.

1.2.1 Specifying kinetochore location

The centromeric region (*CEN*) of *S. cerevisiae* was the first one to be cloned and sequenced. It is 125 bp long and contains three conserved elements CDEI, II and III (Fitzgerald-Hayes et al., 1982; Hieter et al., 1985). The 8 bp long CDEI and the 26 bp long CDEIII regions represent imperfect palindromes. Between them the AT-rich (>90%) CDEII element of 78-87 bp length is located (Clarke and Carbon, 1980). Only CDEIII and part of CDEII are essential. Point mutations within CDEIII abolish kinetochore function (McGrew et al., 1986; Ng and Carbon, 1987). Together these three sequences form the platform necessary for the assembly of the protein complexes that build the kinetochore.

1.2.2 Components of an active kinetochore

Due to the huge number of kinetochore proteins identified in the last decades, the kinetochore turns out to be a very complex structure. The majority of these proteins could be assigned to different sub-complexes on basis of yeast two-hybrid interactions, co-immunoprecipitation, or tandem affinity purification. Components of a specific kinetochore sub-complex mainly show related mutant phenotypes. Their association with *CEN* DNA can be tested by chromatin immunoprecipitations (ChIP) *in vivo*. Fluorescent labelling allows for co-localization together with an established kinetochore protein.

The following components are part of the *S. cerevisiae* kinetochore:

Cbf1 (Centromere binding factor 1):

Cbf1, also called Cep1, is a dimer which directly binds to CDEI (Bram and Kornberg, 1987; Baker et al., 1989; Jiang and Philipsen, 1989). Although its deletion increases the probability of chromosome loss and results in hypersensitivity to spindle drugs, the protein is nonessential (Baker and Masison, 1990; Cai and Davis, 1990).

The CBF3-complex:

This complex consists of four essential proteins: Ndc10 (Cbf3a), Cep3 (Cbf3b), Ctf13 (Cbf3c) and Skp1 (Cbf3d) (Connelly and Hieter, 1996; Doheny et al., 1993; Espelin et al., 1997; Goh and

Kilmartin, 1993; Lechner and Carbon, 1991; Stemmann and Lechner, 1996, Strunnikov et al., 1995). This kinetochore sub-complex was originally identified by its *in vitro* binding to CDEIII (Lechner and Carbon, 1991). It has been shown that the association of all other kinetochore proteins depends on the presence of the CBF3 complex (Ortiz et al., 1999; Janke et al., 2001; Goshima and Yanagida, 2000). Therefore it is not surprising that temperature sensitive (*ts*) mutants of all four components cause defects in microtubule attachments that abolish the separation of sister chromatids (Goh and Kilmartin, 1993). Additionally, Ndc10 has been shown to locate to the mitotic spindle (Müller-Reichert et al., 2003; Bouck and Bloom 2005) and *ndc10-1* mutants have a defective spindle attachment checkpoint (Espelin et al., 1997; Gardner et al., 2001). Lately it has been demonstrated that the Bub1 protein interacts with Skp1, and that this interaction is essential for cells to detect tension at kinetochores (Kitagawa et al., 2003).

Cse4 (chromosome segregation):

Cse4 shows homology to the histone-fold domain of histone 3 and is essential for chromosome segregation (Stoler et al., 1995). It is believed that Cse4 replaces H3 forming a specialized nucleosome present at the *CEN* DNA (Meluh et al., 1998; Stoler et al., 1995). Cse4 interacts with CDEI and II and thus also contributes to centromere specification (Cheeseman et al., 2002b; Meluh et al., 1998).

Mif2 (Mitotic fidelity):

Mif2 is an essential protein, extremely rich in prolines, an indication of possible interactions with AT-rich sequences (Meluh and Koshland, 1995; 1997). It seems to localize in close proximity of Cse4, since histones and Cse4 are present in affinity purifications of Mif2 (Westermann et al., 2003).

The Okp1-complex:

The Okp1-complexes comprises at least eleven different proteins. Only two of them, Okp1 and Ame1, are essential whereas the others, Mcm21, Mcm22, Mcm16, Mcm19, Ctf19, Ctf3, Chl4, Nkp1 and Nkp2 are dispensable for growth (Cheeseman et al., 2002b; Measday et al., 2002; Ortiz et al., 1999). Even though all eleven proteins co-purify, they may organize in two to three different sub-complexes as indicated by sedimentation analysis (De Wulf et al., 2003). Okp1, Ame1, Mcm21 and Ctf19 are found in a sub-complex called Ctf19, whereas all others form the Ctf3 complex. Deletions of Mcm21 and Ctf19 increase the probability of chromosome loss. Deletion of Chl4 and Mcm19 cause defects in chromosome segregation and sensitivity against antimitotic drugs (Roy et al., 1997; Ghosh et al., 2001).

The Mtw1-complex:

The Mtw1 complex contains at least four essential proteins: Mtw1, Nsl1, Dsn1 and Nnf1 (Goshima and Yanagida, 2000; Euskirchen et al., 2002; Pinsky et al., 2003; De Wulf et al., 2003; Scharfenberger et al., 2003). An *mtw1* mutant strain shows loss of tension across sister chromatids (Goshima and Yanagida, 2000) and Nsl1 and Mtw1 are required for bipolar spindle attachment (Scharfenberger et al., 2003; Pinsky et al., 2003).

The Spc105-complex:

This complex is composed of two essential proteins, Spc105 and Ydr532 (Nekrasov et al., 2003). Spc105 is necessary for chromosome segregation, since mutant forms of this protein cause chromosome loss. It genetically interacts with the Ndc80 and the Mtw1 complex.

The Ndc80-complex:

The Ndc80 complex comprises four proteins: Ndc80, Nuf2, Spc24 and Spc25. All of which are essential (Janke et al., 2001; Wigge and Kilmartin, 2001). Nuf2 and Ndc80 are well conserved from yeast to human. Mutations in components of the Ndc80 complex result in complete detachment of kinetochores from the mitotic spindle (Janke et al., 2001; Wigge and Kilmartin, 2001). In addition, mutants of Spc24 and Spc25 are unable to maintain an activated spindle attachment checkpoint (Janke et al., 2001; McClelland et al., 2003).

The DDD complex:

The DDD complex contains nine or more subunits, all of which are essential: Dad1, Dad2, Dad3, Dad4, Dam1, Duo1, Spc19, Spc34 and Ask1 (Cheeseman et al., 2001; Janke et al., 2002; Li et al., 2002). This complex locates to both kinetochore and spindle microtubules *in vivo* (Li et al., 2002; Janke et al., 2002). Mutants of this complex show monopolar distribution of chromatides and shortened or broken spindles (Janke et al., 2002; Cheeseman et al., 2001). *In vitro* studies suggest that Ask1, Dam1 and Spc34 are phosphorylated by the Ipl1 kinase (Cheeseman et al., 2002a). Since Ipl1 corrects improper attachments (syntelic attachments; see 1.3.2 for details), also the modification of DDD components may therefore contribute to this process.

Regulatory proteins:

Ipl1 is a kinase located at the kinetochore that mediates bipolar attachment of kinetochores to microtubules (see 1.3.2 for details; Tanaka et al., 2002; Buvelot et al., 2003). *Ipl1* is also involved in the induction of the spindle assembly checkpoint by missing tension (Tanaka et al., 2002; Biggins and Murray, 2001; Pinsky et al., 2006). In anaphase it can be found on the spindle midzone together with Sli15 where it promotes spindle stabilization (see 1.4.5 for details; Zeng et al., 1999; Sullivan et al., 2001; Pereira and Schiebel, 2003). A recent publication also suggests a role of *Ipl1* in cytokinesis, where it inhibits abscission until the cleavage plane has been cleared of chromosomes (Norden et al., 2006).

Checkpoint proteins cause a mitotic arrest if chromosomes are not correctly attached to the spindle (see 1.4.1 and 1.4.2 for details). The kinetochore localization of these proteins depends on the Ndc80 complex, especially on Spc24 and Spc25 (Janke et al., 2001).

Stu1 is a microtubule binding protein located at the spindle midzone (Yin et al., 2002). It is important for spindle pole body separation by preventing spindle collapse.

Stu2 is located at kinetochores and at cortical tips demonstrating the preference of this protein for the plus end of microtubules (He et al., 2001). *Stu2* is generally involved in the regulation of spindle microtubule dynamics (Pearson et al., 2003). *Stu2* has been shown to destabilize microtubules *in vitro* (Van Breugel et al., 2003), but there is also evidence for a role of *Stu2* in microtubule stabilization (Severin et al., 2001; Tanaka et al., 2005). Mutant forms of the protein decrease microtubules dynamics (Kosco et al., 2001). Although, these mutants can perform bipolar microtubule attachments they are unable to transiently separate sister chromatides. Additionally, *Stu2* is implicated in the recruitment of microtubules to the kinetochore were it on the other hand promotes stabilization of microtubules (see 1.3.2 for details; Tanaka et al., 2005).

Slk19 is cleaved at the transition from metaphase to anaphase by the separase Esp1. The C-terminal fragment of this protein dissociates from kinetochores and can thereafter be found at the spindle midzone were it might play a role in spindle stabilization (see 1.4.5 for details; Zeng et al., 1999; Sullivan et al., 2001). Additionally, *Slk19* is also involved in the induction of FEAR (see 1.4.3 for details; Pereira et al., 2002; Stegmeier et al., 2002; Yoshida et al., 2002).

Microtubule-associated proteins and *motor proteins* are involved in the regulation of many microtubule-based processes (reviewed in Hunter and Wordeman, 2000; Akhmanova and Hoogenraad, 2005; Moore and Wordeman, 2004; Tytell and Sorger, 2006). Kip1 and Cin8 for example are required for correct alignment and clustering of kinetochores in metaphase (Hildebrandt and Hoyt, 2000; Hoyt et al., 1992). Kip3 on the other hand is involved in the coordination of the movement of sister chromatides to spindle poles in anaphase (Moore and Wordeman, 2004) and Kar3 plays a role in the lateral sliding of minichromosomes along microtubules during the capture of newly formed kinetochores by microtubules (Tanaka et al., 2005).

1.2.3 Kinetochore architecture

The simplest known kinetochore is that of *S. cerevisiae*. Nevertheless, it already contains at least 65 different proteins that together form a platform for microtubule attachment (McAinsh et al., 2003). Although numerous interactions between individual kinetochore proteins are known (Ito et al., 2001; Uetz et al., 2000; De Wulf et al., 2003; Westermann et al., 2003), the architecture of the kinetochore is not elucidated in all details so far.

Theoretically, two alternative ways of kinetochore assembly can be imagined. The kinetochore may either preassemble in solution or sequentially associate at the centromere. Experimental data strongly favour the latter possibility and the existence of a multilayered structure (Figure 2). Kinetochore formation initiates after DNA replication with the binding of the CBF3 complex and Cse4 to the centromere (Lechner and Carbon 1991; Meluh et al., 1998). The CBF3 complex is required for Cse4 maintenance at kinetochores (Ortiz et al., 1999). It resembles a scaffold for

kinetochore assembly, since the recruitment of all other complexes depends on CBF3, whereas the reciprocal is not true. Immunoprecipitation and two-hybrid interactions locate the Okp1 complex in proximity to the inner DNA binding complex CBF3 and Cse4. Okp1, Mtw1 and Ndc80 complexes assemble with the kinetochore independently of each other and their localization depends only upon CBF3 (Wigge and Kilmartin, 2001; Janke et al., 2001; He et al., 2001; De Wulf et al., 2003). This characterizes them as components of the central layer. The only complex that requires microtubules for its kinetochore localization is the DDD complex (Li et al., 2002; Enquist-Newman et al., 2001). Its interaction with the kinetochore also depends on the CBF3 and Ndc80 complexes (Li et al., 2002; Cheeseman et al., 2002b; Janke et al., 2002; Jones et al., 2001). Together with the Ndc80 complex the DDD complex is required for kinetochore-microtubule attachment (He et al., 2001; Janke et al., 2001; Janke et al., 2002; Jones et al., 2001). Although DDD mutants interact with microtubules, they do not resist tension applied on their kinetochores. This implies that the DDD complex is not involved in the recruitment of microtubules, but rather strengthens their attachment. Only this way stable bipolar attachment necessary for chromosome segregation may be achieved (Janke et al., 2002).

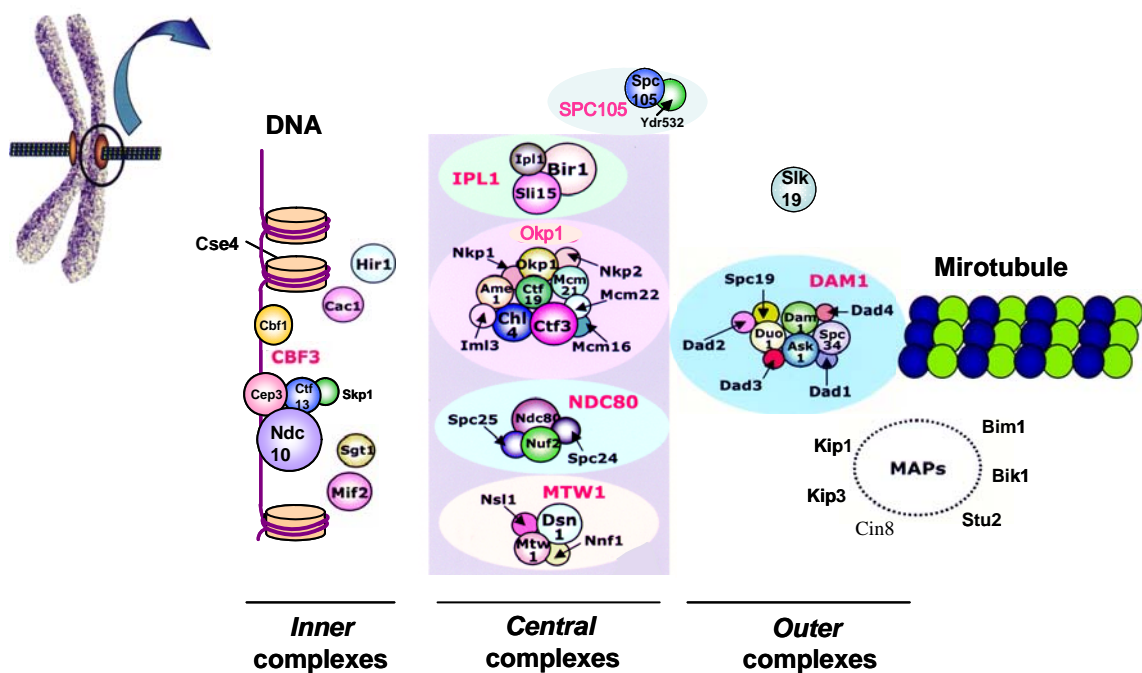


Figure 2. Kinetochore architecture (adapted from Tan et al., 2005). The kinetochore consists of an inner, central and outer layer. The inner layer makes direct contact to the DNA, whereas the outer layer contacts microtubules. The inner layer mediates between both.

Apart from its role in microtubule attachment, the kinetochore also provides a platform for the association of checkpoint proteins (Mad2, Bub2, and Mps1) and other factors (Ipl1, Slk19, Stu2, Cin8, Bik1 and Bim1). Recruitment of Cin8, Stu2, and checkpoint proteins to the kinetochore in particular requires the presence of the Ndc80 complex (He et al., 2001; Janke et al., 2001; Janke et al., 2002; Wigge and Kilmartin, 2001).

1.3 Microtubules – the machinery involved in kinetochore capture and chromosome movement

Microtubules (MT) are filamentous structures responsible for many movements within the cell. They are involved in the transport of organelles and chromosomes and are also important for nuclear and cellular division.

1.3.1 Microtubule structure

MTs represent a hollow cylindrical polymer that consists of α/β -tubulin heterodimers that associate to longitudinal protofilaments. Thirteen of them arrange laterally to form together the MT lattice (Desai and Mitchison, 1997). MT assembly is nucleated at the SPB and involves the γ -tubulin ring complex (Schiebel, 2000). It allows the polymerization of MTs at a relatively low concentration of soluble tubulin (Gunawardane et al., 2000). The number of γ -tubulin ring complexes influences the number of MTs emanating from the SPB (Khodjakov and Rieder, 1999). MT polymerization involves head to tail fusion of α/β -tubulin heterodimers and results in a polarized filament, whose minus-end locates at the SPB. The plus-end can associate with the kinetochore. Both ends are characterized by different growth rates *in vitro*: the minus end is polymerizing slower, whereas the plus end grows quicker. The growth under physiological conditions is characterized by dynamic instability (reviewed by Kinoshita et al., 2002): The plus-end changes between phases of slow growth and quick shrinkage. The conversion between these phases is termed “catastrophe”. However, also a rescue phase is often observed. The energy for the polymerization comes from GTP-hydrolysis (Erickson and O’Brian, 1992). Whereas β -tubulin forms the end of the MT and binds GTP, its GTPase activity is triggered by the α -tubulin subunit of the next docking heterodimer. MTs are growing as long as GTP-hydrolysis lags behind polymerization. This way a GTP-cap is formed at the plus-end which stabilizes the growing MT.

The MT’s plus-end is also the attachment site of numerous MAPs (microtubule associated proteins) which either stabilize or destabilize the growing MT (see next paragraphs). Two distinct end-binding classes have been described: One group, MACKs (mitotic centromere-associated kinesins), lead to destabilization of MT ends (Desai et al., 1999). Kip3 is an example of this class. The second group, plus-end-binding proteins like Bim1 and Bik1, are often involved in the stabilization of MTs (Schuyler and Pellman, 2001).

Also some chemical compounds influence the stability of MTs. Taxol leads to stabilization of MTs, whereas nocodazole induces their depolymerization. Nocodazole is also used in the laboratory for a secondary effect: MT depolymerization arrests *S. cerevisiae* cells in metaphase by induction of the spindle attachment checkpoint (see 1.4.1).

1.3.2 Initial encounter and bipolar attachment of kinetochores and microtubules

The mitotic spindle comprises MTs emanating from both SPBs. They are characterized by a very undynamic minus-end on the poles and a highly dynamic plus-end. Some MTs are involved in the interaction with kinetochores (kinetochore MT) being important for chromosome alignment and segregation (McIntosh et al., 2002, Rieder and Salmon, 1998). Further MTs emanate from both SPBs and overlap in the midzone of the cell. These interpolar MTs play an important role in the formation of the metaphase and anaphase spindle and the separation of the SPBs (Scholey et al., 2003). Additionally, another set of MT connects the nucleus with the cell cortex (astral microtubules), playing a role in the movement of the nucleus and the formation of tension at kinetochores.

Of major importance for correct segregation of sister chromatids is their attachment to MTs emanating from opposing poles. This leads to their alignment, bi-orientation, and prepares them for separation. MTs in metaphase are highly dynamic, a property very important for kinetochore capture. This process is facilitated by mechanisms that favour MT growth and mediated by plus-end-binding proteins. The initial encounter between MTs and kinetochores happens laterally. Protein Stu2 plays an important role in the docking process (Tanaka et al., 2005). Upon initial contact it migrates from the captured kinetochore to the plus-end of the attached MT, where it promotes its stabilization. This prevents the kinetochore from sliding off the MT. Next, the chromosome is moved towards the pole by the activity of the minus-end directed kinesin Kar3. Once the pole is reached, the second chromatide is attached to a MT emanating from the opposing pole and the lateral attachment matures into an end-on attachment.

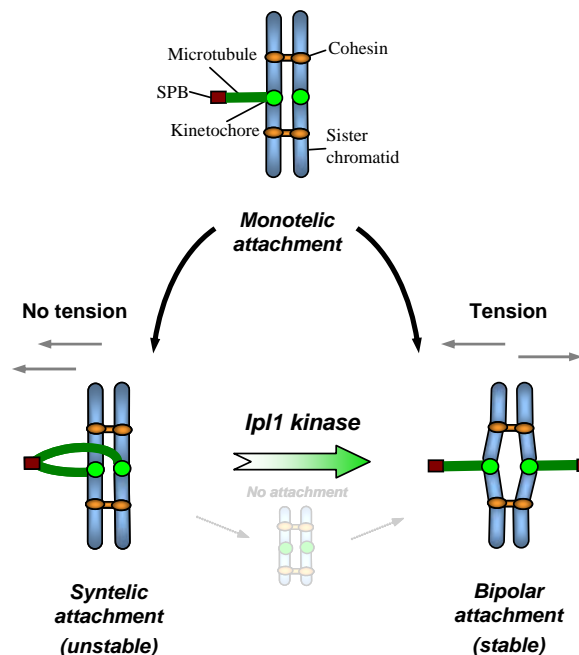


Figure 3. Ipl1 resolves syntelic attachments thereby promoting bipolar spindle attachments. Missing tension due to syntelic attachments of kinetochores to microtubules leads to the activation of Ipl1. The kinase corrects the lack of tension leading to the formation of bipolar attachments (probably through a state without any attachment at all).

Bipolar attachment is controlled by another set of proteins, the Ipl1 kinase complex and its substrates (Biggins and Walczak, 2003; Figure 3). There are indications that syntelic attachment (both sister kinetochores are attached to the same pole) may precede bipolar spindle attachment. In absence of Ipl1 kinetochore interactions with MTs emanating from the old SPB are favoured leading to the monopolar distribution of chromosomes, preferentially into the daughter (Tanaka et al., 2002). Accordingly, Ipl1 does not only serve to resolve syntelic attachment. The protein also redistributes kinetochore-MT interactions between old and new spindle pole body, since unreplicated chromatids show no preference for either pole (Tanaka, 2002). Ipl1 activity is regulated by tension (Dewar et al., 2004). As long as tension is missing, as in case of syntelic attachment, Ipl1 promotes detachment of MTs. However, once bipolar attachment is reached, tension is built up between sister chromatids and Ipl1 activity drops.

1.3.3 Spindle positioning and chromosome movement

Next to the bipolar attachment of sister chromatids, the mitotic spindle needs to be properly aligned along the mother-bud axis. This process is under the control of the spindle positioning checkpoint (see 1.4.2 for details). Astral microtubules, which emanate from the SPB into the cytoplasm and contact the cell cortex, play a major role in the positioning of the mitotic spindle. Shortly after the emergence of a bud, the duplicated SPBs are separated. Astral MTs of the old SPB, which is in close proximity to the daughter cell, begin to enter the bud (Byers and Goetsch, 1975; Vallen et al., 1992). They start to pull on the mitotic spindle by lateral sliding along the bud cortex (Shaw et al., 1997, Adames and Cooper, 2000). At the same time the new SPB moves to the most distal point in the mother cell. In combination, both movements lead to the positioning and alignment of the mitotic spindle.

One group of proteins involved in spindle positioning comprises dynein and dynactin (Stearns, 1997; Hildebrandt and Hoyt, 2000). Dynein is required for the lateral sliding of astral MTs along the bud cortex (Adams and Cooper, 2000). However, since neither dynein nor dynactin are essential in yeast, cells deficient in these proteins are only delayed in cell cycle (Yeh et al., 1995). Also the Kip3 pathway influences spindle positioning. It includes the kinesin motor protein Kip3, the formin Bni1, the cortex and MT associated protein Kar9, and the MT binding protein Bim1 (DeZwaang et al., 1997; Lee et al. 1999; Fujiwara et al., 1999; Miller and Rose, 1998). Kar9 is located at the plus-end of MTs that extend into the bud. It is transported to the bud along actin cables by Myo2 (Miller et al., 1999; Yin et al., 2000). Its interaction with MTs is mediated via Bim1, which increases MT dynamics and thus supports their search for binding sites within the bud (Carminati and Stearns, 1997, Tirnauer et al., 1999). The Bim1/Kar9 complex might promote the depolymerization of MTs, once they are attached at the bud cortex. This shortening creates a force on spindle and nucleus, which pulls them towards the bud. Kip3 may also contribute to this depolymerization process.

Once the spindle has the right orientation and chromosomes are bipolarly attached, chromosome segregation can start. Separation of sister chromatides is initiated by cleavage of cohesins and by the pulling force applied on them via MTs. Their segregation occurs in two phases: During anaphase A kinetochore MTs are shortened, leading to a movement of the sister chromatides towards opposite poles. This is achieved by the pac-man method, the active depolymerization of MTs from the plus-end located at the kinetochore. Kip3 is a kinesins possibly involved in this process (Cottingham and Hoyt, 1997; Tytell and Sorger, 2006). Stu1 has high affinity for β tubulin (Pasqualone and Huffaker, 1994) and may also influence GTP hydrolysis and MT depolymerization. During anaphase B, the overall distance between the two poles is increased by successive polymerization and lengthening of interpolar MTs. This process involves the stabilization of the spindle midzone (see 1.3.4). However, mechanistic details of MT polymerization during anaphase B are currently unknown. After successful separation of sister chromatides between mother and daughter cell, the spindle disassembles and the cells progress towards cytokinesis. These processes are controlled by another pathway, the mitotic exit network (MEN, see 1.4.4 for details).

1.3.4 Anaphase spindle stability

As mentioned before, sister chromatide separation and spindle elongation are initiated by the activation of the separase Esp1. However, Esp1 is also involved in the stabilization of the anaphase spindle either through direct localization to the spindle midzone or through the activation and release of Cdc14 from the nucleolus (FEAR) (see 1.4.3 for details; Jensen et al., 2001, Zeng et al., 1999; Sullivan et al., 2001; Pereira and Schiebel, 2003; Higuchi and Uhlmann, 2005). Cdc14 recruits other spindle stabilizing proteins to the spindle midzone, e.g. Ipl1-Sli15 or Slk19 (see 1.4.5 for details). Additional proteins that are also found at the spindle midzone are Ase1 and Stu1 (Yin et al., 2002; Pellman et al., 1995). But also kinetochore components like Ndc10 or members of the DDD complex can locate to the anaphase spindle where they may play a role in spindle stabilization (Müller-Reichert et al., 2003; Bouck and Bloom 2005; Li et al., 2002; Janke et al., 2002).

1.4 Faithful chromosome segregation is monitored by checkpoints

To ensure reliable chromosome segregation evolution has developed conserved mechanisms to survey this process: the spindle assembly (see 1.4.1 for details) and the spindle positioning checkpoint (see 1.4.2 for details). The first of which is activated, when cells encounter defects in spindle assembly or chromosome attachment to microtubules. The second is induced, when the mitotic spindle is mispositioned along the mother-bud axis. Both checkpoints arrest the cell-cycle unless all chromosomes are bipolarly attached and the mitotic spindle is correctly positioned. They prevent anaphase entry, induction of the mitotic exit network (MEN) and cytokinesis.

The spindle checkpoint was originally defined in mutants of *S. cerevisiae* that fail to arrest in the cell cycle upon treatment with microtubule-depolymerizing drugs. This phenotype led to the identification of several checkpoint proteins: Mad1, Mad2, Mad3 (mitotic arrest deficient; Li and Murray, 1991); Bub1, Bub2, Bub3 (budding uninhibited by benzimidazole; Hoyt et al., 1991); and Mps1 (monopolar spindle; Weiss and Winey, 1996). Experiments have shown that many of these proteins are part of the same signal transduction cascade. All proteins except Bub2 are involved in the control of anaphase entry by the spindle assembly checkpoint. Bub2 on the other hand is part of the spindle positioning checkpoint and also a regulator of the mitotic exit network (MEN; see 1.4.4 for details). All of these factors have homologues in higher eukaryotes and vertebrates (Taylor, 1998; Chan et al., 1999; Cahill et al., 1999). It has also been shown that they locate to the kinetochore during mitosis (Martinez-Exposito et al., 1999; Chan et al., 1999). This allows to conclude that they monitor events at kinetochores. Interference with checkpoint activity causes cells to enter anaphase prematurely and results in genomic instability.

1.4.1 The spindle assembly checkpoint

Cells that maintain an active spindle assembly checkpoint due to defective kinetochore-microtubule attachment arrest in metaphase. Accordingly, the spindle checkpoint is able to inhibit the transition from metaphase to anaphase (Figure 4). As mentioned before this transition is regulated by ubiquitin mediated proteolysis and involves the anaphase promoting complex (APC) (Zachariae and Nasmyth, 1999). Activation of the APC requires the accessory protein Cdc20 (Visintin et al., 1997; Hwang et al., 1998; Fang et al., 1998b). If all kinetochores are bipolarly attached, APC/Cdc20 triggers the degradation of Pds1. This protein is an inhibitor of the separase Esp1, which proteolytically cleaves Scc1, a subunit of the cohesion complex that connects sister chromatides (Uhlmann et al., 1999). Once liberated, sister chromatides are pulled to opposing poles by microtubules, spindle pole bodies move apart, and anaphase is initiated.

If the spindle checkpoint is maintained active by unattached kinetochores, the checkpoint protein Mad2 is recruited to these kinetochores (Chen et al., 1996; Li and Benzra, 1996). Mad2 inactivates Cdc20, the inductor of APC (Howell et al., 2000). In consequence, inactivation of the

APC induces a metaphase arrest with high Pds1 levels. High Pds1 levels are thus indicative of an active spindle assembly checkpoint. If all kinetochores are bipolarly attached, Mad2 does no longer associate with kinetochores. This leads to an interaction and activation of APC/Cdc20 and anaphase onset.

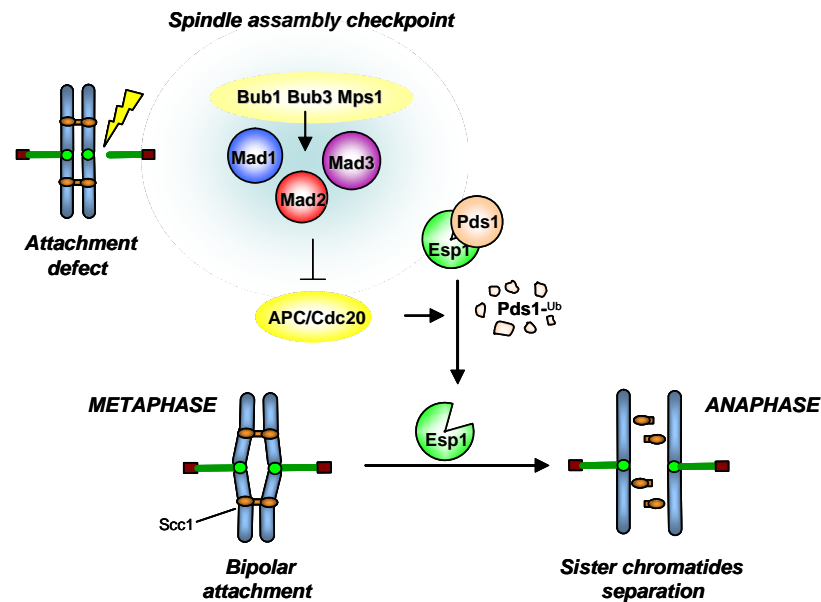


Figure 4. The spindle assembly checkpoint. Unattached kinetochores are activating the checkpoint, thus inhibiting the APC and consequently the degradation of Pds1. Esp1 is therefore kept inactive and unable to promote Scc1 cleavage and separation of sister chromatides.

1.4.1.1 Attachment versus tension

Faithful chromosome segregation is of major importance. Therefore, the inactivation of the spindle assembly checkpoint involves two different aspects: (1) occupancy, meaning the attachment of all kinetochores to MTs (Rieder et al., 1994; Rieder et al., 1995) and (2) tension applied on kinetochores via microtubules emanating from opposing poles (McIntosh et al., 1991; Li and Nicklas, 1995). Dual induction of the spindle assembly checkpoint by missing occupancy and tension may increase the accuracy of bipolar attachment. Whereas the occupancy checkpoint monitors only the overall association of kinetochores and microtubules, tension allows the cell to distinguish between kinetochores attached to microtubules emanating from the same pole (syntelic attachment) and those kinetochores that are bipolarly attached.

Occupancy is controlled by checkpoint protein Mad2, which locates to free kinetochores (see above; Chen et al., 1998; Chen et al., 1999; Sironi et al., 2001). Much less is known about how tension is monitored. In mutants defective in sister chromatides replication, *cdc6* for example, the spindle assembly checkpoint gets activated (Stern and Murray, 2001). The same is true if sister chromatides cohesion is prevented (Biggins and Murray, 2001). Although both situations allow for an attachment of kinetochores to MTs, no tension is formed between them. These experiments

indicate that tension also influences the spindle assembly checkpoint. A possible mechanistic explanation of this observation is the tension dependent phosphorylation of kinetochore proteins (Gorbsky and Ricketts, 1993; Nicklas et al., 1995).

In yeast, the Ipl1 kinase plays an important role in tension dependent checkpoint signalling (Biggins and Murray, 2001). In spite of syntelic attachment, *ipl1* mutants precede through the cell cycle (Biggins et al., 1999). Ipl1 activity is therefore crucial for the formation of bipolar interactions and tension across kinetochores (Tanaka et al., 2002). MT-depolymerizing drugs activate the spindle checkpoint in an Ipl1-independent manner, thus indicating a role of this protein in tension sensing. As mentioned before, Ipl1 promotes bipolar attachment through the detachment of incorrectly bound microtubules. Unattached kinetochores created this way lead to an activation of the spindle assembly checkpoint (Pinsk et al., 2003; Pinsky et al., 2006). Noteworthy, nocodazole induced detachment of microtubules from kinetochores leads to a much stronger arrest than the delay in the cell cycle induced by loss of tension. The inter-relation of attachment and tension makes it difficult to distinguish which one is the primary defect sensed by the spindle assembly checkpoint. In yeast, kinetochores interact with MTs throughout most of the cell cycle. Thus, monitoring tension might be of greater importance since mono-orientation always leads to mis-segregation. This might be different in higher eukaryotes where more than one microtubule is attached to the kinetochore.

1.4.1.2 A single unattached kinetochore can induce the spindle assembly checkpoint

In order to ensure correct chromosome segregation, the cell cycle has to pause until all kinetochores are properly attached. This means that a single unattached kinetochore has to be able to arrest the cell cycle. Normally, Mad2 is recruited to unattached kinetochores via an interaction with Mad1 (Chen et al., 1998). Mad2 on the other hand sequesters Cdc20 to kinetochores preventing its association with the APC and thereby its activation. But how can a single unattached kinetochore produce a signal strong enough to inhibit the APC? It has been shown that there are two different pools of Mad2 in the cell: one stably associated with kinetochores via Mad1, the other in transient contact with kinetochores interacting with Cdc20 (Shah et al., 2004). The connection between these pools is achieved by the dimerization of Mad2. Dimers however, are only formed between Mad2 subunits that are in different conformations (De Antoni et al., 2005). Binding of Mad2 by Mad1 induces such a conformational change (Sironi et al., 2001) and allows the binding of free Mad2 by the Mad1-Mad2 complex. This second Mad2 molecule recruits Cdc20, undergoes also a conformational change, dissociates from the kinetochore as a Mad2/Cdc20-heterodimer and prevents APC activation. It is intriguing to speculate that the liberated Mad2/Cdc20 complex triggers the formation of further heterodimers and thus induces a catalytical enhancement of the checkpoint signal. Inactivation of the spindle assembly checkpoint may therefore involve a disruption of Mad2-Mad2 interactions and thereby prevent the formation of Mad2/Cdc20 complexes.

1.4.2 The spindle positioning checkpoint

Correct chromosome segregation requires proper spindle positioning. This process is controlled by another surveillance mechanism, the spindle positioning checkpoint (Figure 5). It monitors the entry of the old SPB into the bud, regardless of correct chromosome attachment (Gardner et al., 2001; Goh and Kilmartin, 1993). The positioning of the spindle involves growth and shrinkage of astral microtubules. Mutants with defects in astral microtubules, motor proteins or cortical proteins are impaired in spindle orientation and elongate the spindle only within the mother (Palmer et al., 1992; Schuyler and Pellman, 2001; Segal and Bloom, 2001). Noteworthy, even a transient penetration of one SPB into the bud neck is sufficient to induce cell cycle progression (Adames et al., 2001).

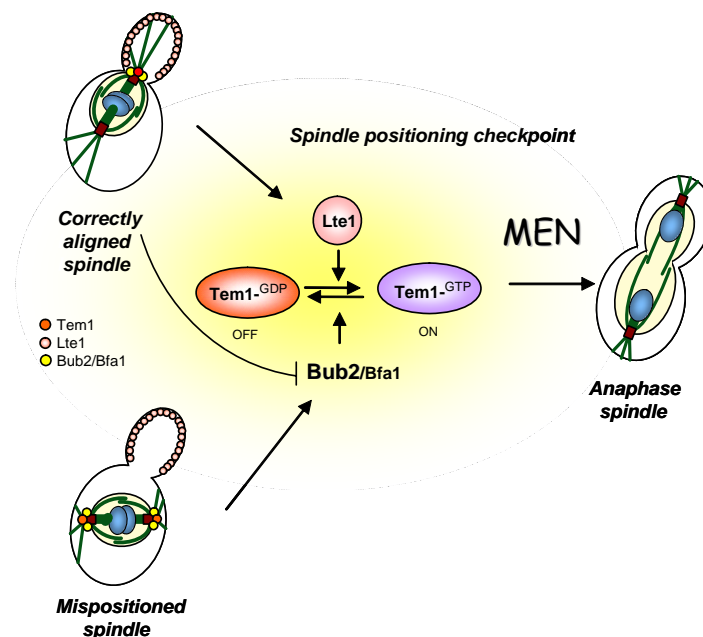


Figure 5. The spindle positioning checkpoint. Mispositioned spindles inhibit an activation of MEN (mitotic exit network) by recruitment of Bub2 to the SPB. Once the SPB enters the bud neck, Bub2 gets inactivated and cells progress towards anaphase.

If the spindle is misoriented, mitotic progression is inhibited by the spindle positioning checkpoint. This process involves Bub2, a protein that monitors the position of the SPBs (Bardin et al., 2000; Pereira et al., 2002; Bloecher et al., 2000). During mitosis, Bub2 asymmetrically locates to the bud oriented SPB (Cerutti and Simanis, 1999; Pereira et al., 2000; Bloecher et al., 2000; see also next chapters). It inactivates Tem1, the upstream kinase of the mitotic exit network (MEN) (Geymonat et al., 2002; Furge et al., 1998). Only as the daughter-bound SPB passes the bud neck, Bub2 is inactivated and MEN induced. This allows for mitotic progression from metaphase to anaphase.

1.4.3 Cdc14 early anaphase release - FEAR

In early anaphase FEAR (Figure 6) promotes a transient release of the Cdc14 phosphatase from the nucleolus to the nucleoplasm (Pereira et al., 2002; Stegmeier et al., 2002; Yoshida et al., 2002). Retained in the nucleolus by interactions with Cfi/Net1 and Fob1 (Shou et al., 1999), the release of Cdc14 from this compartment involves two parallel pathways (Stegmeier et al., 2002; Stegmeier et al., 2004). The first comprises protease Esp1, its substrate Slk19 and the protein kinase Cdc5. Although the interplay of these factors is not well understood, Cdc5 promotes phosphorylation of Net1 and Cdc14. This modification weakens their interaction, but may alone not be sufficient to release Cdc14 from the nucleolus (Shou et al., 2002; Yoshida and Tohe, 2002; Visintin et al., 2003). The second pathway involves phosphoprotein Spo12 and its binding partner Fob1. Phosphorylated Spo12 induces a conformational change in Fob1, which in turn promotes the release of Cdc14 from Cfi1/Net1 (Stegmeier et al., 2002). Cdc14 released by these pathways plays an important role in anaphase spindle stability, nuclear positioning and segregation of repetitive DNA.

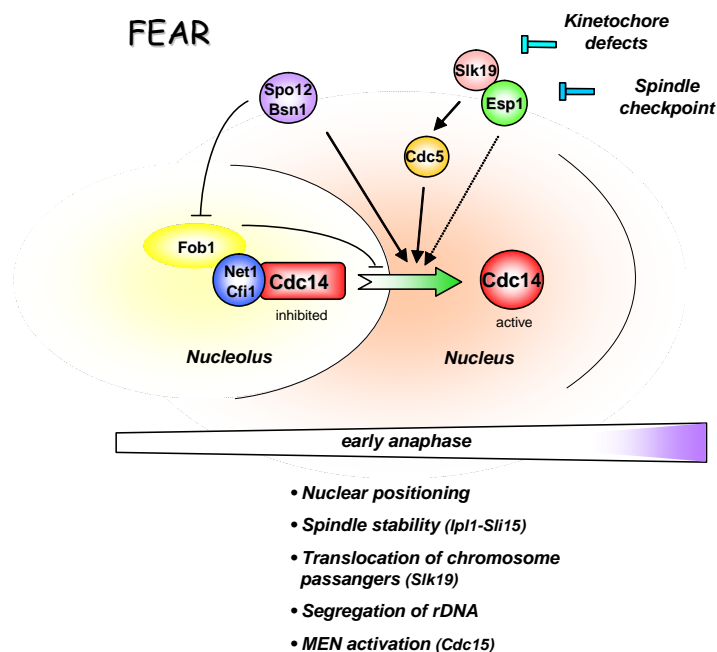


Figure 6. FEAR (Cdc14 early anaphase release). FEAR promotes a transient release of Cdc14 from the nucleolus to the nucleus, where it contributes to spindle stability, nuclear positioning and MEN activation.

In contrast to sister chromatid separation the proteolytic activity of Esp1 is not required for the induction of FEAR (Sullivan and Uhlmann, 2003). Nevertheless, also the non-proteolytic function of Esp1 is inhibited by Pds1 (Sullivan and Uhlmann, 2003). Thus, chromosome separation, anaphase spindle stability, and nuclear positioning are all connected via Pds1. Interestingly, also the anaphase-specific cleavage of Slk19 by Esp1 is not required for FEAR induction (Stegmeier et al., 2002; Sullivan and Uhlmann, 2003). It is rather the binding of Esp1 to Slk19 that is important for Cdc14 release (Sullivan et al., 2001; Sullivan and Uhlmann, 2003).

1.4.4 Mitotic exit network - MEN

In contrast to FEAR, MEN induces a release of Cdc14 from the nucleolus into the nucleus and from there on into the cytoplasm (Figure 7) (Asakawa et al., 2001; Visintin et al., 1998; Xu et al., 2000; Bardin et al., 2000; Lee et al., 2001; Mah et al., 2001). This kinase cascade is initiated by the upstream regulator Tem1 (Shirayama et al., 1994b). Tem1 is a small G protein, whose activity is regulated by the GEF (guanine nucleotide exchange factor) Lte1 (Shirayama et al., 1994a) and the GAP (GTPase activating protein) Bub2/Bfa1 (Furge et al., 1998; Geymonat et al., 2002). Bub2 is part of the spindle positioning checkpoint (see before) and thus connects MEN with proper spindle alignment.

Next to Tem1, the MEN cascade includes protein kinases Cdc15 and Dbf2/Mob1. Except for Lte1, all components of MEN preferentially locate to the cytoplasmic face of the SPB (Fraschini et al., 1999, Frenz et al., 2000, Luca et al., 2001; Menssen et al., 2001; Pereira et al., 2002; Pereira et al., 2003, Yoshida et al., 2002). In line with this observation, mutations in the outer plaque of the SPB cause defects in mitotic exit (Gruneberg et al., 2000).

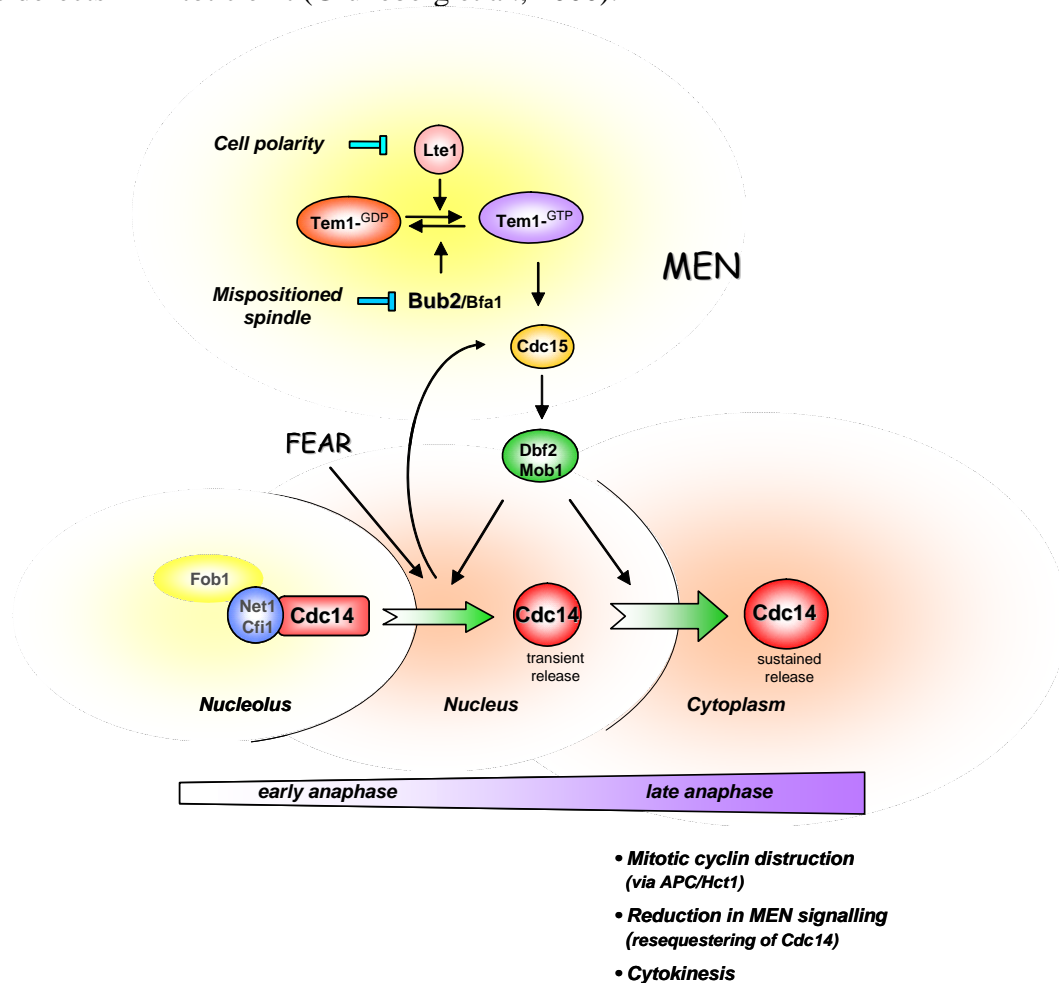


Figure 7. MEN (mitotic exit network). MEN promotes the release of Cdc14 from the nucleolus to the cytoplasm during late anaphase. The release of this phosphatase leads to the degradation of cyclins and cytokinesis; functions distinct from those of FEAR released Cdc14.

During anaphase Bub2/Bfa1 locate to the bud-oriented SPB where they recruit and inactivate Tem1 (Luca et al., 2001; Visintin et al., 1999; Pereira et al., 2000). Activation of Tem1 requires Lte1, the only component of MEN not found at the SPB but at the bud cortex (Bardin et al., 2000; Pereira et al., 2000; Jensen et al., 2002; Seshan et al., 2002). Accordingly, activation of Tem1 and induction of MEN necessitates entry of the bud-oriented SPB into the daughter cell. However, this can't be the only activating mechanism since Lte1 is nonessential in yeast (Adames et al., 2001). Noteworthy, Tem1 has a comparatively high spontaneous nucleotide exchange rate. The activity status of Tem1 can thus also be regulated via the GAP Bfa1/Bub2 alone. Accordingly, inactivation of Bfa1/Bub2 by the polo kinase Cdc5 concomitantly increases the activity of Tem1 (Hu et al., 2001; Hu and Elledge, 2002; Geymonat et al., 2003). The kinase cascade triggered by Tem1 finally leads to a release of Cdc14 from the nucleolus. In contrast to FEAR, the MEN induced dissociation of Cdc14 from Net1/Cfi involves phosphorylation of Net1/Cfi by Dbf2 (Shou et al., 2002; Yoshida et al., 2002). Cdc14 that has been released via MEN inactivates cyclin dependent kinases and stimulates cytokinesis.

1.4.5 The role of the Cdc14 phosphatase

Major events during anaphase and mitotic exit involve the effector protein Cdc14. Either released by FEAR or MEN, the Cdc14 phosphatase has distinct functions in mitosis.

Anaphase spindle stability

During anaphase B the mitotic spindle starts to elongate. This process requires spindle dynamics and stabilization of the overlap region of polar microtubules. The latter involves the recruitment of spindle stabilizing factors to the spindle midzone. This is under the control of separase Esp1 and Slk19. In absence of either of these proteins the spindle collapses (Zeng et al., 1999; Sullivan et al., 2001). FEAR-released Cdc14 during early anaphase or MEN-released Cdc14 during late anaphase dephosphorylates Sli15, leading to the midzone localization of the Ipl1/Sli15 complex (Zeng et al., 1999; Sullivan et al., 2001; Pereira and Schiebel, 2003). This complex in turn recruits Slk19 to the midzone (Zeng et al., 1999). Additionally, also phosphorylation of Slk19 by Ipl1 may influence its association with the spindle.

Nuclear positioning

During anaphase the nucleus has to be partially moved from the mother cell into the daughter cell. However, in order to prevent chromosome mis-segregation, it has to be ensured that the nucleus does not entirely leave the mother cell. The sub-cellular location of the nucleus and its distribution between mother and daughter involves astral microtubules anchored at the cortex. Prior to anaphase, asters located in the mother push the nucleus towards the daughter, whereas microtubules anchored in the bud pull (Pearson and Bloom, 2004). In anaphase a reversal of pulling and pushing forces at the mother pole takes place (Ross and Cohen-Fix, 2004). This process involves Kar9 which in its phosphorylated state locates to the daughter-bound SPB (Liakopoulos et al., 2003; Maekawa et al., 2003). However,

dephosphorylated by Cdc14 released in early anaphase (FEAR), the protein relocates to the mother oriented SPB and thus reverts pushing to pulling forces (Ross and Cohen-Fix, 2004).

Segregation of repetitive DNA

The nucleolus, containing ribosomal DNA, separates much later than the rest of the nucleus (Granot and Snyder, 1991; Buonomo et al., 2003). Moreover, *cdc14* mutants show defects in the division of the nucleolus (Granot and Snyder, 1991). Both observations together indicate that nucleolar segregation may be regulated independent of euchromatin. Cdc14 released by FEAR leads to an enrichment of condensins at heterochromatic and repetitive DNA through sumoylation of a condensin subunit (D'Amours et al., 2004; Wang et al., 2004). Chromosome condensation and compaction facilitates the separation of these DNA regions. Accordingly, the segregation of ribosomal and telomeric DNA appears to be particularly dependent on FEAR released Cdc14 (Sullivan et al., 2004).

Activation of MEN by FEAR

FEAR mutants delay cell cycle progression through late anaphase (Stegmeier et al., 2002), suggesting that FEAR released Cdc14 activates MEN. Cdc14 dephosphorylates and thus activates Cdc15, an intermediate kinase in the MEN cascade (Visintin and Amon, 2001). Moreover, phosphoproteins Bfa1 and Lte1 are substrates of Cdc14 *in vitro* (Pereira et al., 2000; Pereira et al., 2002; Seshan et al., 2002). Dephosphorylation alters the function and localization of both factors. However, the FEAR pathway alone is insufficient to fully activate MEN.

Closing mitosis

Cdc14 released by MEN promotes the degradation of cyclins and induces the accumulation of kinase inhibitor Sic1 (Visintin et al., 1998). Both processes lead to an inactivation of mitotic cyclin dependent kinases. Cdc14 dephosphorylates Hct1, which associates with the APC only in its unmodified state. Activated this way, the APC mediates ubiquitin-dependent proteolysis of cyclins (Jaspersen and Morgan, 2000; Visintin et al., 1998; Zahariae et al., 1998). Cdc14 also dephosphorylates Sic1 and its transcription factor Swi5, which leads to an accumulation of this kinase inhibitor (Moll et al., 1991; Toyn et al., 1997; Verma et al., 1997; Visintin et al., 1998). Degradation of cyclins and inhibition of cyclin dependent kinases resets the cell cycle to G1. Moreover, Cdc14 is part of a negative feed-back mechanism which eventually inactivates MEN. It dephosphorylates Bfa1 and this way attenuates the upstream kinase of the pathway.

Next to its role in mitotic exit, Cdc14 and other components of the MEN pathway are also implicated in the regulation of cytokinesis. During late anaphase and telophase Cdc15, Dbf2, Mob1 and Cdc5 locate to the bud neck (Frenz et al., 2000; Luca et al., 2001; Song et al., 2000; Song and Lee, 2001; Xu et al., 2000; Yoshida and Toh-e, 2001). Their accumulation in this area apparently involves dephosphorylation by Cdc14, as has been documented for Dbf2 and Mob1 at least (Frenz et al., 2000; Yoshida and Toh-e, 2001).

1.5 Goal of the present work

One of the fundamental requirements of life is that each individual cell is able to propagate its genetic material from one generation to the other. Accurate chromosome segregation involves bipolar attachment of replicated sister chromatids to microtubules and an equal distribution of DNA between mother and daughter cells. The attachment of microtubules occurs via a specialized chromosome structure, the so called kinetochore. One of the simplest and thus best studied kinetochores is that of the budding yeast *Saccharomyces cerevisiae*. Nevertheless it comprises more than sixty different components, several of which not functionally characterized so far. Kinetochore proteins are organized in a number of complexes and sub-complexes, which bridge between centromeric DNA and microtubules. Based on genetic data and successive affinity-purifications a hierarchical organization of the kinetochore starts to emerge. However, direct physical interactions between individual kinetochore complexes have not been analyzed to date.

In line with these considerations the present thesis focuses on the following two aspects:

The first of which is a functional analysis of Ame1, a previously uncharacterized protein of the yeast kinetochore. It is part of the Okp1 complex located in the central layer of kinetochore complexes. To investigate the role of this essential protein in kinetochore function, temperature-sensitive mutants have to be created. Since kinetochores are involved in the attachment of centromeric DNA to microtubules, it has to be determined if mutations in Ame1 have an influence on these interactions. As the kinetochore is also implicated in diverse surveillance mechanisms of mitosis, a possible contribution of Ame1 to checkpoint function has to be investigated. Moreover, several kinetochore mutants are known to influence the polymerization of the mitotic spindle. Accordingly, also this aspect of mitosis has to be analyzed. Finally, if Ame1 had an influence on spindle formation, further investigations will be needed to determine the role kinetochores play in spindle stability.

The second goal concerns the identification of *in vitro* binding partners amongst the different kinetochore complexes. For this purpose the complexes shall be isolated individually from yeast using the TAP technology and subsequently tested for pair-wise interactions. This way direct biochemical evidence for interrelations between kinetochore complexes can be provided. To gain further insight into the structural organisation of the kinetochore, also the previously mentioned mutant of *AME1* can be used. Its influence on the DNA binding of individual kinetochore complexes can be determined. This analysis can help to establish the dependency in the localization of all other complexes on the Okp1 complex. This structural knowledge can furthermore serve to explain some of the phenotypes of the *ame1* temperature-sensitive mutant analyzed before.

Thus, a functional characterization of Ame1 in combination with a biochemical mapping of intra-kinetochore interactions may help to refine our understanding of the structural organisation of the yeast kinetochore. Moreover this could lead to a better understanding of its implications in microtubule attachment, checkpoint control, and chromosome segregation. One day we might be able to reconstitute a three dimensional model of all kinetochore proteins, not only for the simple kinetochore of the budding yeast *S. cerevisiae*, but also for that of the very complicated human one. It would help us in understanding how faithful chromosome segregation is achieved. Thus, we can anticipate that someday we might be able to better understand how this process contributes to the development of cancer.

2. RESULTS

2.1 Functional analysis of *ame1-2* temperature-sensitive mutants

2.1.1 Generation of an *ame1-2* temperature-sensitive mutant

For the investigation of the *in vivo* role of Ame1, an essential protein of the *S. cerevisiae* kinetochore, temperature-sensitive mutant alleles were generated in an error-prone PCR reaction. One conditional allele, *ame1-2*, was isolated, sequenced and integrated into the genome. This allele encodes for a mutant protein with 10 amino acid changes (Figure 8). The influence of this mutated allele on different processes in mitosis was investigated in the present work.

<i>AME1</i>	MDRDTKLAFR LRGSHSRRTD DIDDDVIVFK TP NAVYREEN SPIQSPVQPI	50
<i>ame1-2</i>	MDRDTKLAFR LRGSHSRRTD DIDDDVIVFK TL NAVYREEN SPIQSPVQPI	50
<i>AME1</i>	LSSPKLANSF EFPITTNNVN AQDRHEHGY Q PLDAEDYPMI DSENKSLISE	100
<i>ame1-2</i>	LSSPKLANSF EFPITTNNVN AQDRHEHGY R PLDAEDYPMI DSENKSLISE	100
<i>AME1</i>	SPQNVNRNDED LTTRYNF DDI PIRQLSSSIT SVTTIDVLSS LFINLFENDL	150
<i>ame1-2</i>	SPQNVNRNDED LTTRYNF E DI PIRQLSSSIT SVTTIDVLSS LFINLFENDL	150
<i>AME1</i>	I PQALKDFNK SDDDQFRKLL YKLDLRL F QT ISDQMTRDLK DILDINVSNN	200
<i>ame1-2</i>	MP QALKDFNK SDDDQFRKLL YKLDLRL HF QT ISDQMTRDLK DILDIN S NN	200
<i>AME1</i>	ELCYQLKQVL ARKEDLNQQI ISVRNEIQEL KAGKDWHDL Q NEQAKLNDKV	250
<i>ame1-2</i>	ELCYQLKQVL ARKEDLNQQI ISVRNEIQEL KAGKDWHDM Q NLQAKLNDKV	250
<i>AME1</i>	KLNKRLNDLT STLLGKYEGD RKIMSQDSED DSIRDDSNIL DIAHFVDLMD	300
<i>ame1-2</i>	KLNKRLND S T STLLGKYEGD RK L MSQDSED DSIRDDSNIL DIAHFVDLMD	300

Figure 8. Amino acid sequence comparison of wild type and mutant Ame1 protein. Mutant residues are highlighted in bold and indicated by asterisks.

To verify the temperature-sensitivity of the *ame1-2* mutant, cells were spotted in several serial dilutions on plates and incubated at permissive and restrictive temperature. *ame1-2* cells showed a pronounced growth defect at 37°C (Figure 9A). This condition was used for all subsequent experiments as the restrictive temperature.

The *ame1-2* strain was also analyzed for its sensitivity to benomyl. Benomyl is a microtubule destabilizing drug also known for the weakening of kinetochore-microtubule interactions. When incubated at 23°C, *ame1-2* cells showed the same benomyl sensitivity as a corresponding wild type strain (Figure 9B). At 30°C, a temperature still permissive for growth, increased benomyl sensitivity was observed (Figure 9B). Accordingly, a combination of elevated temperature and benomyl causes synthetic enhancement, suggestive of impaired kinetochore-microtubule interactions or spindle defects in the *ame1-2* mutant strain.

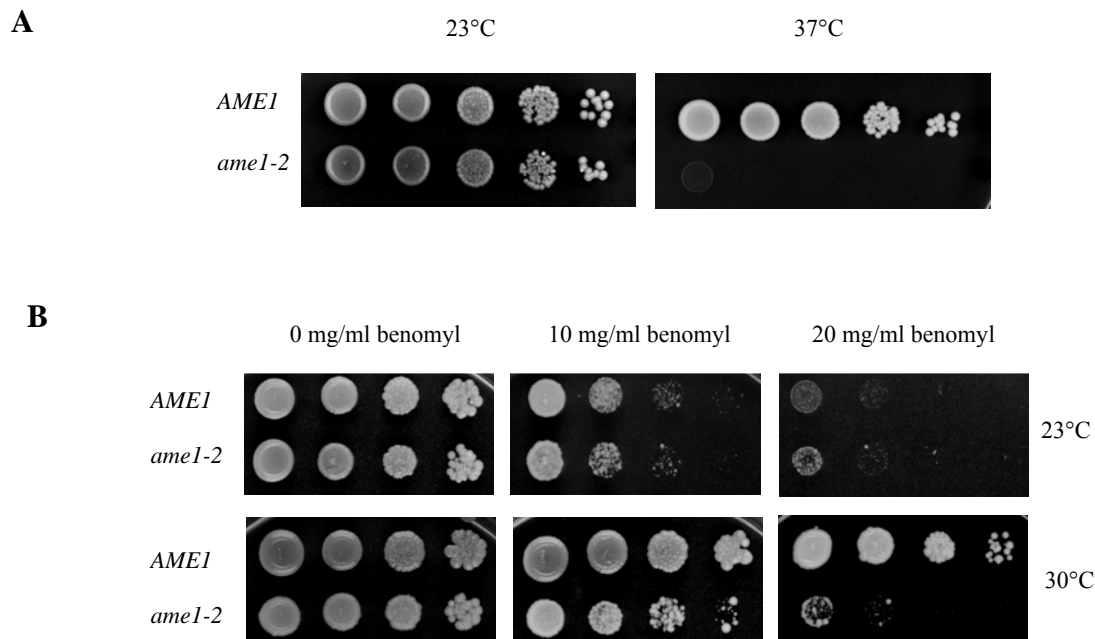


Figure 9. Growth defects of the *ame1-2* mutant strain.

- (A) *Temperature effects.* 1 OD₅₇₈ of a logarithmically growing culture was harvested and resuspended in 1 ml YPD (2×10^7 cells). Five successive 1:10 dilutions were spotted on YPD plates and incubated for 3 days at 23°C or 37°C.
- (B) *Benomyl sensitivity.* 1 OD₅₇₈ of a logarithmically growing culture was harvested and resuspended in 1 ml YPD (2×10^7 cells). Four successive 1:10 dilutions were spotted on YPD plates supplemented with 0, 10, or 20 mg/ml benomyl. Plates were incubated for 4 days at 23°C or 30°C.

2.1.2 Analysis of kinetochore-microtubule attachments in *ame1-2*

The observed temperature and benomyl sensitivity of the *ame1-2* mutant strain may reflect defective kinetochore-microtubule interactions. As a result, chromosomes may not get properly segregated between mother and daughter cell, thus leading to cell death.

2.1.2.1 Tension between sister chromatides is not maintained in *ame1-2*

Formation of tension at kinetochores during metaphase can be used as an indication for correct bipolar attachment of microtubules to kinetochores. As described in the introduction, tension can be visualized by GFP-tagging of the centromeric region of a chromosome with the tetO/tetR system (Michaelis et al., 1997). In order to keep cells arrested in metaphase, depletion of Cdc20 was performed. This way the spindle checkpoint remains activated and sister chromatide separation is inhibited.

When Cdc20 was depleted for 3 hours at RT, both wild type and *ame1-2* cells showed two distinct GFP signals in more than 90% of the cells. This is indicative of tension that has been build up

between kinetochores (Figure 10). Whereas a subsequent temperature shift to 37°C had no effect on tension in wild type cells, the GFP signals gradually collapsed in the *ame1-2* strain. Within three hours after transfer to the restrictive temperature, more than 90% of the mutant cells showed only one distinct GFP dot.

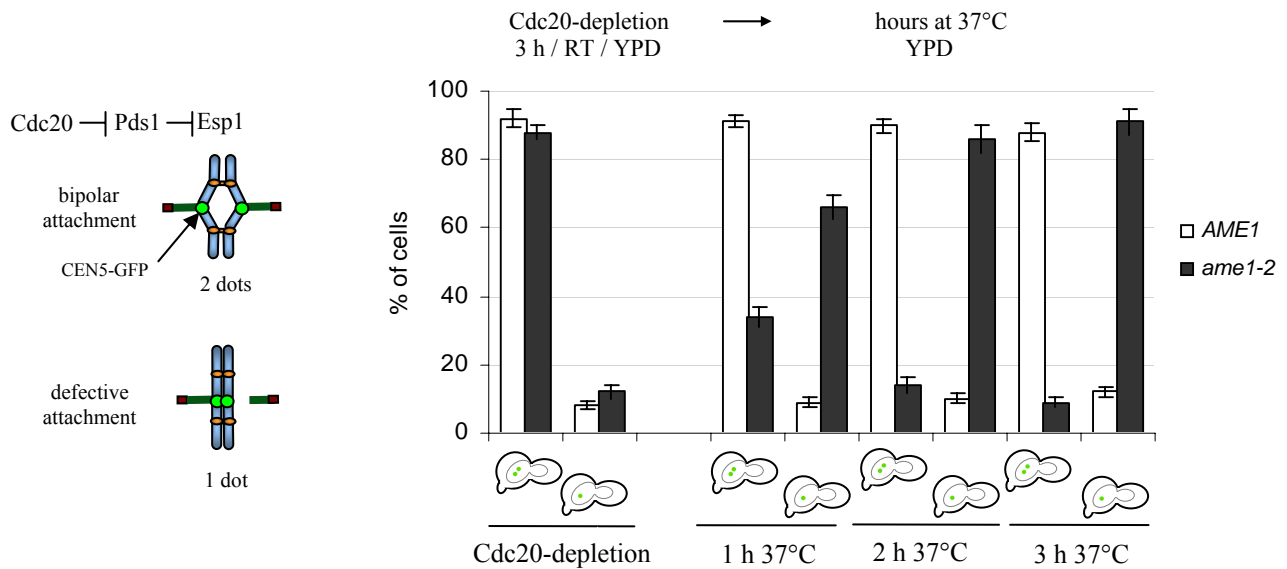


Figure 10. Loss of tension in *ame1-2* during *Cdc20* arrest. *CEN5* was tagged with GFP by the tetO/tetR system (Michaelis et al., 1997). Cells with *CDC20* under the control of a *GAL* promoter were grown o/n in medium containing galactose, shifted to glucose medium and incubated for 3 h at RT. Temperature was subsequently increased to 37°C and the sub-cellular distribution of *CEN5*-GFP analyzed after 1, 2, and 3 hours. At least 100 cells per time point were counted.

The inability of *ame1-2* to maintain tension at kinetochores is indicative of defects in kinetochore microtubule attachments.

2.1.2.2 *ame1-2* mutants show defects in the distribution of sister chromatides

Loss of tension at the kinetochore in the *ame1-2* mutant strain may either result from a syntelic attachment (interaction with microtubules emanating from the same pole) or no kinetochore-microtubule attachment at all. In mutants of the Ndc80 or CBF3 complexes for example, kinetochore-microtubule interactions are lost (Janke et al., 2001; Wigge and Killmartin, 2001; Goh and Killmartin, 1993). This causes retention of DNA in the mother cell.

In order to analyze the attachment defect in *ame1-2* the distribution of sister chromatides (by *CEN5*-GFP) and DNA masses (by Hoechst) was analyzed (Figure 11). *ame1-2* mutant cells were able to segregate DNA between mother and daughter. However, they failed to distribute sister chromatides (Figure 11A). Instead, in 97% of all cases sister chromatides were segregated to one

of the poles (Figure 11B). No clear preference for mother or daughter cell was observed. In 53% of the cells the *CEN5*-GFP signal remained in the mother and in 44 % of the cells the signal was segregated into the daughter. Noteworthy, besides cells with a single GFP signal in either mother or daughter also cells with a second signal were observed, indicative of sister chromatide separation at least in a subset of cells.

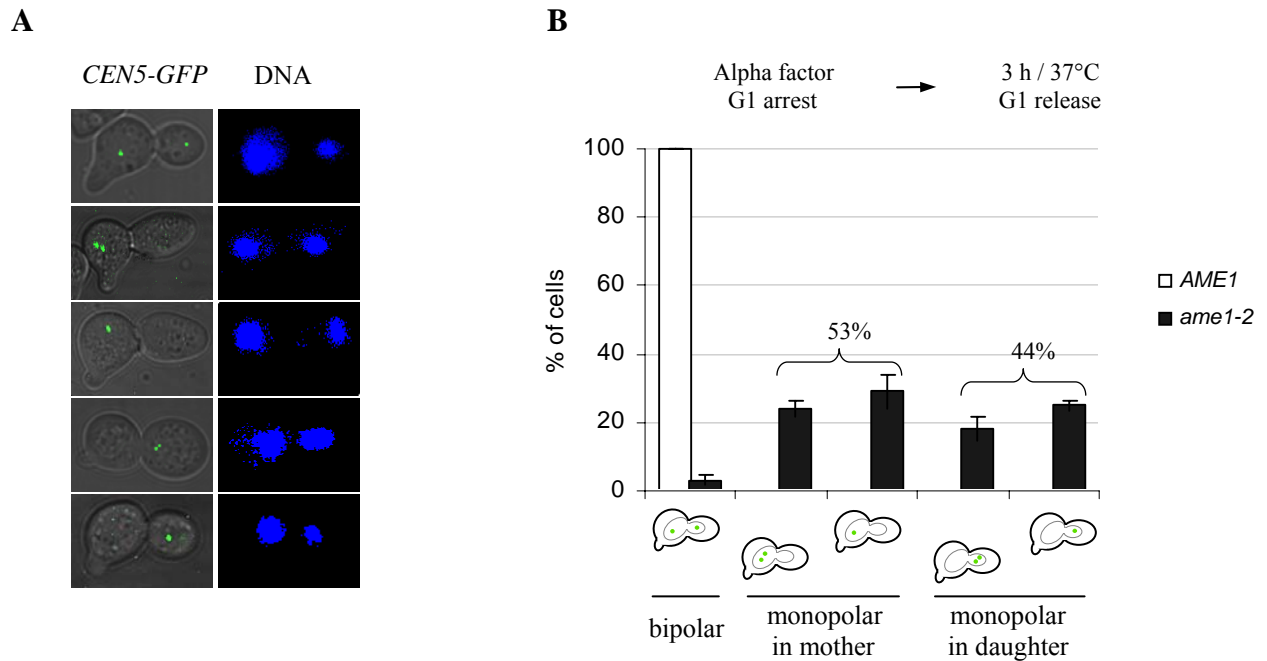


Figure 11. Monopolar distribution of sister chromatides in *ame1-2*.

- (A) Distribution of *CEN5*-GFP signal and corresponding DNA stain. *CEN5* was tagged with GFP by the tetR/tetO system (Michaelis et al., 1997) and the DNA was stained with Hoechst. Cells were synchronized with alpha factor for 2.5 h and released in medium at 37°C. Sub-cellular distribution of the signals was analyzed after 3 h.
- (B) Quantification of (A). After 3 h at 37°C 100 cells with segregated DNA masses (>90%) were counted for the distribution of the *CEN5*-GFP signal.

Since the *ame1-2* mutant is still able to segregate its DNA, kinetochore-microtubule interactions are still formed in this strain. Furthermore, *ame1-2* displays a monopolar distribution of sister chromatides, with no preference for either mother or daughter. This monopolar segregation defect indicates a requirement of the Ame1 protein in the establishment of bipolar spindle attachment.

2.1.3 Checkpoint analysis in *ame1-2* mutant cells

During the transition from metaphase to anaphase sister chromatide separation and spindle elongation are regulated by the spindle assembly checkpoint. This checkpoint is inactivated once all chromosomes are bipolarly attached to microtubules emanating from the opposing poles. A marker for the spindle attachment checkpoint is Pds1, a protein degraded during this transition. In metaphase Pds1 levels are high, start to decrease at the onset of anaphase and become very low at the end of anaphase. Defects in kinetochore-microtubule attachment delay the inactivation of the spindle checkpoint and lead to elevated Pds1 levels. These cause a G2/M arrest, since the sister chromatides separating protein Esp1 is kept inactive by Pds1. Once all kinetochores are properly attached to microtubules, sister chromatide cohesion is resolved and the spindle starts to elongate. During this process, the orientation of the growing anaphase spindle relative to the mother-bud axes is monitored by the spindle positioning checkpoint. Hence, several aspects of mitosis involve control mechanisms.

2.1.3.1 The occupancy checkpoint is active in *ame1-2*

A number of kinetochore mutants (e.g. *ndc10-1*, *spc24-2*, *spc25-7*) have a defective checkpoint response, being unable to initiate a checkpoint arrest in the presence of spindle or attachment defects (Goh and Kilmartin, 1993; McClelland et al., 2003; Janke et al., 2001). The occupancy checkpoint monitors if all kinetochores are correctly attached to microtubules. A single unattached kinetochore is sufficient to prevent its inactivation. To analyze the functionality of the occupancy checkpoint in the *ame1-2* background, Pds1 levels were determined in the presence of nocodazole, a microtubule depolymerizing drug. In a wild type situation nocodazole leads to a fully active checkpoint with persisting high Pds1 levels and an arrest with a 2N DNA content.

ame1-2 mutant cells were alpha factor arrested in G1 and released at 37°C into medium containing nocodazole. The amount of Pds1 was determined by immunoblotting and the DNA content was analyzed by FACS (Figure 12). In presence of nocodazole, both *ame1-2* and wild type maintained high Pds1 levels and arrested with a 2N DNA content (Figure 12A, B upper panel). The arrest of *ame1-2* with a 2N DNA content can either be attributed to the activation of the spindle assembly checkpoint, which inhibits sister chromatides separation and MEN (mitotic exit) or to an activation of the spindle positioning checkpoint which also interferes with the execution of MEN. To differentiate between these possibilities, Bub2, a regulator of this checkpoint (see introduction; 1.4.2) was deleted in *ame1-2*. Deletion of Bub2 makes it possible to attribute the metaphase arrest and the defect in mitotic exit solely to an active spindle assembly checkpoint. In absence of Bub2 both, *ame1-2* and wild type cells behaved similarly (Figure 12B, middle panel). After an initial arrest with a 2N DNA content for 4 hours, rereplication was initiated, which indicates the beginning of a new cell cycle. This occurred despite the induction of the occupancy checkpoint by the addition

of nocodazole. In comparison, wild type cells with both checkpoints fully active remain in mitosis for at least 7 hours (Figure 12B, upper panel), whereas wild type cells with both checkpoints defective ($\Delta bub2\Delta mad2\Delta AME1$) perform mitotic exit and produce cells with a 4N DNA content already after 2.5 hours (Figure 12B, lower panel).

These results indicate that the occupancy checkpoint can be induced in *ame1-2* and that it is fully active. In order to additionally verify the induction of the occupancy checkpoint, the localization of checkpoint proteins Mad2 and Bub1 was analyzed (Figure 12C). In wild type and *ame1-2* cells, GFP-tagged versions of both proteins were found at the kinetochore in presence of nocodazole. This further confirms the functionality of the occupancy checkpoint in *ame1-2*.

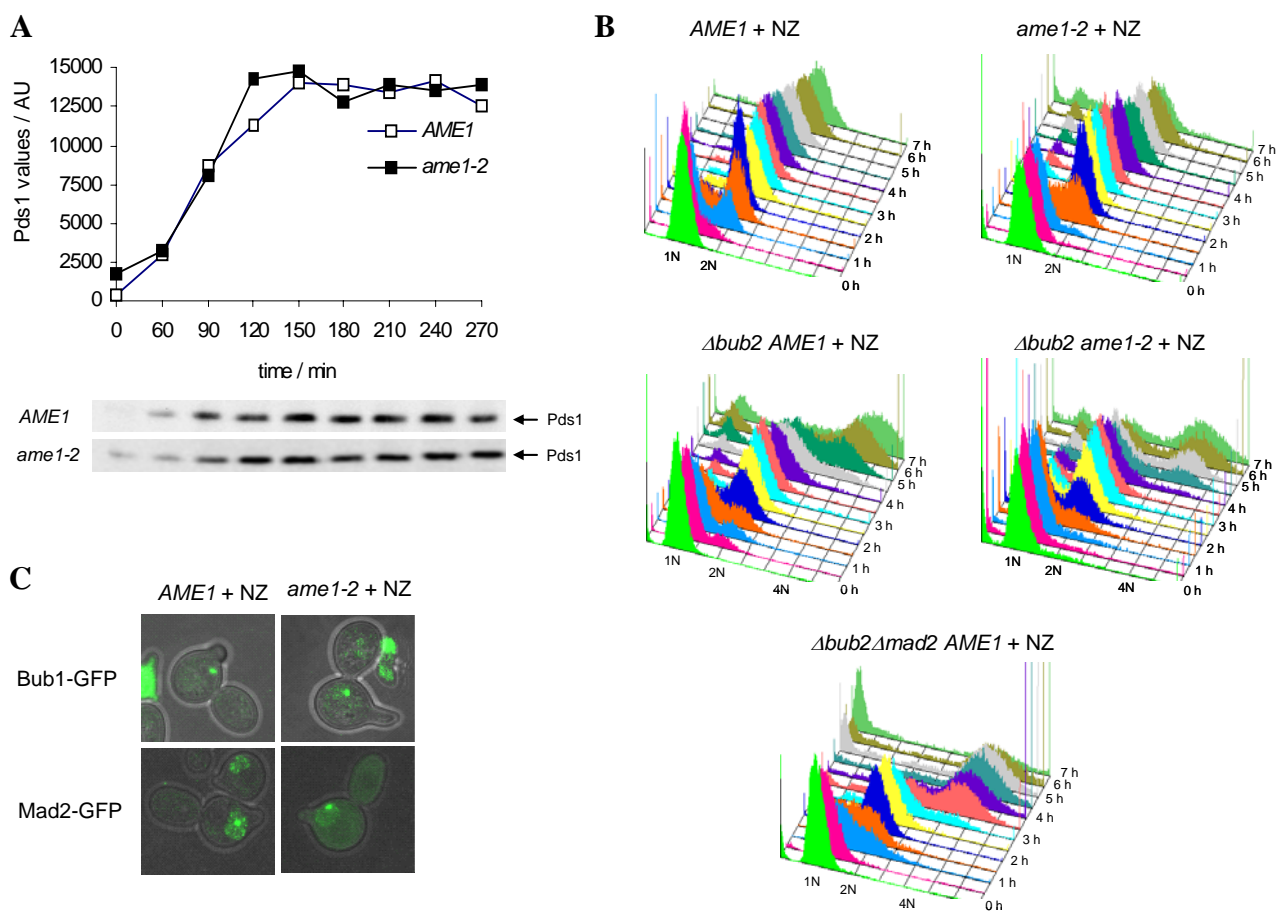


Figure 12. The *ame1-2* mutant has no effect on the occupancy checkpoint.

- (A) *Pds1* levels. Cells with myc-tagged *Pds1* were arrested in G1 with alpha factor at RT and released at 37°C into medium supplemented with 15 µg/ml nocodazole (t=0). Aliquots were taken every 30 min, protein extracts prepared and the amounts of *Pds1* determined by immunoblotting (anti-myc). AU, arbitrary units.
- (B) *FACS analysis*. Same conditions as in (A). Aliquots were analyzed by FACS for their DNA content.
- (C) *Localization of Bub1 and Mad2*. Cells with GFP-tagged Bub1 or Mad2 were arrested in G1 with alpha factor at RT (t=0) and released at 37°C in medium containing nocodazole. After 3 h fluorescence microscopy was performed.

2.1.3.2 *ame1-2* shows a delay in Pds1 degradation and arrests with a 2N DNA content

ame1-2 mutant cells show defects in bipolar spindle attachment and a monopolar distribution of sister chromatides. These effects should delay or prevent the inactivation of the spindle assembly checkpoint. To analyze this, cells were synchronized in G1 with alpha factor and released in medium at 37°C. In order to see if cells are able to perform cytokinesis, the entry in a new cell cycle was prevented by the re-addition of alpha factor after the appearance of the bud (90-120 minutes after the release from the initial alpha factor arrest). Aliquots were taken in 30 minute intervals and analyzed for the amount of Pds1 by immunoblotting and for the DNA content by FACS (Figure 13).

In the *ame1-2* mutant the degradation of Pds1 is delayed by about 60 minutes in comparison to wild type cells (Figure 13A). This indicates a partial induction of the spindle assembly checkpoint in the *ame1-2* mutant. In order to verify this, a deletion of checkpoint protein Mad2 was performed in the *ame1-2* mutant strain. Inactivation of the spindle assembly checkpoint by Mad2-deletion should abolish the *ame1-2* induced delay in Pds1 degradation. However, the *ame1-2 Δmad2* double mutant turned out to be sick and slow growing already at the permissive temperature and could thus not be analyzed in this assay.

Although Pds1 degradation in *ame1-2* is only delayed by 60 minutes, the mutant cells still arrest with a DNA content of 2N even 4 hours after corresponding wild type cells performed cytokinesis (Figure 13B). This can have different causes:

1. A defect in DNA segregation would lead to the formation of cells with no DNA and cells with a DNA content of 2N. However, this can already be excluded since the *ame1-2* mutant is able to distribute its DNA between mother and daughter (see 2.1.2.2 and Figure 11).
2. An activation of the spindle positioning checkpoint would lead to a delay in mitotic exit and thus interfere with cytokinesis. In order to exclude that an activation of the spindle positioning checkpoint is the cause for the observed arrest, FACS analysis were performed in the absence of Bub2 (regulator of this checkpoint; see introduction; 1.4.2). In spite of the lack of Bub2, *ame1-2* cells permanently arrested with a 2N content for 6 hours and were unable to perform cytokinesis similar to the *ame1-2* mutant alone (Figure 13C; compare with Figure 13B). This indicates that an activation of the spindle positioning checkpoint is not responsible for the arrest of *ame1-2* cells.
3. An activation of the spindle assembly checkpoint on the other hand would lead to a metaphase arrest and to a delay in mitotic exit. As a consequence of both, cytokinesis would be prevented. However, this is unlikely the cause for the arrest of the *ame1-2* mutant since degradation of Pds1 is only delayed by 60 minutes and not permanently inhibited like in a strain with an activated spindle assembly checkpoint (Figure 13A, see Figure 12A for comparison). Additionally, an *AME1 Δbub2* strain is able to form a 4N peak after 4 hours even in presence of a fully active spindle assembly checkpoint (nocodazole treatment, Figure 12B, middle panel). Thus, the arrest of the *ame1-2 Δbub2* double mutant cannot be due to an activation of the spindle assembly checkpoint. To further confirm this, FACS analysis in the *ame1-2 Δbub2* double mutant were performed without a secondary addition of

alpha factor, so to allow for an analysis of rereplication (i.e. MEN, mitotic exit). Although a broadening of the 2N peak was observed after 3.5 hours no clear accumulation of cells with a DNA content of 1N or 4N took place, indicating that cytokinesis could not be performed (Figure 13C).

4. Finally also an intrinsic defect in the MEN (mitotic exit network) pathway can account for the inability of *ame1-2* cells to leave the 2N state and perform cytokinesis. However, functionality of MEN in *ame1-2* had already been proven, since an *ame1-2* Δ *bub2* double mutant is able to perform rereplication when treated with nocodazole (4N peak in Figure 12B, middle panel).

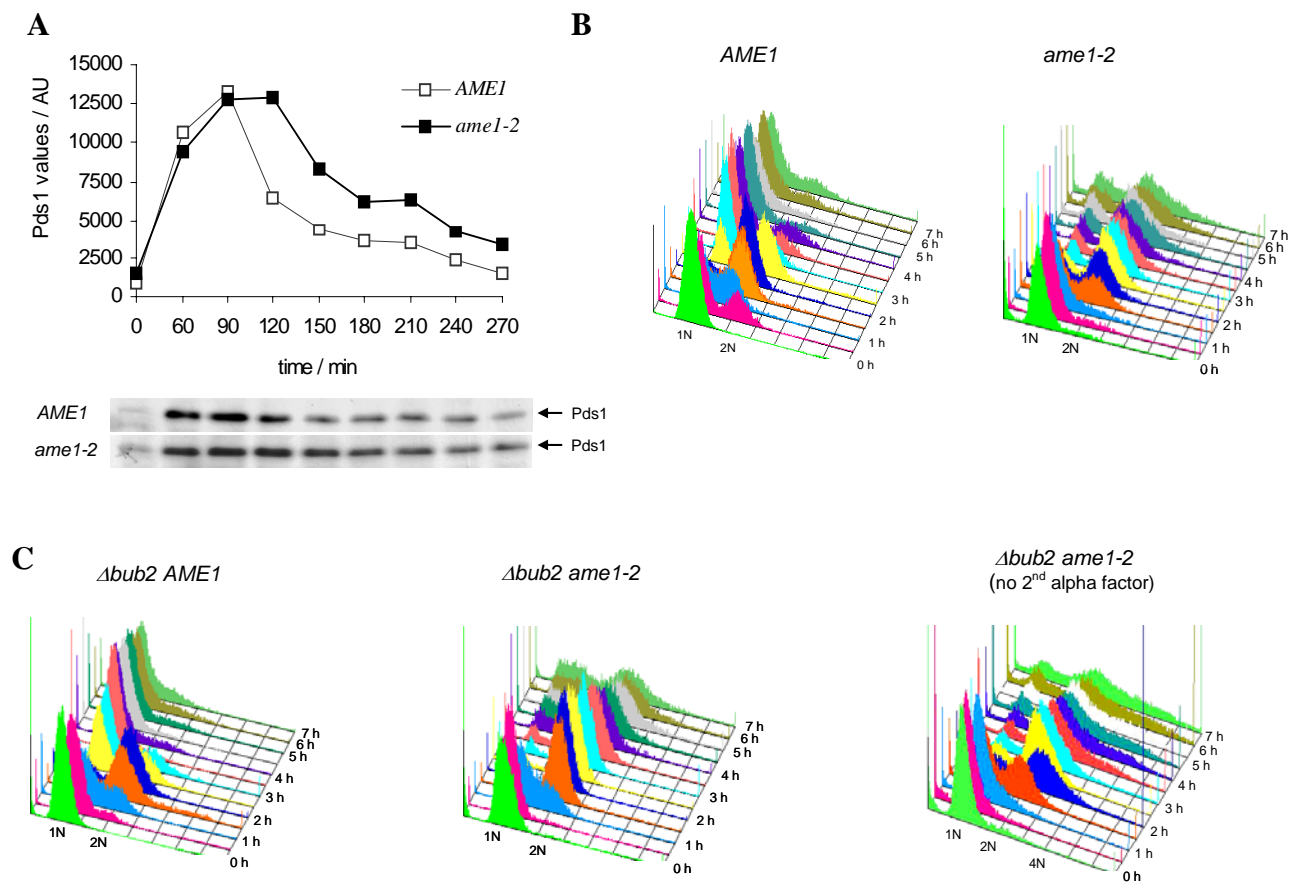


Figure 13. *ame1-2* leads to delayed spindle checkpoint inactivation and to a G2/M arrest.

- (A) *Pds1* levels. Cells with myc-tagged Pds1 were arrested in G1 with alpha factor at RT and released into medium at 37°C (t=0). When the appearing bud was about 2/3 of the size of the mother, alpha factor was re-added. Aliquots were taken every 30 min, protein extracts prepared and the amounts of Pds1 determined by immunoblotting (anti-myc). AU, arbitrary units.
- (B) *FACS analysis*. Same conditions as in (A). Aliquots were analyzed by FACS for their DNA content.
- (C) *FACS analysis*. Same conditions as in (B), except for the Δ *bub2**ame1-2* strain, were FACS analyses were performed with or without a secondary addition of alpha factor.

These data allow to conclude that the 2N peak in the FACS analysis of the *ame1-2* mutant cannot be due to an activation of the spindle assembly checkpoint, but can more likely be attributed to the monopolar segregation defect of the *ame1-2* mutant accompanied by an intrinsic defect in cytokinesis. This might lead to an uneven distribution of the replication machinery and thus may possibly prevent rereplication.

2.1.3.3 The delay in Pds1 degradation in *ame1-2* is conform with an induction of the tension checkpoint

The delay observed in the degradation of Pds1 (Figure 13A) still indicates an activation of the spindle assembly checkpoint. This can either be due to an activation of the tension checkpoint, since the *ame1-2* mutant is unable to maintain tension at its kinetochores (see Figure 10; Biggins and Murray, 2001; Stern and Murray, 2001), or to a single or a few unattached kinetochores that lead to an induction of the occupancy checkpoint. However, missing tension induces the spindle assembly checkpoint only temporarily, whereas a detachment of all kinetochores from microtubules would lead to a permanent arrest.

In order to compare the induction of the spindle assembly checkpoint in *ame1-2* with tension-dependent checkpoint activation, Pds1 degradation was analyzed in a strain depleted of the cohesin Scc1. Loss of cohesion leads to loss of tension despite bipolar attachment and causes an activation of the tension checkpoint (Biggins and Murray, 2001). A comparison between the *ame1-2* strain and a wild type strain depleted for Scc1 revealed that the degradation kinetics of Pds1 in both strains are similar (Figure 14). This indicates that the delay in Pds1 degradation observed in *ame1-2* is conform with an activation of the tension checkpoint. However, this does not necessarily exclude a partial induction of the occupancy checkpoint by a single or a few unattached kinetochores.

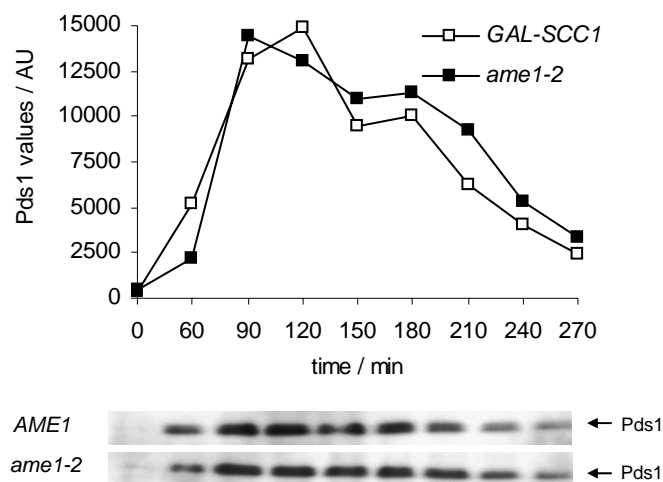


Figure 14. The tension checkpoint is activated in *ame1-2* cells. A *GAL-SCC1* and an *ame1-2* mutant strain with myc-tagged Pds1 were grown o/n in medium containing galactose and shifted to glucose containing medium supplemented with alpha factor. Incubation was continued for 5h at RT and cells released at 37°C into medium containing glucose. Aliquots were taken every 30 min and analyzed by immunoblotting (anti-myc). AU, arbitrary units.

2.1.4 *ame1-2* mutants are unable to perform cytokinesis despite a functional MEN (mitotic exit network)

As seen in the preceding chapter (2.1.3.2), the *ame1-2* mutant arrests with a 2N DNA content even four hours after the wild type has undergone cytokinesis (Figure 13B). As previously shown, this arrest can neither be attributed to an activation of the spindle assembly checkpoint nor to a nonfunctional MEN due to an active spindle positioning checkpoint.

In order to further confirm the functionality of the MEN cascade in the *ame1-2* mutant, the release of the Cdc14 effector-phosphatase from the nucleolus was analyzed. However, as mentioned in the introduction, Cdc14 can not only be released from the nucleolus by MEN but also by FEAR (Pereira et al., 2002; Stegmeier et al., 2002; Yoshida et al., 2002; Visintin et al., 1998; Xu et al., 2000; Bardin et al., 2000; Lee et al., 2001). Nevertheless, since FEAR releases Cdc14 only transiently during mitosis and MEN induces a sustained release, it is possible to distinguish between both. In order to follow the sub-cellular distribution of Cdc14, a genomic GFP-fusion construct of Cdc14 was analyzed in the *ame1-2* mutant background by time-lapse microscopy (Figure 15). For this experiment cells were synchronized with alpha factor in G1 and released at 37°C. In more than 95% of the cells the initial Cdc14 signal concentrated in the nucleolus and was released about 28 minutes after the appearance of a medium sized bud. Since the Cdc14 release was sustained in *ame1-2*, this observed release can be attributed to the mitotic network (MEN). The cytokinesis defect in *ame1-2* can therefore not be due to a nonfunctional MEN.

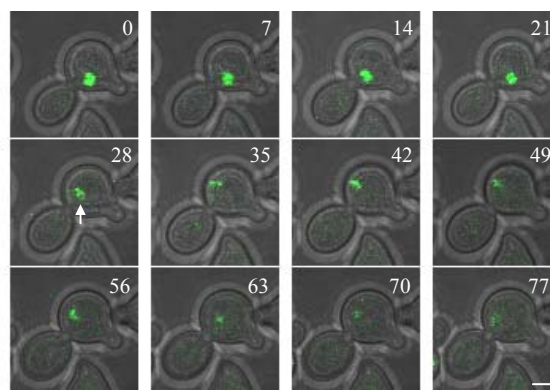


Figure 15. The *ame1-2* mutant has a functional MEN. Cells with GFP-tagged Cdc14 were arrested in G1 with alpha factor at RT and released into medium at 37°C. Time-lapse sequences were recorded in 60 sec intervals by scanning through 5 z stacks. For all pictures maximal intensity projections were calculated. Depicted are images of an exemplary cell, collected in 7 min intervals after the appearance of a medium sized bud (t=0). Arrow indicates the disappearance of the nucleolar Cdc14-GFP signal. Bar, 2 µm.

Analysis of the budding index of the *ame1-2* strain also indicates that the mutant is unable to perform cytokinesis (Figure 16). Whereas a wild type control strain showed virtually no buds after three hours at the restrictive temperature, the *ame1-2* mutant predominantly displayed either one or two buds (Figure 16A). More than 30% of the mutant cells had still one bud seven hours after alpha factor release, also indicating a defect in cytokinesis. However, this defect cannot be attributed to failures in MEN, since about 30% of the cells were able to form an additional bud.

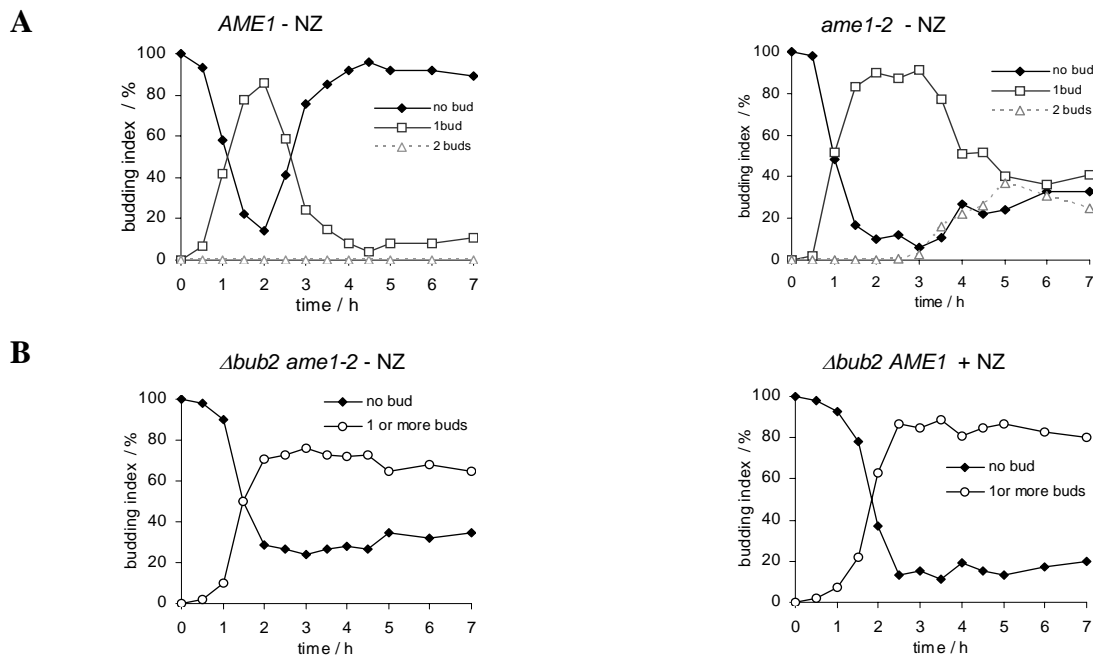


Figure 16. Analysis of the budding index of an *ame1-2Δbub2* double mutant in absence or presence of nocodazole.

- (A) Budding index without NZ. Cells were arrested in G1 with alpha factor at RT (t=0) and released in medium at 37°C. At the indicated time points cells were analyzed for the presence or absence of buds. For each time point at least 100 cells were counted. The relative abundance of each population is depicted over time.
- (B) Budding index in the presence or absence of NZ. Same conditions as in (A), but *Δbub2AME1* cells were released at 37°C in medium supplemented with 15 μg/ml nocodazole.

The preceding analyses indicated that the cytokinesis defect in *ame1-2* cannot be attributed to a failure in MEN. However, the real cause of the defect still remained to be determined. Defects in cell division may also result from instability of the spindle midzone (Norden et al., 2006). That this is also likely the cause for the cytokinesis defect in *ame1-2* is supported by the comparison of the budding index of an *ame1-2 Δbub2* double mutant with that of an *AME1 Δbub2* strain treated with nocodazole (Figure 16B). Both strains display a high number of cells with one or more buds (more than 60% in *ame1-2Δbub2* and about 80% in *AME1 Δbub2*). Nocodazole treatment leads to the dpolymerization of microtubules. Thus, the cytokinesis defect of the *ame1-2* mutant may be attributed to defects of this mutant in spindle polymerization. Accordingly, the spindle morphology in *ame1-2* was focus of subsequent analyses.

2.1.5 *ame1-2* exhibits a spindle defect

Proper DNA segregation requires the polymerization of a mitotic spindle. It comprises three different kinds of filaments: Astral microtubules attach the spindle pole bodies to the cell cortex, kinetochore microtubules connect centromeres with spindle pole bodies, and overlapping polar microtubules form the spindle midzone and push the poles apart. As shown in the previous chapters, the *ame1-2* mutant is defective in chromosome segregation and cytokinesis. Monopolar segregation defects are also observed in mutants of the Mtw1 or DDD complex (Scharfenberger et al., 2003; Janke et al., 2002; Cheeseman et al., 2001). However, these strains also display an abnormal spindle morphology (polar microtubules). More recently also cytokinesis has been linked to the presence of a spindle midzone (Norden et al., 2006). Accordingly, the influence of the *ame1-2* allele on the assembly and stability of the mitotic spindle was analyzed.

2.1.5.1 *ame1-2* interferes with anaphase spindle formation

In order to follow the formation of the mitotic spindle, a GFP-tagged version of the microtubule protein Tub1 was integrated into the *ame1-2* mutant. Cells were alpha factor arrested in G1 and released into medium at the restrictive temperature. The polymerization of the spindle was followed by life time microscopy. Time-lapse sequences were recorded and are displayed in Figure 17. Shortly after the appearance of the bud, spindle pole bodies are duplicated and start to separate in wild type cells (Figure 17A). This goes along with the formation of a short metaphase spindle six to twelve minutes after the appearance of a small bud. This structure elongates to an anaphase spindle and is depolymerized at the end of mitosis. In contrast, anaphase spindle formation in *ame1-2* is severely compromised. The spindle pole bodies can be resolved as two distinct spots throughout mitosis. They are either not connected by an anaphase spindle at all or only by a very faint one (Figure 17B). Moreover, in *ame1-2* cells spindle pole bodies are not separated as far as in wild type cells, where they eventually reach the ends of the mother and daughter cell. This phenomenon in *ame1-2* can be attributed to the missing anaphase spindle that normally contributes to spindle pole body separation in anaphase B. That spindle pole bodies are separated at all in *ame1-2* is due to the pulling force of the astral microtubules anchored at the poles.

Quantification of the *ame1-2* spindle morphology revealed that only 2% of the *ame1-2* cells are able to form a spindle comparable to an anaphase spindle in wild type (Figure 17C). Instead, 11% of the cells displayed a very faint anaphase spindle, whereas the majority of the cells were unable to polymerize an anaphase spindle at all (87%). Thus, anaphase spindle formation is strongly compromised by the *ame1-2* mutation.

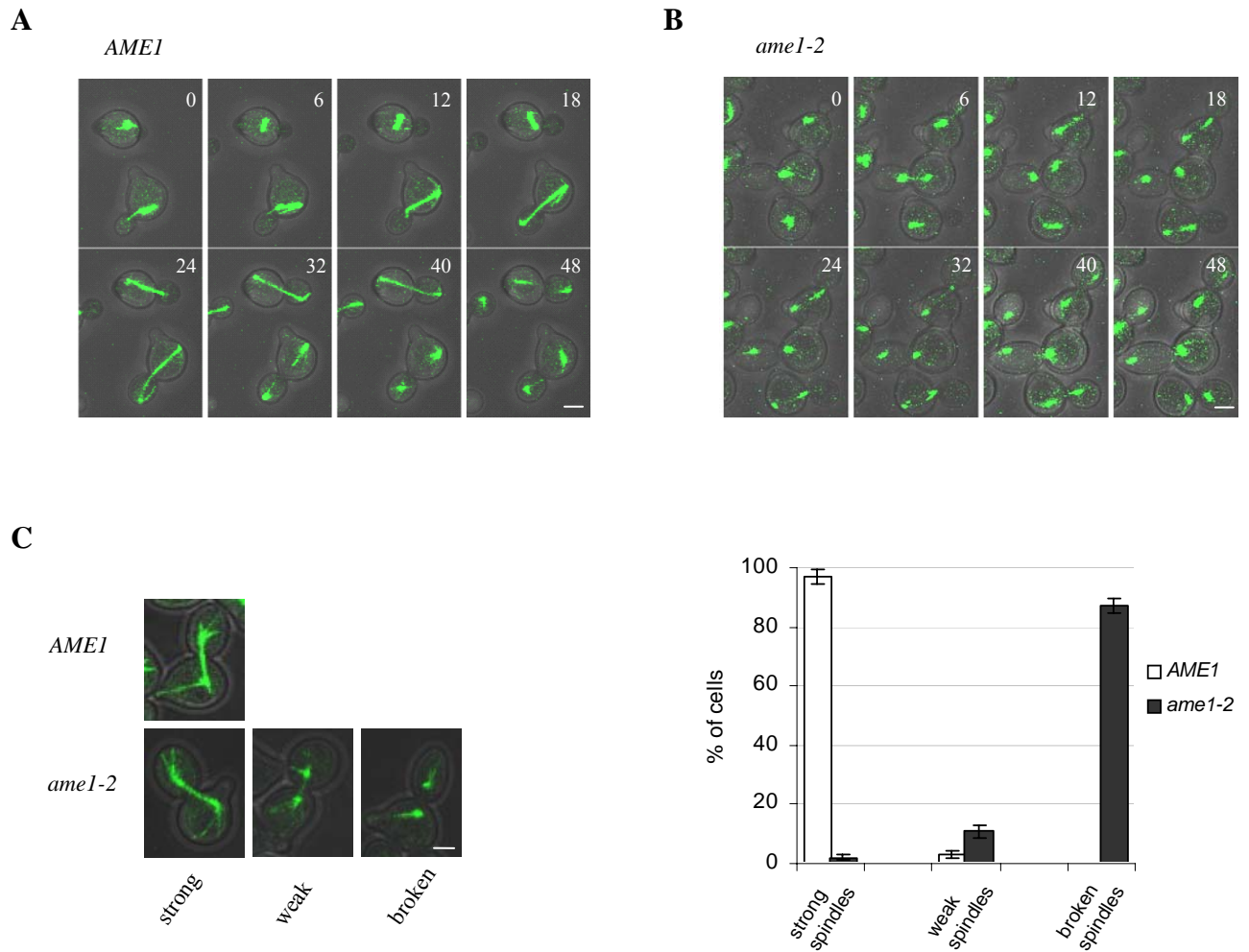


Figure 17. Spindle morphology in *ame1-2*.

- (A) *Formation of an anaphase spindle in wild type cells.* Cells were arrested in G1 with alpha factor at RT and released into medium at 37°C. Time-lapse sequences were recorded in 60 sec intervals by scanning through 5 z stacks. For all pictures maximal intensity projections were calculated. Depicted are images of exemplary cells, collected every 6 min after the initiation of metaphase (time 0). Bar, 2 μ m.
- (B) *Spindle formation in *ame1-2* is severely compromised.* Same experimental setup as in (A).
- (C) *Quantification of the observed spindles.* Cells were arrested in G1 with alpha factor at RT and released into medium at 37°C. Spindle morphology was analyzed 165 min after the release. At least 100 cells were counted.

2.1.5.2 Ame1 is not a microtubule-associated protein (MAP)

Some kinetochore proteins, like Ndc10 or components of the DDD complex for example, are not only located at the kinetochore but can also be found along the anaphase spindle (Müller-Reichert et al., 2003; Bouck and Bloom 2005; Li et al., 2002; Janke et al., 2002). There they may play a role in spindle stabilization. If Ame1 was also a MAP, mutations in this protein could potentially affect its microtubule localization and thereby the overall stability of the spindle. To examine this, cells were double labeled with a 3 x GFP version of Ame1 and CFP-Tub1 for the visualization of spindles (Figure 18).

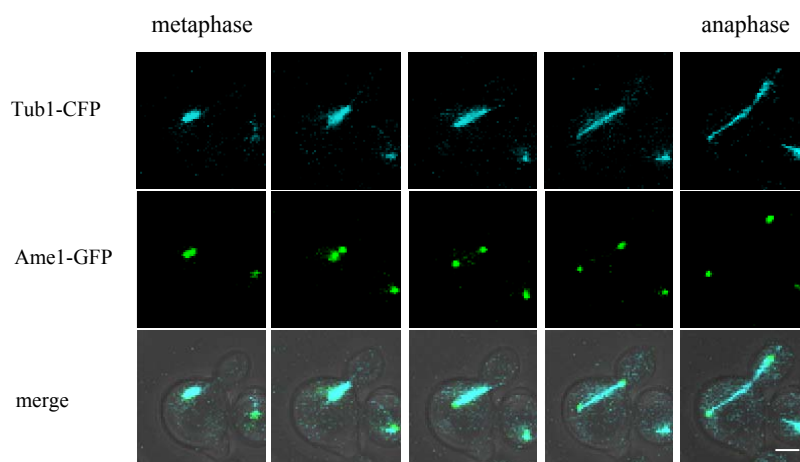


Figure 18. Ame1 localization during mitosis. Cells were double labeled with Tub1-CFP (blue) and Ame1-3GFP (green), arrested in G1 with alpha factor, and released into medium at RT. Images were taken by scanning through 5 z stacks. For all pictures maximal intensity projections were calculated. Bar, 2 μ m.

During mitosis, the spindle elongates at the transition from metaphase to anaphase. At the same time Ame1-GFP can be visualized as two separate signals representing kinetochores. In anaphase, the Ame1 signal can still be observed at kinetochores, close to the spindle pole bodies. However, a localization of Ame1 along the spindle could not be detected at any given time. Accordingly, Ame1 does not seem to be a MAP. The spindle defect of the *ame1-2* mutant may thus be attributed to indirect, Ame1-dependent processes.

2.1.5.3 Investigating the cause of the *ame1-2* spindle defect

In wild type, anaphase spindle formation is initiated after the inactivation of the spindle assembly checkpoint by the bipolar attachment of kinetochores to microtubules. Checkpoint inactivation leads to the degradation of Pds1 and subsequently to the activation of separase Esp1. Esp1 does not only play a role in sister chromatide cleavage but also contributes to anaphase spindle stabilization. The latter may either result from its translocation to the spindle or from an activation of FEAR and the subsequent transient release of Cdc14 from the nucleolus (Jensen et al., 2001, Zeng et al., 1999; Sullivan et al., 2001; Pereira and Schiebel, 2003; Higuchi and Uhlmann, 2005). Cdc14 in turn leads to the recruitment of spindle stabilizing factors to the spindle midzone. One of these factors is Slk19 which translocates from the kinetochore to the spindle midzone in anaphase, upon Cdc14 release. However, Slk19 also plays together with Esp1 a role in FEAR induction.

The inability of the *ame1-2* mutant to perform a bipolar attachment causes an activation of the spindle attachment checkpoint (see Figure 13A and 14). This leads to a delay in the degradation of Pds1 and thus to a delay in Esp1 activation. In consequence, also the Cdc14 release from the nucleolus would be delayed. Accordingly, spindle stability in *ame1-2* may be compromised by premature spindle pole body separation (due to the inability to perform bipolar attachment) in presence of low Esp1 and Cdc14 activity.

2.1.5.3.1 The *ame1-2* mutant interferes with a nucleolar Cdc14 release in early anaphase (FEAR)

In order to investigate whether FEAR is functional in *ame1-2*, cells labeled with Cdc14-GFP were analyzed by video microscopy (Figure 19). All experiments were performed in a *cdc15-1* background (inhibits mitotic exit), so that a Cdc14 release due to an induction of MEN could be excluded.

In wild type cells the release of Cdc14 from the nucleolus was observed 30 minutes after the appearance of a small sized bud (Figure 19A; arrows). 10-15 minutes later the Cdc14 signal was resequenced in the divided nucleoli. In contrast, in the *ame1-2* mutant the Cdc14 signal did not disappear, but persisted in the nucleolus of the mother cell even for 2 hours after the appearance of the bud (Figure 19B and data not shown). More than 85% of wild type cells showed an active FEAR, whereas no single *ame1-2* mutant cell displayed a nucleolar release of Cdc14-GFP (Figure 19D).

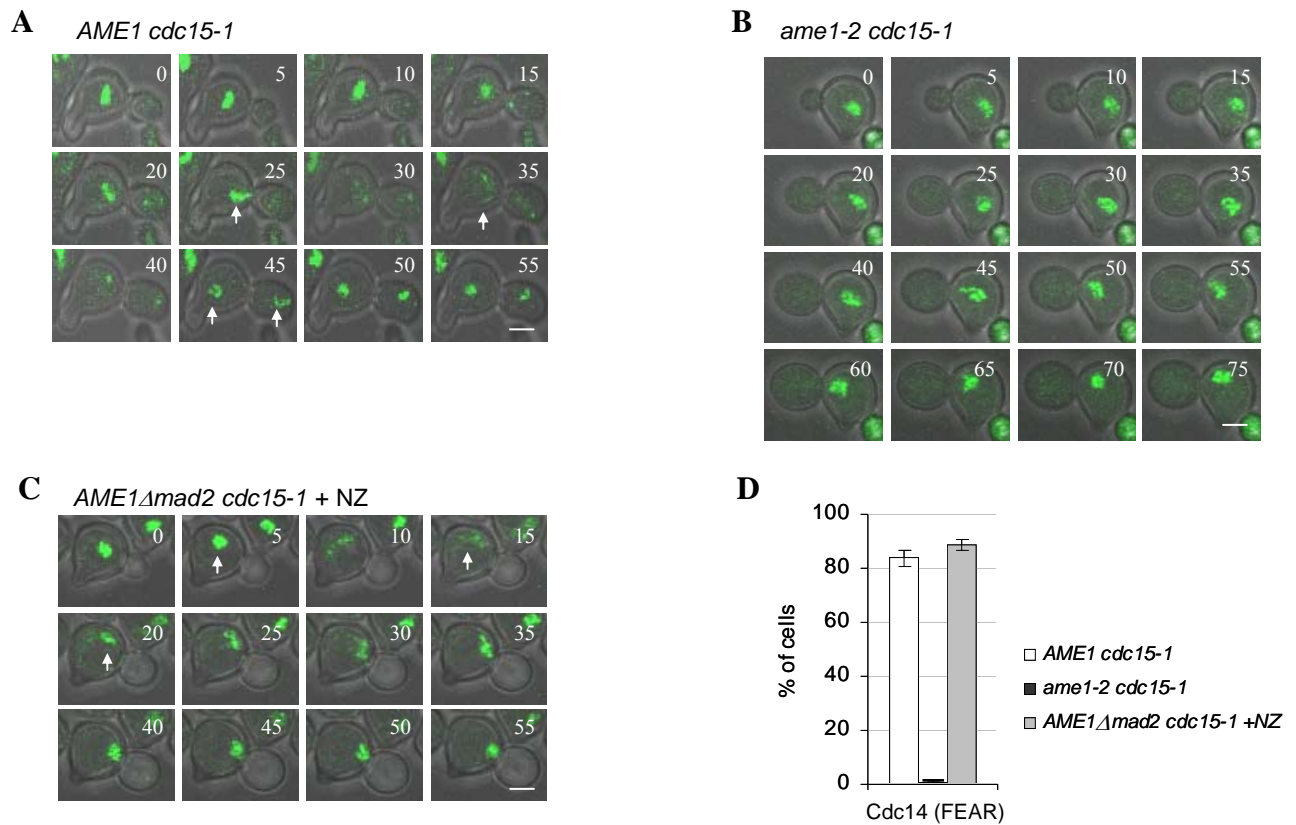


Figure 19. Analysis of FEAR in the *ame1-2* mutant strain.

All experiments were performed in a *cdc15-1* background to omit induction of MEN. Cells with GFP-tagged Cdc14 were arrested in G1 with alpha factor at RT and released into medium at 37°C. Time-lapse sequences were recorded in 60 sec intervals by scanning through 5 z stacks. For all pictures maximal intensity projections were calculated. Depicted are images of exemplary cells collected in 5 min intervals after the appearance of a small sized bud (time 0). Arrows indicate the disappearance and reappearance of a nucleolar Cdc14-GFP signal. Bar, 2 μ m.

(A) *Cdc14* release in wild type cells.

(B) Nucleolar *Cdc14* release is abolished in *ame1-2*.

(C) *Cdc14* release in an *AME1Δmad2* strain released into medium supplemented with 15 μ g/ml nocodazole.

(D) Quantification of A-C. At least 50 cells were counted.

Retention of the Cdc14 signal in the mother cell in *ame1-2* indicates that this mutant is unable to distribute its nucleolus. This may reflect the monopolar segregation defect observed in *ame1-2* (see Figure 11). However, this is not the reason why Cdc14 could not be released from the nucleolus in *ame1-2*, since a wild type strain depleted of the checkpoint protein Mad2 and treated with nocodazole was able to induce FEAR. Nocodazole interferes with DNA separation by the depolymerisation of microtubules, thus keeping the nucleolus in the mother. The additional removal of Mad2 inactivates the spindle assembly checkpoint (activated by missing occupancy in presence of nocodazole) and thus allows activation of FEAR. Under these circumstances, Cdc14 was released from the nucleolus of the mother in more than 90% of the cells (Figure 19C and 19D). Hence, a persistence of the nucleolus in the mother does not interfere with a transient release of Cdc14. The observed FEAR defect of *ame1-2* is therefore not a consequence of the monopolar distribution of the nucleolus in this strain.

Taken together, the *ame1-2* mutant allele interferes with a nucleolar release of Cdc14 in early anaphase. Inactive Cdc14 may thus contribute to the spindle defect observed in *ame1-2*.

2.1.5.3.2 Tension-like activation of the spindle assembly checkpoint prevents FEAR induction

The FEAR defect in *ame1-2* may either be attributed to a defective kinetochore *per se* or to the observed activation of the spindle assembly checkpoint (see Figure 13). In order to investigate the latter, the Cdc14 release in cells depleted of cohesion protein Scc1 was analyzed. Kinetochore in this strain are undamaged and able to attach to microtubules. However, in lack of cohesion no tension is build up between sister chromatides. In absence of Scc1 (in absence of tension) no Cdc14 release was observed (Figure 20A). Accordingly, loss of tension can abolish an induction of FEAR. Also the failure in FEAR induction of *ame1-2* may therefore result from loss of tension at the mutant kinetochore.

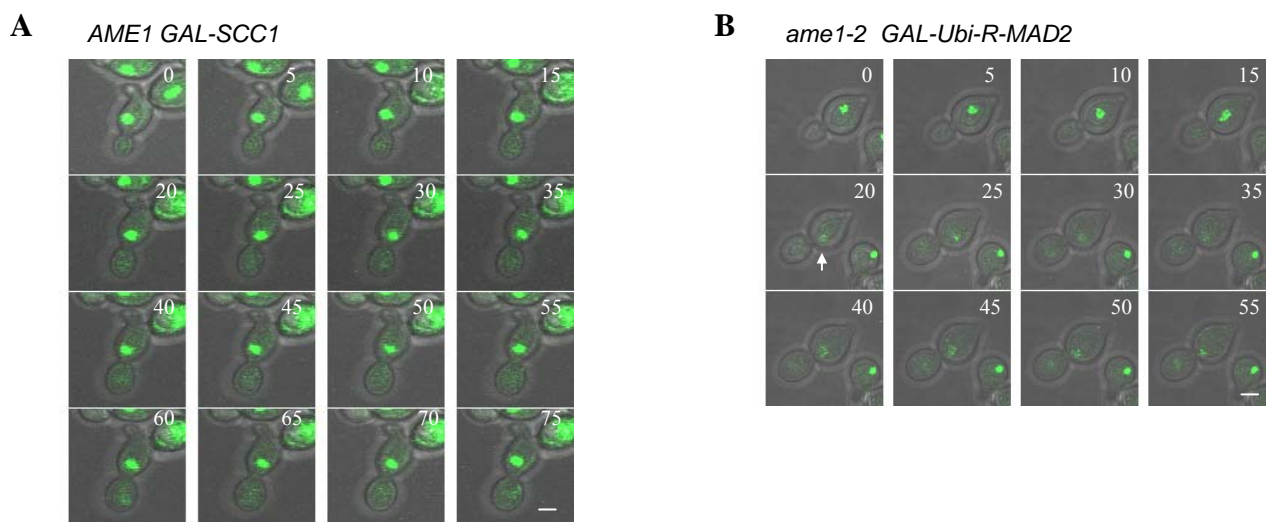


Figure 20. FEAR in wild type cells depleted of Scc1 and *ame1-2* cells depleted of Mad2.

- (A) *Failure in the Cdc14 release of Scc1 depleted cells.* Scc1 gene expression was repressed during a 5 h alpha factor arrest at RT and cells released into glucose containing medium at 37°C. The localization of Cdc14-GFP was determined by fluorescence microscopy. The experiment was performed in a *cdc15-1* background to omit induction of MEN. Time-lapse sequences were recorded in 60 sec intervals by scanning through 5 z stacks. For all pictures maximal intensity projections were calculated. Depicted are images of exemplary cells collected in 5 min intervals after the appearance of a small sized bud (time 0). Bar, 2 μ m.
- (B) *Cdc14 release in Mad2 depleted *ame1-2* cells.* Depletion of Mad2 was achieved during 12 h growth in glucose containing medium at RT. After a 3 h arrest with alpha factor in G1, cells were released into medium at 37°C. Video microscopy was performed as in (A). Mad2 depletion was verified by immunoblotting (see Figure 22C).

A contribution of an active spindle assembly checkpoint to the failure in FEAR induction observed in *ame1-2* is also supported by the analysis of a mutant strain depleted of Mad2. Checkpoint inactivation led to a nucleolar release of Cdc14 in 90% of these cells (Figure 20B). However, it remains unclear why FEAR is permanently inactive in *ame1-2*, since the spindle assembly checkpoint is only temporarily activated in this mutant (Pds1 degradation is only delayed, see Figure 13A) and also Esp1 activation eventually occurs (see below; 2.1.5.3.6). FEAR induction might only be possible during a very short period in mitosis. Once this time point has been passed, no further activation of FEAR may take place.

2.1.5.3.3 Cdc14 overexpression does not rescue anaphase spindle formation in *ame1-2*

As previously mentioned one of the causes for the spindle defect in *ame1-2* mutant cells could be the spindle formation in presence of low Esp1 and Cdc14 activity. It has recently been reported that defects in spindle formation due to spindle pole body separation in presence of low Esp1 activity can be rescued by overexpression of Cdc14 (Higuchi and Uhlmann, 2005). The corresponding strain Y1539 allows cohesion cleavage by an inducible TEV protease in presence of low Esp1 levels (Cdc20 depletion). Under these conditions spindle pole body separation is induced in presence of high Pds1 levels (low Esp1 activity). This leads to defects in spindle formation. However, Cdc14 overexpression in this strain is able to rescue the spindle defect. If the *ame1-2* spindle defect is only caused by an inactive FEAR due to a slight activation of the spindle assembly checkpoint, than overexpression of Cdc14 should also be able to rescue the spindle defect in the mutant strain. The *ame1-2* allele was genomically integrated into the Y1539 strain resulting in YAW988. As will be described later in more detail, the establishment of bipolar attachments prior to the induction of the *ame1-2* mutation allows for spindle formation (see 2.1.5.3.8). In order to circumvent this and also to ensure that both strains enter anaphase from a common defined point in the cell cycle, both strains were arrested in metaphase by the addition of nocodazole (induces microtubule depolymerization) and subsequently shifted to 37°C. Only Y1539 was depleted of Cdc20 during the nocodazole arrest. Both strains were released from the metaphase arrest by nocodazole washout. At the same time sister chromatide separation was induced by expression of Esp1. Furthermore Cdc14 overexpression was initiated one hour prior to the release from metaphase. As a consequence of Cdc20 depletion the control strain (Y1539) separates spindle pole bodies in presence of persistently high Pds1 levels (low Esp1 activity). In contrast, the Pds1 concentration does decline in the *ame1-2* strain (YAW988), although in a delayed manner as compared to an *AME1* wild type strain (see Figure 13A). Whereas 80% of control cells were able to polymerize anaphase spindles, spindle formation was only observed in less than 10% of *ame1-2* mutant cells (Figure 21A). Thus, an overexpression of Cdc14 is insufficient to rescue the *ame1-2* spindle defect. Accordingly, absence of Cdc14 activity due to low Esp1 activity cannot account for the *ame1-2* spindle phenotype.

To further confirm the above findings, spindle formation in presence of a Sli15(6A) variant was analyzed. It has previously been reported that dephosphorylation of Sli15 by Cdc14 leads to the localization of the Sli15-Ipl1 complex to the spindle midzone where both proteins may contribute to spindle stabilization (Pereira and Schiebel, 2003). If the spindle defect in *ame1-2* resulted from a mislocalization of Sli15 (due to lacking Cdc14 activity), than expression of a Sli15 variant whose midzone localization is independent of Cdc14 (Sli15(6A)), may be able to restore spindle formation in *ame1-2*. However, even in the presence of constitutively dephosphorylated Sli15, spindle formation was only observed in 20% of *ame1-2* cells (Figure 21B). In contrast, anaphase spindles were polymerized in over 90% of wild type cells.

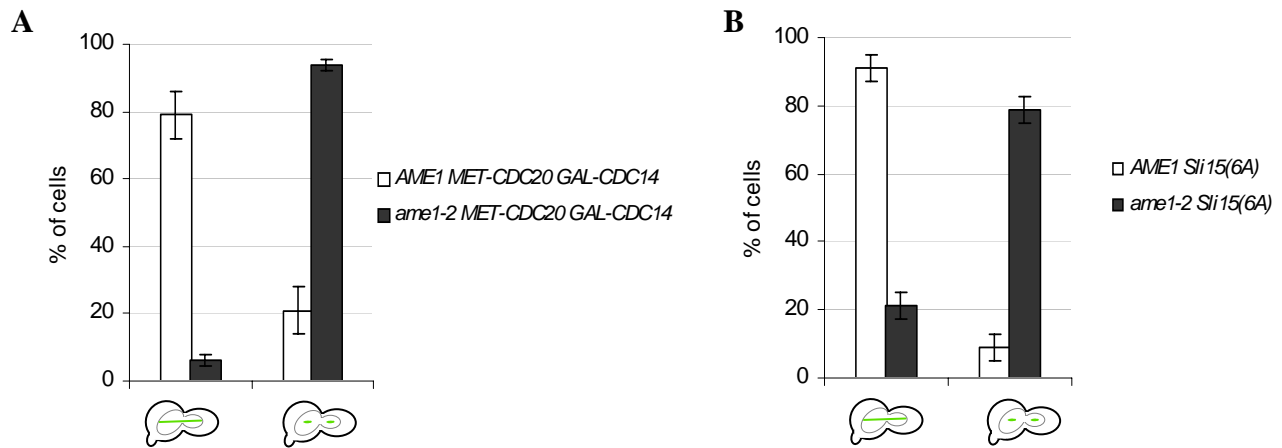


Figure 21. Overexpression of Cdc14 does not restore anaphase spindle formation.

- (A) *Cdc14* overexpression. The *MET-CDC20 GAL-CDC14* (Y1539) strain was grown o/n in medium containing raffinose and lacking methionine. Cells were arrested by the addition of 2 mM methionine for 3 h at RT, shifted to 37°C in the presence of 15 µg/ml nocodazole for 3 h and released into medium containing 3% galactose without nocodazole to induce TEV expression. The *ame1-2* (YAW988) strain in the same background was arrested with nocodazole for 3 h at RT, shifted to 37°C in the presence of 15 µg/ml nocodazole for 3 h and released into medium containing 3% galactose without nocodazole to induce TEV expression. Cdc14 expression was induced 1 h prior metaphase release. The spindle integrity was analyzed by GFP marked tubulin.
- (B) *Influence of dephosphorylated Sli15 on spindle morphology.* Cells were arrested with alpha factor and released into medium at 37°C. Spindle integrity was analyzed after 180 minutes by GFP marked tubulin.

These results indicate that neither Cdc14 nor its substrate Sli15 are responsible for the spindle defect in *ame1-2*. Thus, although FEAR is impaired in *ame1-2*, it cannot be the sole cause for the aberrant spindle phenotype.

2.1.5.3.4 Inactivation of checkpoint protein Mad2 partially rescues the spindle defect of *ame1-2*

Even though overexpression of Cdc14 could not rescue the spindle defect in *ame1-2*, this phenotype may still be attributed to a partial activation of the spindle assembly checkpoint. Low Esp1 activity does not only interfere with Cdc14 release by FEAR, but may also directly influence spindle stability through its midzone localization (Higuchi and Uhlmann, 2005; Jensen et al., 2001). In order to abolish the activation of the spindle checkpoint, *ame1-2* was depleted of checkpoint protein Mad2. In absence of Mad2 cells are not able to maintain elevated Pds1 levels and thus precociously activated Esp1, despite the defective *ame1-2* kinetochore. Depletion of Mad2 was achieved by placing the *MAD2* gene under the control of a repressible *GAL* promoter followed by an ubiquitine and a single arginine residue, and by growing the cells for 12 hours in glucose containing medium. Following a three hours alpha factor arrest, cells were subsequently released at 37°C into fresh medium containing glucose and analyzed for the integrity of the anaphase spindle (Figure 22). Depletion of Mad2 was verified by immunoblotting and FACS analysis. Twelve hours after Mad2 removal no protein signal could be detected (Figure 22C). Also the loss of the 2N peak after 3 hours

post G1 release and the appearance of cells with a DNA content greater than 2N in presence of nocodazole indicated that Mad2 had been successfully removed (Figure 22D).

Deletion of Mad2 could partially rescue the polymerization defect of anaphase spindles in *ame1-2* (Figure 22B). Anaphase spindle formation was increased from 13% to 50% in absence of Mad2. However, wild type-like anaphases were only observed in 7% of the cells whereas the remaining 44% displayed only weak anaphase spindles (Figure 22A and B). This result indicates that elevated Pds1 levels, due to a partial activation of the spindle assembly checkpoint, play only a subordinate role in the spindle defect of *ame1-2*.

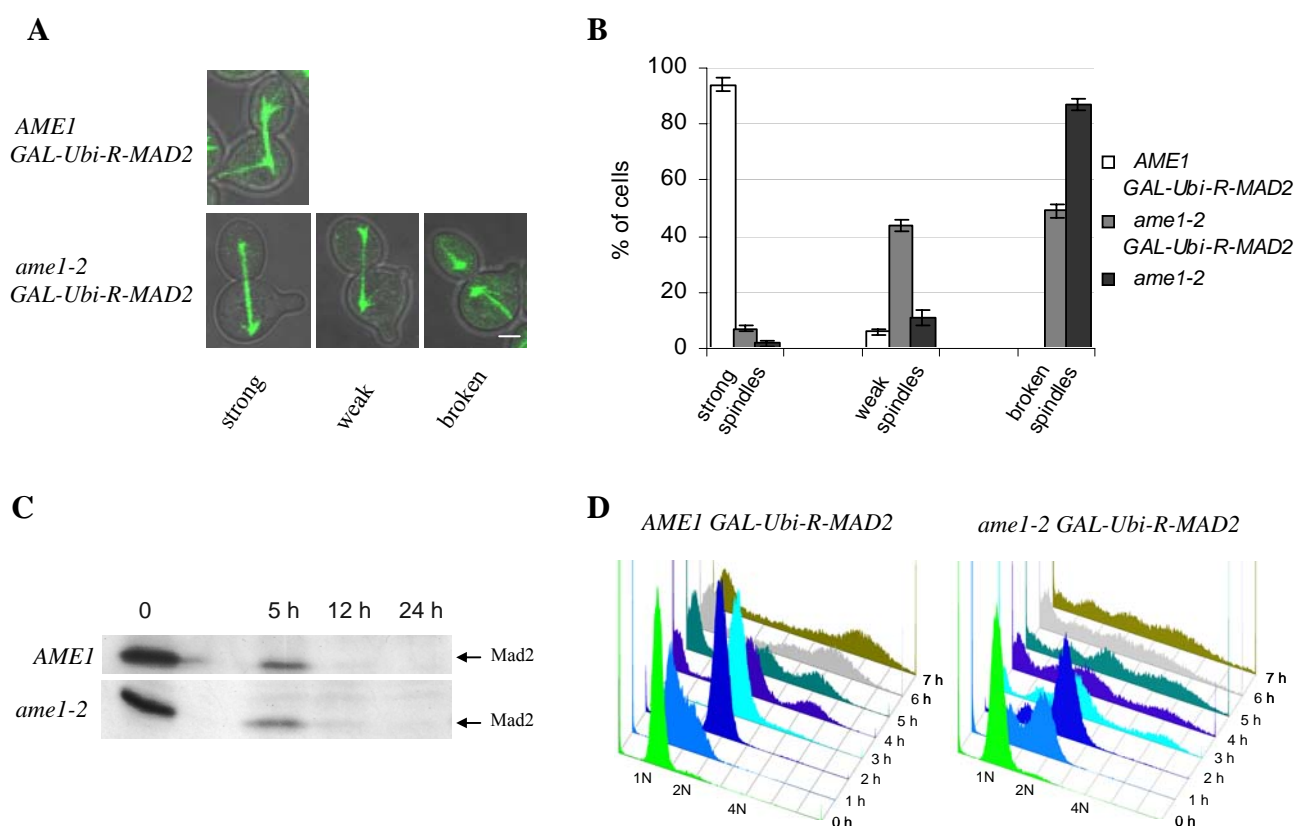


Figure 22. Mad2 depletion partially rescues anaphase spindle formation in *ame1-2*.

- (A) Examples of anaphase spindles in wild type and *ame1-2* cells depleted of Mad2. Depletion of Mad2 was achieved during 12 h growth in glucose containing medium at RT. After a 3 h arrest with alpha factor in G1, cells were released into medium at 37°C. Spindle integrity was analyzed after 165 min by fluorescence microscopy of GFP-Tub1. Bar, 2 μ m.
- (B) Quantification of anaphase spindles from (A).
- (C) Depletion of Mad2 verified by immunoblotting. Depletion of Mad2 during growth in glucose containing medium at RT. Aliquots were taken at indicated time points and analyzed by immunoblotting (anti-Mad2).
- (D) Depletion of Mad2 verified by FACS analysis. Same experimental setup as in (A) but cells were released at RT from the alpha factor arrest ($t=0$). Aliquots were taken at indicated time points and analyzed for their DNA content by FACS.

2.1.5.3.5 Overexpression of Esp1 in *ame1-2* allows for a partial rescue of anaphase spindles

Defective spindles formed in presence of elevated Pds1 levels can either be rescued by an increase in the amount of Cdc14, or by overexpression of Esp1 (Higuchi and Uhlmann, 2005). To verify this published data, a wild type strain with Cdc20 under the control of a repressible promoter and Esp1 under that of an inducible promoter was constructed (*AME1 MET-CDC20 GAL-ESP1*). Depletion of Cdc20 in the wild type strain leads to a metaphase arrest from which cells can be released by overexpression of Esp1 (cohesion cleavage). This effect is irrespective of Pds1. Additionally, an inducible promoter was also introduced in front of the *ESP1* gene in the *ame1-2* mutant strain (*ame1-2 GAL-ESP1*). Finally, also the *ame1-2* mutant alone was analyzed. In order for all strains to enter anaphase from a defined point in the cell cycle, a metaphase arrest by addition of nocodazole was performed. In the control strain (*AME1 MET-CDC20 GAL-ESP1*) Cdc20 was additionally depleted. Subsequent to the metaphase arrest, all strains were shifted to 37°C to induce the *ame1-2* mutation. Induction of Esp1 expression was performed with galactose during the last hour of this incubation. Cells were then released from the metaphase arrest by nocodazole washout and the spindle morphology was visualized with GFP-Tub1 (Figure 23).

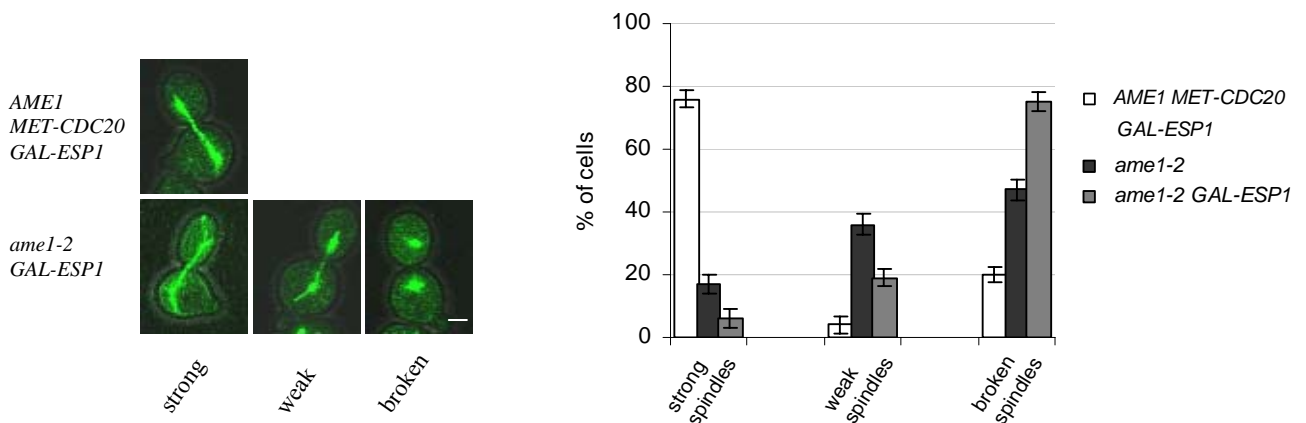


Figure 23. Overexpression of Esp1 partially rescues anaphase spindles in *ame1-2*. The *AME1 MET-CDC20 GAL-ESP1* strain was grown o/n in raffinose containing medium lacking methionine. It was arrested by the addition of 2 mM methionine for 3 h at RT, shifted to 37°C in the presence of 15 µg/ml nocodazole for 3 h, and released into medium containing 3% galactose. The *ame1-2* strains were grown o/n in medium containing raffinose, arrested at RT for 3 h with nocodazole, shifted for another 3 h to 37°C and released into medium containing 3% galactose. In all 3 strains Esp1 expression was induced 1 h prior to metaphase release. Spindle integrity was analyzed with GFP-Tub1. At least 100 cells were counted.

Interestingly, although the degradation of Pds1 is only delayed in *ame1-2*, an overexpression of Esp1 did not allow for a comparable rescue of spindle formation as in the *AME1 MET-CDC20 GAL-ESP1* strain, although the latter is characterized by permanently high Pds1 levels. Under these conditions anaphase spindle formation was observed in 80% of *AME1 MET-CDC20 GAL-ESP1* cells (Figure 23).

In contrast overexpression of Esp1 in *ame1-2* increased the total number of cells with anaphase spindles from 25% to only 53%, with the majority of the spindles being weaker than in a corresponding wild type strain. Accordingly, overexpression of Esp1 only partially rescues anaphase spindle formation in *ame1-2*, and the slight activation of the spindle assembly checkpoint in *ame1-2* cannot be the sole cause for the observed defect.

2.1.5.3.6 The spindle defect in *ame1-2* cannot be attributed to lacking Esp1 activity

As previously demonstrated a temporal activation of the spindle assembly checkpoint interferes with the induction of FEAR (see 2.1.5.3.2 and Figure 20). Since Esp1 does not only promote spindle formation through the activation of FEAR but can also accomplish this alone through its localization to the spindle (Jensen et al., 2001), the activation of this protein in *ame1-2* was investigated. Esp1 activity can be analyzed by the cleavage of its substrates Scc1 or Slk19 (Uhlmann et al., 1999; Zeng et al., 1999; Sullivan et al., 2001). In contrast to Scc1 cleavage, cleavage of Slk19 results in the formation of a stable product. Esp1 activity was thus monitored by the proteolytic cleavage of Slk19. Cells with myc-tagged Slk19 were arrested with alpha factor and released into medium at 37°C. Aliquots were taken every 20 minutes and the cleavage pattern of Slk19 was analyzed by immunoblotting (Figure 24, lower panel). The cleavage product visible at the beginning of the analysis represents the fragment left from the preceding cell cycle. During the following synthesis phase full length Slk19 is formed and subsequently cleaved by Esp1. Whereas the C-terminal fragment of Slk19 appears after 120 minutes in wild type cells, its occurrence is delayed by about 40 minutes in *ame1-2*. This coincides with the delayed degradation of Pds1 in the mutant (see Figure 13) and thus may be attributed to the slight activation of the spindle attachment checkpoint.

To determine if the *ame1-2* spindle defect is due to a premature separation of spindle pole bodies in absence of Esp1, cleavage of Slk19 was correlated with the distances between the spindle poles (Figure 24). A typical metaphase spindle has a length of about 2 μm . However, to ensure that anaphase had been initiated, only distances between spindle poles greater than 3 μm were considered. In wild type cells proteolytic cleavage of Slk19 occurs approximately 120 minutes after the alpha factor release. This coincides with the separation of spindle poles. In *ame1-2* both, the separation of spindle poles and Slk19 cleavage are delayed in respect to wild type. Noteworthy, in about 35% of *ame1-2* cells spindle pole body separation precedes an activation of Esp1 (compare 140 and 160 minutes time points). These 35% represent cells that separate spindle poles in absence of active Esp1. However, when Esp1 is activated (160 to 180 minutes) the number of cells with spindle pole bodies separated by more than 3 μm is further increased by about 40%. These additional cells separate their poles while Esp1 is active. Nevertheless, they still exhibit defects in spindle formation. Therefore, the absence of Esp1 activity cannot be the sole cause for the spindle defect.

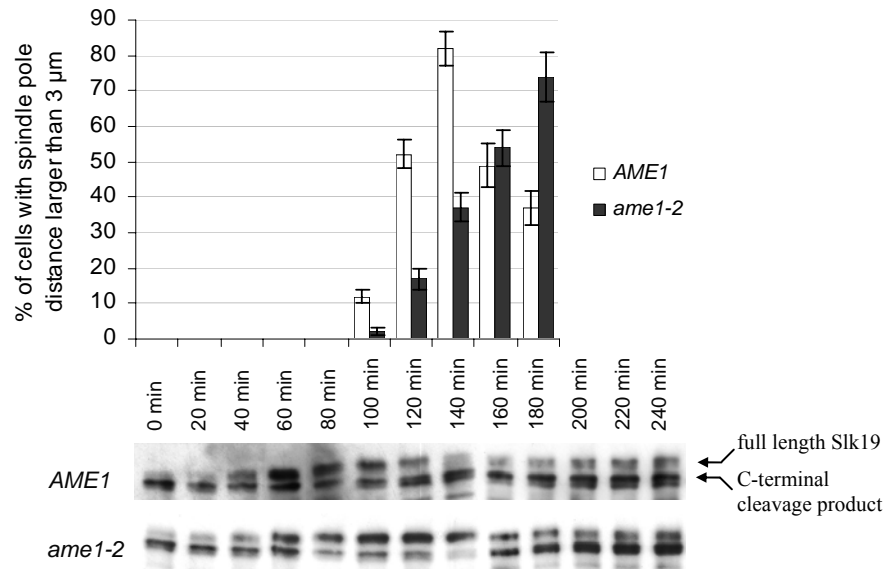


Figure 24. Separation of spindle pole bodies and proteolytical cleavage of Slk19 in *ame1-2*. Cells with GFP-Tub1 were released from an alpha factor arrest at 37°C and analyzed for the distance between the two SPB signals. At least 100 cells were counted. To determine the cleavage of Slk19, cells with myc-tagged Slk19 were also released from alpha factor arrest at 37°C. Aliquots were taken every 20 min and analyzed by immunoblotting. Note that the C-terminal cleavage product of Slk19 visible at the beginning of the analysis represents the fragment left from the preceding cell cycle.

2.1.5.3.7 The *ame1-2* spindle defect already occurs when spindle pole separation resembles a metaphase

Spindle defects can either arise during initial polymerization in metaphase or during spindle elongation in anaphase (Saunders and Hoyt, 1992; Scharfenberger et al., 2003; Janke et al., 2002; Cheeseman et al., 2001). To determine at which point in the cell cycle the spindle defect in *ame1-2* occurs, spindle formation was followed by fluorescence microscopy (Figure 25). Whereas 100% of wild type cells displayed a metaphase spindle, spindle formation was strongly impaired in *ame1-2*. The majority of the mutant cells displayed two separated spindle poles without a connecting metaphase spindle. At a pole distance of 1.5 μm, more than 80% of these cells had defective spindles. The same was also observed at distances of 2 μm and 2.5 μm. Thus, the spindle defect in *ame1-2* can occur when the distance between the poles resembles that of at metaphase spindle.

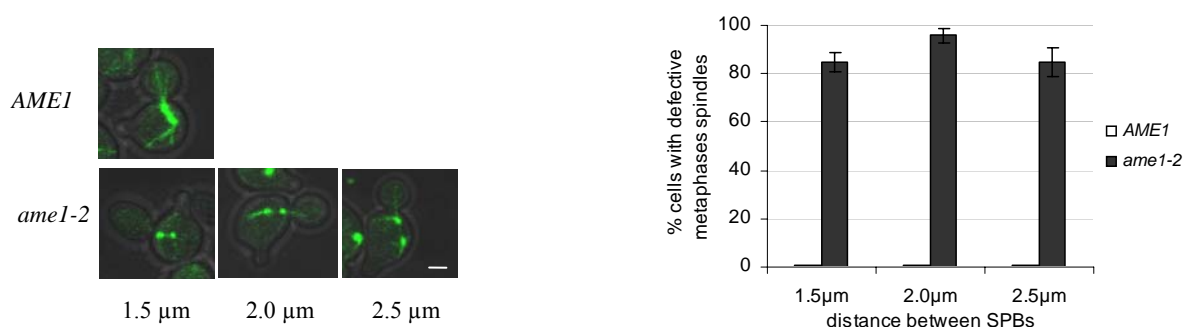


Figure 25. The *ame1-2* mutant displays a spindle defect at a metaphase spindle length. Cells with GFP-tagged tubulin were alpha factor arrested and shifted to 37°C. The distance between the spindle pole bodies was determined. The percentage of cells with defective spindles at pole distances of 1.5 μm, 2 μm, and 2.5 μm was analyzed. More than 70 cells for each distance were counted. Bar, 2 μm.

2.1.5.3.8 Establishment of bipolar attachments prior to the induction of *ame1-2* leads to the formation of stable anaphase spindles, despite defective kinetochores

To further confirm that the spindle defect in *ame1-2* is evoked at a metaphase spindle length, the mutant was arrested in metaphase by Cdc20 depletion prior to the induction of the *ame1-2* mutation. Spindle formation was analyzed by fluorescence microscopy (Figure 26). Surprisingly, under these experimental conditions an intact metaphase spindle was observed in 96% of *ame1-2* cells. Accordingly, a metaphase spindle formed at permissive temperature is maintained also during the subsequent induction of the *ame1-2* mutation.

Furthermore, when the *ame1-2* mutant cells were released from the metaphase arrest by expression of Cdc20, also normal anaphase spindles were formed (Figure 26). Notably, this experiment was performed in a *cdc15-1* background (inhibits mitotic exit) in order to distinguish between spindle defects and spindle depolymerization due to mitotic exit. Anaphase spindle formation was observed in over 75% of *ame1-2* cells under these conditions. The remaining cases may reflect spindle depolymerization due to leakiness of the *cdc15-1* allele, since also in the corresponding *AME1* control strain only 85% of the cells were able to form intact anaphase spindles.

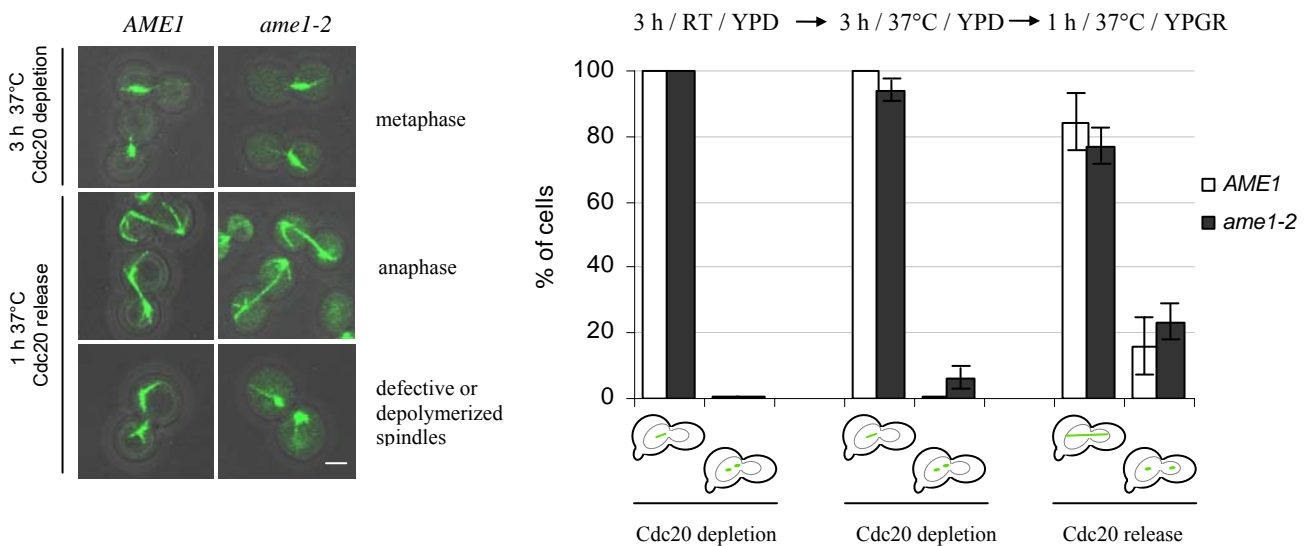


Figure 26. A preceding Cdc20 arrest allows for spindle formation in *ame1-2*. Cells with *CDC20* under the control of a *GAL* promoter were arrested for 3 h at RT in medium containing glucose and shifted to 37°C for another 3 h. Expression of Cdc20 was re-induced with galactose medium. The spindle integrity was analyzed by GFP marked tubulin 3 h after the metaphase arrest at RT, 3 h after the shift to 37°C, and 1 h after re-induction of Cdc20. Bar, 2 μ m.

Pre-arresting *ame1-2* cells in metaphase apparently has a beneficial influence on spindle formation. It can therefore be asked if the establishment of bipolar attachment prior the induction of the *ame1-2* mutation has also a positive influence on the defective kinetochore. To address this question, the activation of the spindle assembly checkpoint, segregation of sister chromatides and the induction of FEAR were analyzed.

A. The spindle assembly checkpoint is activated in *ame1-2* cells pre-arrested in metaphase

When the *ame1-2* mutation was induced after a metaphase arrest and cells were subsequently released from this block by expression of Cdc20, the degradation of Pds1 was delayed in comparison to the wild type control (Figure 27). Thus, *ame1-2* released from a metaphase arrest induced prior to the mutation exhibits a similar spindle assembly checkpoint response as *ame1-2* cells released immediately from G1 at the restrictive temperature (see Figure 13A). This indicates that kinetochores are still defective under these conditions, since they lead to an activation of the spindle checkpoint. Furthermore, spindle elongation in presence of a slight activation of the spindle assembly checkpoint cannot be the only explanation for the spindle defect in *ame1-2*, as anaphase spindles can be formed in this experiment despite elevated Pds1 levels.

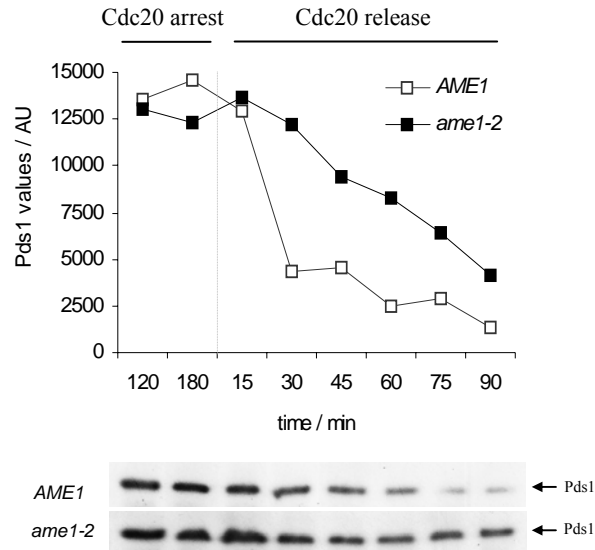


Figure 27. Analysis of Pds1 levels in *ame1-2* after a Cdc20 arrest. Cells with myc-tagged Pds1 were arrested in metaphase at RT by the depletion of Cdc20. They were shifted to 37°C for 3 h and released into medium containing galactose to induce Cdc20 expression (t=0). Aliquots were taken at the indicated time points, protein extracts prepared and the amount of Pds1 determined by immunoblotting (anti-myc). AU, arbitrary units.

B. *ame1-2* cells pre-arrested in metaphase still display a monopolar segregation defect

The analysis of the DNA distribution in *ame1-2* cells pre-arrested in metaphase further confirmed that kinetochores in these cells are still susceptible to defects. Tension at the respective kinetochores was lost (see Figure 10) indicating that the kinetochore interferes with the establishment of a stable bipolar attachment. Upon the release from the Cdc20 arrest, *ame1-2* still exhibited a monopolar segregation defect as severe as without pre-arrest in metaphase (Figure 28; see also Figure 11 for comparison). More than 95% of the *ame1-2* cells were able to segregate their DNA, but sister chromatids were distributed together into either mother (56%) or daughter (33%) cell. Bipolar segregation on the other hand was only observed in 11% of the cells.

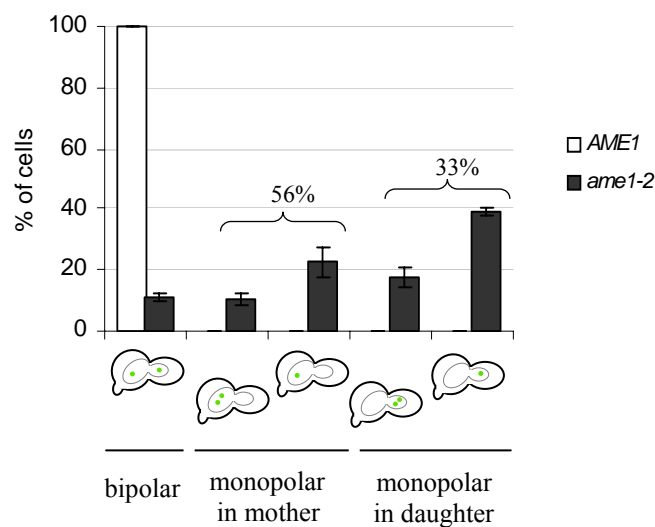


Figure 28. Analysis of sister chromatides segregation in *ame1-2* after a Cdc20 arrest. *CEN5* was tagged with GFP by the tetR/tetO system (Michaelis et al., 1997). Cells were synchronized with alpha factor and arrested in metaphase by Cdc20 depletion at RT. They were subsequently shifted to 37°C and released from metaphase into galactose containing medium. After 1 h DNA distribution was visualized by Hoechst and chromosome segregation followed with *CEN5*-GFP. A total of 100 cells was analyzed.

C. FEAR induction is still abolished in *ame1-2* cells despite a pre-metaphase arrest

Another evidence for a kinetochore defect of *ame1-2* cells released from a pre-metaphase arrest prior to the induction of the mutation was obtained from their inability to release Cdc14 from the nucleolus (Figure 29). Whereas wild type cells were able to induce FEAR 10 minutes after the release from the metaphase arrest, no nucleolar release of Cdc14 was observed in *ame1-2* mutant cells up to 75 minutes after metaphase release. However, as mentioned above, the mutant cells are able to form an anaphase spindle despite an inactive FEAR. This further confirms the previous assumption that lacking Cdc14 activity is not the cause for the spindle defect observed in *ame1-2* mutant cells (see 2.1.5.3.3).

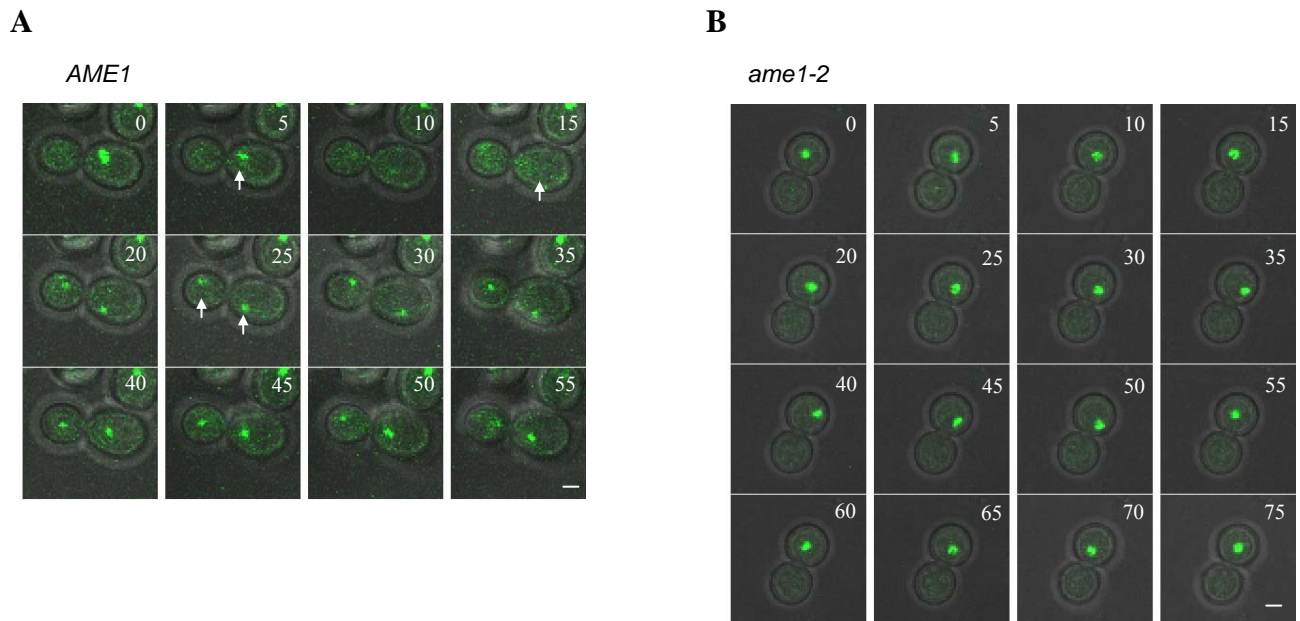


Figure 29. Cdc14 release in *ame1-2* after a previous Cdc20 arrest.

- (A) *Cdc14* release in wild type cells. Cells with *CDC20* under the control of a *GAL* promoter were arrested for 3 h at RT in medium containing glucose and shifted to 37°C for another 3 h. *Cdc20* protein expression was re-induced by medium containing galactose. Localization of *Cdc14*-GFP was followed by fluorescence microscopy. Experiments were performed in a *cdc15-1* background to omit induction of MEN. Time-lapse sequences were recorded in 60 sec intervals by scanning through 5 z stacks. For all pictures maximal intensity projections were calculated. Depicted are images of exemplary cells collected in 5 min intervals after the appearance of a small sized bud (time 0). Bar, 2 µm.
- (B) No *Cdc14* release in *ame1-2* mutant cells. Same experimental setup as in (A).

Finally, it can be conclude that induction of the *ame1-2* mutation after the establishment of bipolar attachment can lead to the formation of anaphase spindles despite the presence of compromised kinetochores. Cells analyzed under these circumstances display mainly the same kinetochore defects as *ame1-2* cells released from a G1 arrest at the restrictive temperature. In both cases, an activation of the spindle assembly checkpoint and a defect in the nucleolar release of *Cdc14* (FEAR) was observed. Additionally, upon induction of the *ame1-2* mutation bipolar attachment was lost during the *Cdc20* arrest and subsequently a monopolar segregation defect was observed when released from the arrest. However, in contrast to the induction of the *ame1-2* mutation prior to the establishment of bipolar attachment, cells pre-arrested in metaphase appear to maintain sufficient bipolar kinetochore-microtubule attachments to prevent separation of spindle poles beyond the length of a metaphase spindle (2µm). Release from the metaphase arrest leads to the formation of stable anaphase spindles. Thus, the spindle-stabilizing event compromised in *ame1-2* may occur either before or during the establishment of bipolar kinetochore-microtubule attachments.

2.1.5.3.9 Kinetochore preformed in absence of tension still cause a spindle defect

Since anaphase spindles can be formed in *ame1-2* cells pre-arrested in metaphase, it remains to be determined if this effect can be attributed to kinetochore pre-assembly at the permissive temperature or to the pre-assembly of a metaphase spindle. To differentiate between these options, cells were arrested in metaphase prior to the induction of *ame1-2* not by Cdc20 depletion, like in the previous experiments, but rather by addition of nocodazole. Nocodazole allows for kinetochore assembly in absence of microtubules. *ame1-2* cells released from the nocodazole arrest at 37°C were unable to polymerize anaphase spindles (Figure 30). Whereas spindle formation was found in 80% of wild type cells, it was only observed in 25% of *ame1-2* mutant cells.

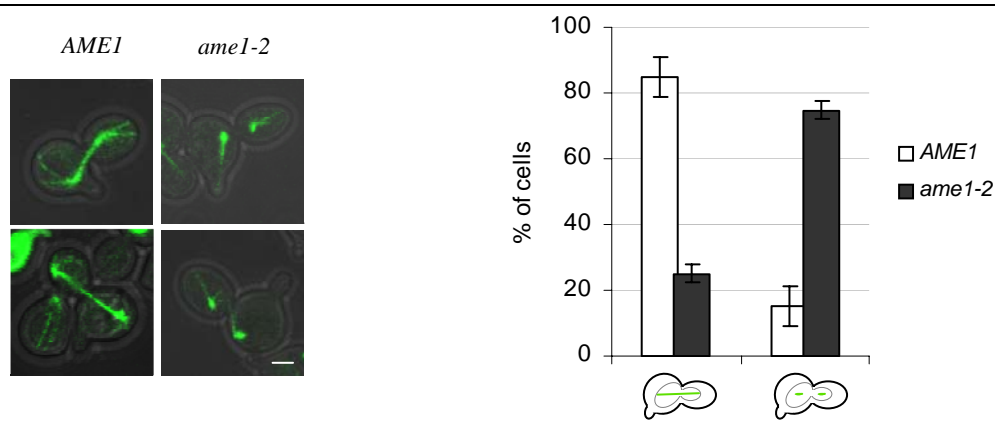


Figure 30. Nocodazole-arrested *ame1-2* cells have defective anaphase spindles. Cells were arrested in metaphase at RT with nocodazole, shifted to 37°C for 3 h and released from the block. Anaphase spindle integrity was analyzed with GFP-Tub1 20 min after the release from the block. Bar, 2 μ m.

Thus, preassembly of kinetochores prior to the induction of the *ame1-2* mutation is not sufficient to allow for spindle formation. It can therefore be speculated that the assembly of a metaphase spindle at the permissive temperature positively influences spindle stability. Alternatively or additionally, bipolar attached kinetochores may be less sensitive towards defects if the *ame1-2* mutation is induced after the bipolar attachment has been established. A similar phenomenon has been reported for the kinetochore protein Nsl1 before (Scharfenberger et al., 2003). Thus, different levels of kinetochore defects may be the reason for the altered phenotype concerning spindle stability and kinetochore function.

2.1.5.3.10 An *ame1-2 ndc80-1* double mutant shows intact anaphase spindles

One other example of spindle formation in presence of an active spindle checkpoint is the kinetochore mutant *ndc80-1*, in which kinetochore-microtubule interactions are abolished (Janke et al., 2002; McClelland et al., 2003). In order to analyze the influence of the *ndc80-1* mutation on the *ame1-2* allele in regard to spindle integrity an *ame1-2ndc80-1* double mutant was constructed. Unfortunately, in contrast to *ame1-2* and *ndc80-1*, the *ame1-2ndc80-1* double mutant does not support the spindle checkpoint anymore (data not shown). Thus, spindle rescue in this strain with wild type like spindles in more than 95% of the cells (Figure 31) may reflect a missing spindle checkpoint. However, this cannot be the reason for the spindle rescue, since an abolishment of the spindle checkpoint in *ame1-2* by deletion of Mad2 or an overexpression of Esp1 only allowed for spindle formation in about 50% of the cells (compare Figure 31 with Figure 22A and B).

Similar to the *ndc80-1* mutant, kinetochore-microtubule interactions are also prevented in the *ame1-2ndc80-1* double mutant (DNA is retained in the mother, Figure 31). Therefore, spindle formation in both mutants may be attributed to the complete detachment of DNA from microtubules. Thus, the monopolar attachment of kinetochores to the spindle in *ame1-2* (Figure 10 and Figure 11) may contribute to the spindle defect observed in this mutant.

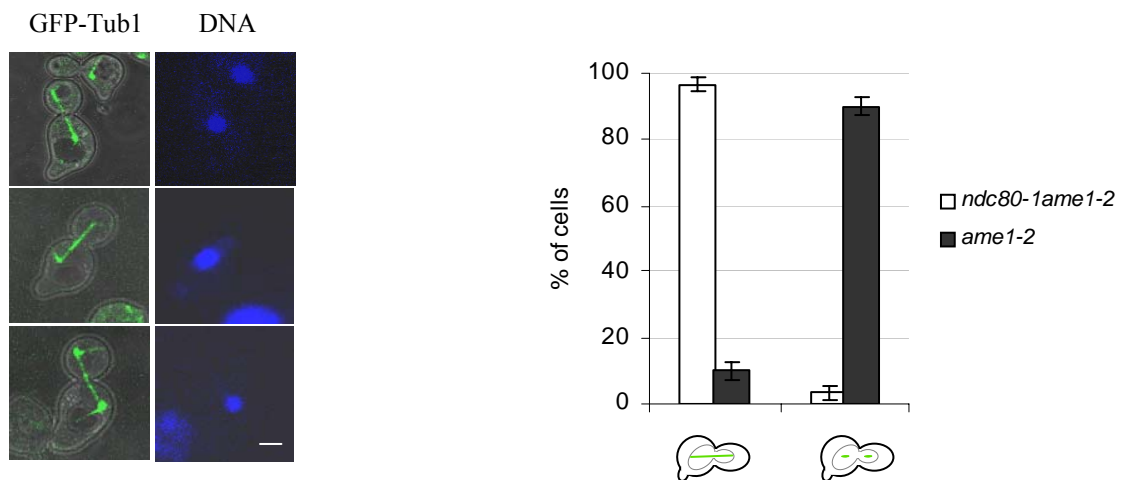


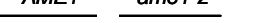

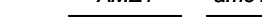
Figure 31. An *ame1-2ndc80-1* double mutant has intact anaphase spindles. Cells with GFP tagged tubulin were arrested in G1 and released at 37°C. The spindle integrity was analyzed after 150 minutes. DNA was stained by Hoechst. Bar, 2 µm.

2.1.6 Influence of the *ame1-2* allele on kinetochore structure

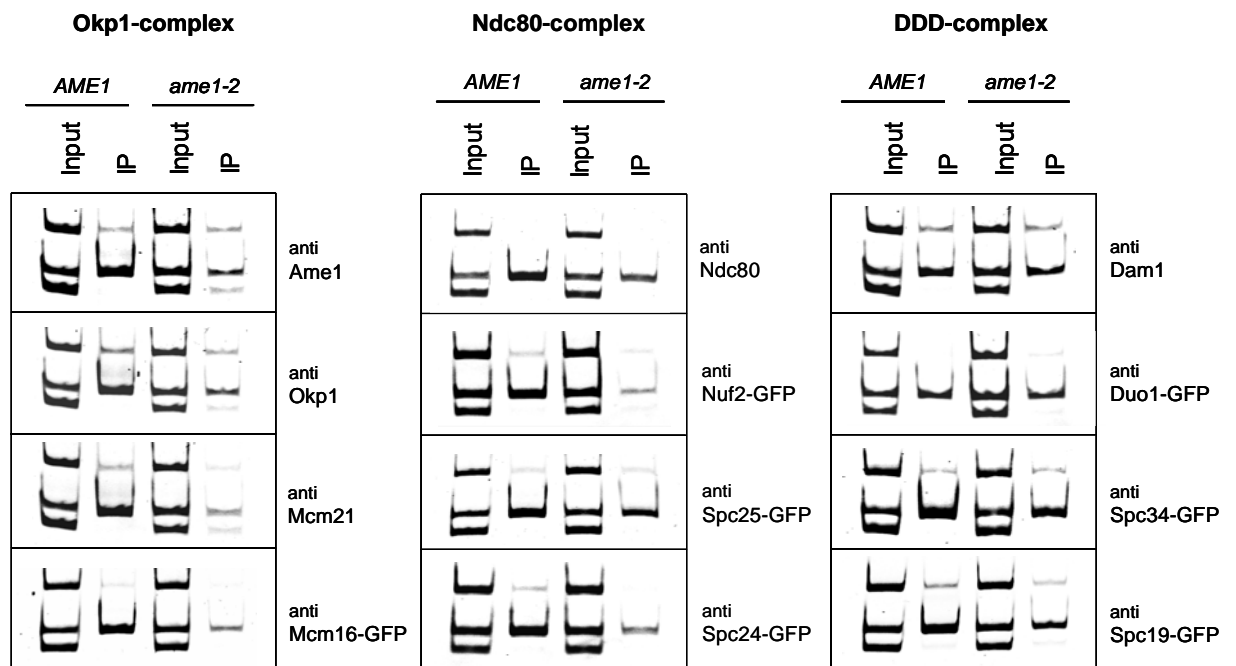
2.1.6.1 Influence of *ame1-2* on the centromere-binding of integral kinetochore proteins

The *ame1-2* allele neither influenced the kinetochore localization of Ndc10 (100%) nor that of Cse4 (100%). Both factors are part of the DNA-binding complex layer. In contrast, *ame1-2* strongly impaired kinetochore association of proteins of its own complex: Okp1 (3%), Mcm21 (3%) and Mcm16 (11%). Also its own association was reduced to 10%. The inner Mtw1 complex was also affected by the *ame1-2* allele as can be deduced from the reduced presence of the Mtw1 (6%) and Nsl1 (17%) proteins. Similarly, also components of the Ndc80 complex were affected: Spc24 (8%), Spc25 (24%), Ndc80 (17%) and Nuf2 (8%). The microtubule associated DDD complex finally was less severely affected than other parts of the kinetochore: Spc19 (31%), Duo1 (40%), Dam1 (36%), Scp34 (58%). This may reflect a potential interaction of the DDD complex with Cse4 or CBF3. However, the DDD complex also interacts with microtubules (Li et al., 2002; Janke et al., 2002), which may also serve to explain the relative higher amounts of this complex at *ame1-2* kinetochores.

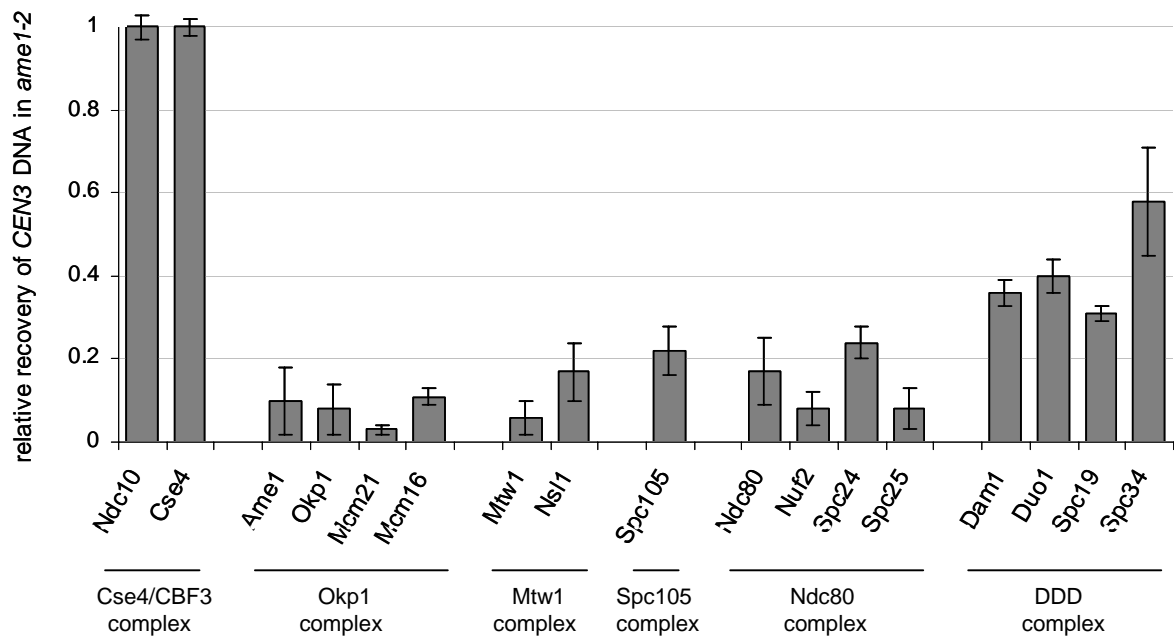
A

Cse4/CBF3-complex				Mtw1-complex				Spc105-complex			
<i>AME1</i>		<i>ame1-2</i>		<i>AME1</i>		<i>ame1-2</i>		<i>AME1</i>		<i>ame1-2</i>	
Input	IP	Input	IP	Input	IP	Input	IP	Input	IP	Input	IP
											

CIII-R →
 CEN3 →
 CIII-L →



B



Accordingly, apart from direct DNA associated components, the kinetochore localization of all analyzed members of the kinetochore is impaired. Thus, the *ame1-2* allele has profound effects on the organization of the kinetochore. These structural alterations may account for the defects observed in the *ame1-2* mutant. The bipolar attachment and monopolar segregation defect of *ame1-2* may be attributed to the reduced kinetochore localization of the Op1, Ndc80 and DDD complex, but not to that of the Mtw1 complex. Increased amounts of the Mtw1 complex at kinetochores still induce monopolar segregation defects (see 2.1.6.3). Although the Ndc80 complex is implicated in spindle checkpoint function (Janke et al., 2001; McClelland et al., 2003) and the localization of all complex members is strongly reduced at the *ame1-2* kinetochore, the checkpoint in *ame1-2* is nevertheless functional. The residual amounts of the Ndc80 complex are therefore sufficient to allow for spindle checkpoint induction. This is in good agreement with published data according to which a reduction of checkpoint proteins Mad1 and Mad2 to 10% is sufficient to activate the spindle checkpoint in mammalian cells (Martin-Lluesma et al., 2002; DeLuca et al., 2003; McClelland et al., 2003).

2.1.6.2 Influence of *ame1-2* on the centromere-binding of kinetochore associated proteins

Next to the already analyzed set of integral kinetochore components, the kinetochore also comprises a number of transiently associated factors. Several of these proteins are important for the stability of the anaphase spindle and translocate from the kinetochore to the spindle at the transition from metaphase to anaphase. Stu1 and Slk19 for example are located at the spindle midzone (Yin et al., 2002; Sullivan et al., 2001; Zeng et al., 1999) and Slk19 is as well implicated in the activation of FEAR (Sullivan et al., 2001). Additionally, Stu1 and Stu2 are involved in the regulation of microtubule dynamics (Yin et al., 2002; Pearson et al., 2003; Severin et al., 2001). Since the *ame1-2* mutant shows defects in anaphase spindle morphology and FEAR, also the kinetochore localization of these proteins was analyzed (Figure 33). In *ame1-2* mutant cells centromeric association of all three proteins was impaired to a similar degree as components of the DDD complex. Whereas kinetochore localization of Stu1 and Slk19 was only reduced to 58% and 57% respectively, Stu2 association was reduced to 27%. Accordingly, also the localization of kinetochore associated proteins is influenced by the *ame1-2* mutant allele, although to a lesser extent than expected. Nevertheless, their reduced presence at the *ame1-2* kinetochore together with their involvement in spindle dynamics may also contribute to the spindle defect in *ame1-2*.

Figure 32. (previous page) *ame1-2* influences the association of individual kinetochore proteins with centromeric DNA.

- (A) *Triplex PCR*. At an OD₅₇₈ of 0.5 cells were shifted for 3.5 h to 37°C and a ChIP assay was performed. Antibodies used for immunoprecipitations are indicated. Each assay was performed at least twice. The presence of *CEN3* DNA and of two flanking sequences (ChIII-R and ChIII-L) was analyzed by triplex PCR. 1/3 of the entire PCR reaction was analyzed on an 8% acrylamide gel.
- (B) *RT-PCR quantification of the ChIPs depicted in (A)*. The amount of the *CEN3* band in input and IP fractions was quantified by RT-PCR using the TagMan method. Samples were analyzed as duplicates in at least two independent runs. Displayed is the relative amount of *CEN3* DNA recovered from *ame1-2* in comparison to wild type. DNA contents were normalized for the difference in the input of the mutant and the wild type. DNA recovery from wild type was set to 1.

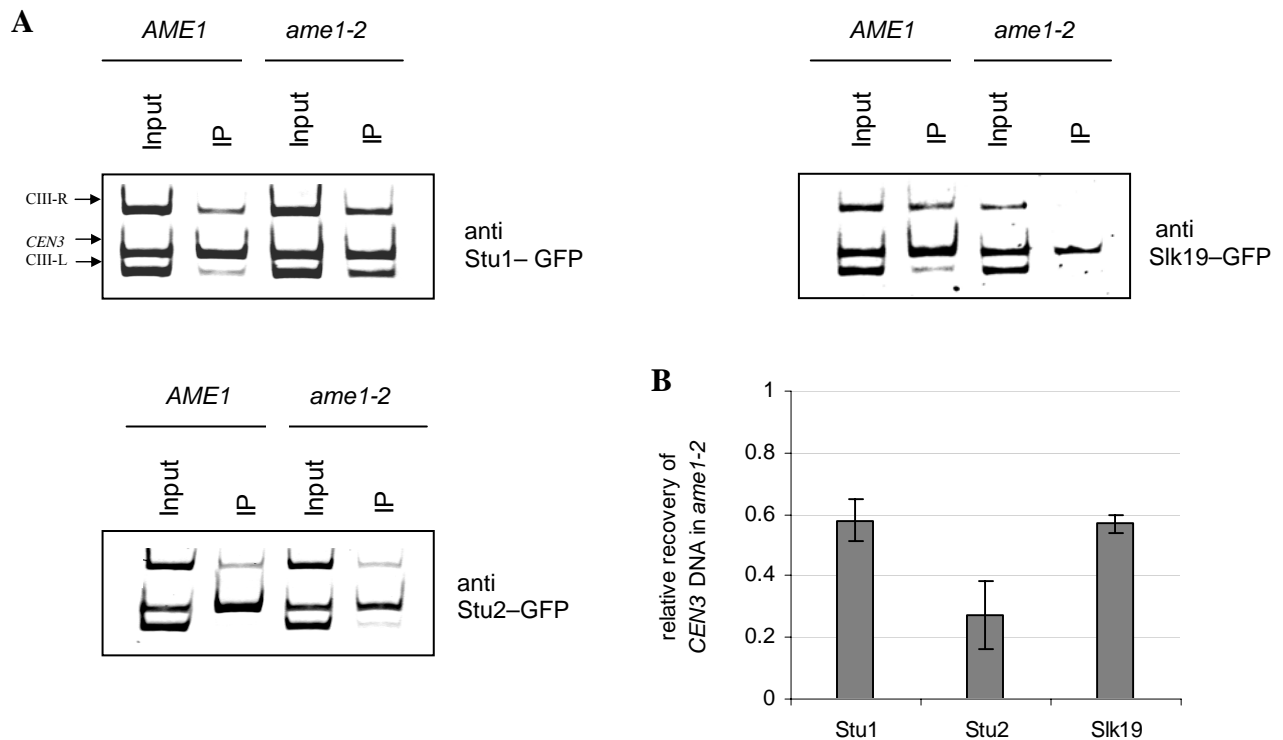


Figure 33. *ame1-2* influences the centromere-binding of kinetochore associated proteins Stu1, Stu2 and Slk19.

- (A) *Triplex PCR*. At an OD_{578} of 0.5 cells were shifted for 3.5 h to 37°C and a ChIP assay was performed. Antibodies used for immunoprecipitations are indicated. Each assay was performed at least twice. The presence of *CEN3* DNA and of two flanking sequences (ChIII-R and ChIII-L) was analyzed by triplex PCR. 1/3 of the entire PCR reaction was analyzed on an 8% acrylamide gel.
- (B) *RT-PCR quantification of the ChIPs depicted in (A)*. The amount of the *CEN3* band in input and IP fractions was quantified by RT-PCR using the TagMan method. Samples were analyzed as duplicates in at least two independent runs. Displayed is the relative amount of *CEN3* DNA recovered from *ame1-2* in comparison to wild type. DNA contents were normalized for the difference in the input of the mutant and the wild type. DNA recovery from wild type was set to 1.

2.1.6.3 Establishment of bipolar attachments prior to the induction of *ame1-2* leads to a less compromised kinetochore structure

As revealed by preceding experiments, a metaphase arrest prior to the induction of the *ame1-2* mutation allowed for a partial rescue of the mutant phenotype. When released from a Cdc20 arrest, *ame1-2* mutant cells were able to form an anaphase spindle despite monopolar DNA segregation and a failure in FEAR induction (see 2.1.5.3.8 and Figure 26 and following). As described, this might reflect a putative change in the structure of the kinetochore as compared to mutant cells released from G1 at the restrictive temperature. To address this, the *ame1-2* mutant was arrested in metaphase by depletion of Cdc20 at room temperature. The arrest was maintained during a subsequent shift to the restrictive temperature and ChIP experiments performed (Figure 34). Also under these conditions the *ame1-2* allele interfered with the centromere association of Okp1 (17%) and Mcm21 (28%). Also the kinetochore localization of Dam1 (36%) was as reduced to a similar extent as before. In contrast, the amounts of Ndc80 (63%) and particularly that of Nsl1 (83%) and Mtw1 (90%) were less severely affected.

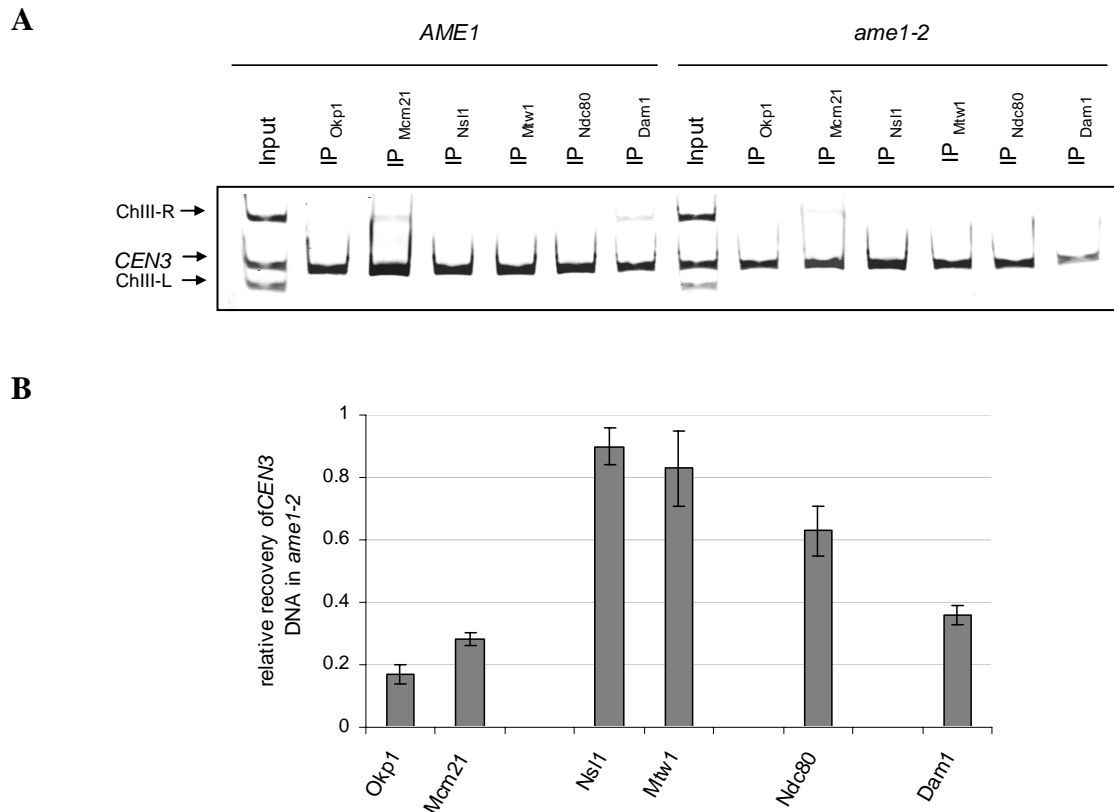


Figure 34. Centromeric DNA association of different kinetochore proteins in a Cdc20 arrested *ame1-2* mutant strain.

- (A) *Triplex PCR.* Cdc20 was depleted in glucose containing medium for 3 h at RT. Cells were subsequently shifted to 37°C and ChIP analysis performed. Antibodies used for immunoprecipitations are indicated. Each assay was performed at least twice. The presence of CEN3 DNA and of two flanking sequences (ChIII-R and ChIII-L) was analyzed by triplex PCR. 1/3 of the entire PCR reaction was analyzed on an 8% acrylamide gel.
- (B) *RT-PCR quantification of the ChIPs depicted in (A).* The amount of the CEN3 band in input and IP fractions was quantified by RT-PCR using the TagMan method. Samples were analyzed as duplicates in at least two independent runs. Displayed is the relative amount of CEN3 DNA recovered from *ame1-2* in comparison to wild type. DNA contents were normalized for the difference in the input of the mutant and the wild type. DNA recovery from wild type was set to 1.

Accordingly, if bipolar kinetochore-microtubule interactions are established at permissive temperature, a subsequent induction of the *ame1-2* mutation has a milder effect on the overall kinetochore structure. This indicates that microtubule-associated kinetochores are protected to a certain extent against the damaging influence of the *ame1-2* allele. The Mtw1 complex in particular becomes independent of the presence of Ame1 and accordingly of the Okp1 complex. Since the kinetochore association of the Mtw1 complex correlates with the ability of the mutant to form stable anaphase spindles, it can be speculated that this complex may play a major role in the regulation of spindle formation.

2.1.6.4 Structural damages of the *ame1-2* kinetochore are not caused by tension and do not require kinetochore assembly during S-phase

Since Amel function is required for stable kinetochore-microtubule interactions, the previously noted defects in the kinetochore structure may result from a tension-induced disruption of the kinetochore. Similar has been postulated for the kinetochore protein Nsl1 (Scharfenberger et al., 2003). To analyze this, ChIP experiments were performed in the presence of a microtubule depolymerizing drug. Cells were alpha factor arrested and released at the restrictive temperature in medium containing nocodazole. For each kinetochore complex the DNA association of two exemplary factors was analyzed (Figure 35). Members of the DDD complex were omitted from the analysis, since their kinetochore association is microtubule dependent (Li et al., 2002; Enquist-Newman et al., 2001). Amongst the tested components only the localization of Ndc10 was not affected in this assay. All other proteins showed a reduced centromere association similar to non-synchronized cells, although microtubules were absent (compare Figure 35 and Figure 32). Only the amount of Ndc80 and Spc24 at the *ame1-2* kinetochore was slightly improved (from about 20% to 45% and from about 20% to 45%, respectively). Therefore, the establishment of tension at kinetochores only moderately contributes to the observed structural defects in *ame1-2*.

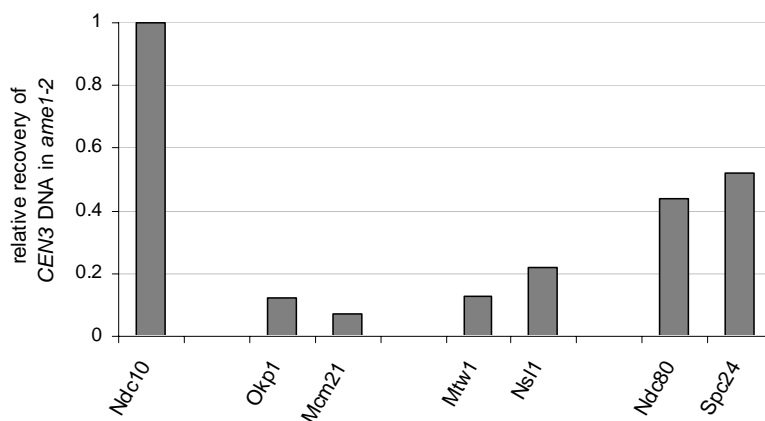


Figure 35. *ame1-2* influences centromere-binding of various kinetochore proteins also in absence of tension.

At an OD₅₇₈ of 0.5 cells were shifted for 3.5 h to 37°C and a ChIP assay was performed. Antibodies used for immunoprecipitations are indicated. The amount of the *CEN3* band in input and IP fractions was quantified by RT-PCR using the TagMan method. Samples were analyzed as duplicates in at least two independent runs. Displayed is the relative amount of *CEN3* DNA recovered from *ame1-2* in comparison to wild type. DNA contents were normalized for the difference in the input of the mutant and the wild type. DNA recovery from wild type was set to 1.

Furthermore, the question arises if the *de novo* assembly of kinetochores is a prerequisite for the structural defects observed in *ame1-2*? To address this, cells were first arrested at room temperature with nocodazole and only thereafter shifted to 37°C. These conditions allow for kinetochore assembly prior to the induction of the *ame1-2* mutation, but did not improve the kinetochore localization of Ndc80 and Spc24 as compared to the previous experiments (data not shown). These results demonstrate that the structural defects of the *ame1-2* kinetochore do not correlate with its *de novo* assembly.

2.2 Biochemical analysis of interactions between individual kinetochore complexes of the central and outer layer

Up to now more than 60 different proteins have been identified in the kinetochore of *S. cerevisiae*. Many of them are functionally organized in complexes or sub-complexes. Five major interaction groups are currently known: the Ndc10, the Mtw1, the Spc105, the Ndc80 and the DDD complex. Their relative location within the kinetochore has been deduced from interactions with DNA or microtubules. Sequential co-purifications and ChIP analysis like those performed for *ame1-2* allowed for conclusions about the hierarchical organization of the kinetochore. However, direct biochemical interactions between isolated kinetochore complexes had not been investigated before. In order to analyze interactions between kinetochore complexes of the central and outer layer *in vitro*, a binding assay based on the tandem affinity purification method of Puig et al., 2001 was established (Figure 36).

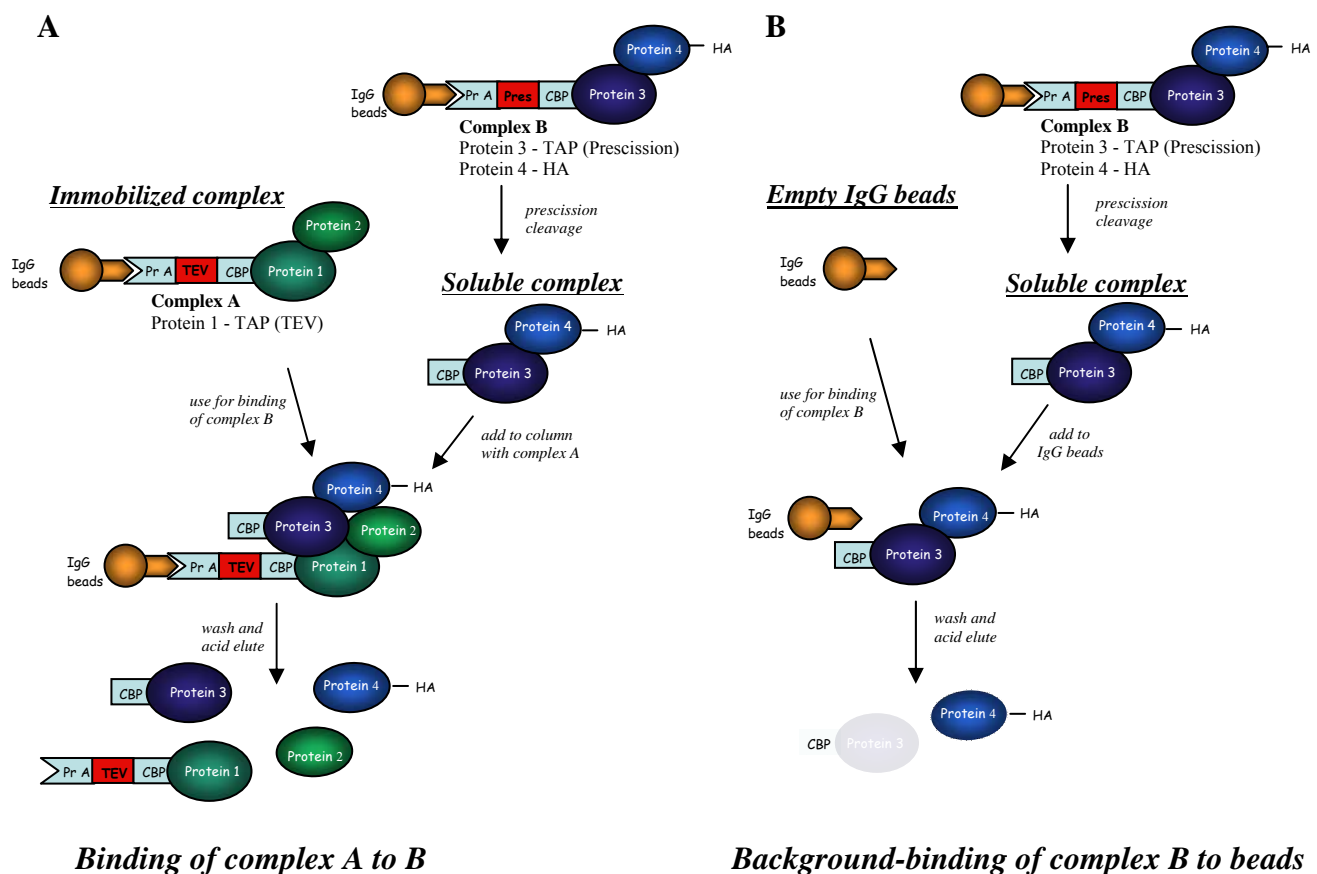


Figure 36. *In vitro* binding assay used for determining kinetochore complex interactions.

- (A) Interaction of affinity-purified kinetochore complex A and B. One component of complex A and one of complex B were TAP-tagged with either a TEV or a prescission protease cleavage site. Additionally, a second component of complex B was HA-tagged to facilitate further detection. Both complexes were individually affinity-purified on IgG Sepharose beads. Whereas complex A was kept immobilized on beads, complex B was solubilized by either TEV or prescission cleavage. Both complexes were subsequently incubated together for 1 h at RT. Beads were washed and samples acid eluted. Binding of complex B to complex A was evaluated by Western analysis of the HA-tagged component of complex B.
- (B) Background binding of soluble complex B to empty IgG beads (negative control). The soluble complex B was also added to empty IgG beads and incubated for 1 h at RT. Beads were subsequently washed and proteins acid eluted to determine non-specific background binding.

2.2.1 The Okp1 complex interacts with the Mtw1 complex

Since mutations in the Ame1 protein, a component of the Okp1 complex, had a strong effect on the kinetochore localization of the Mtw1 complex (Figure 32), the physical interaction between these two complexes was investigated first. Soluble Mtw1 complex was either incubated with immobilized Okp1 complex or empty beads as control (Figure 37A). Interaction between the two complexes was determined after elution by immunoblotting against HA-tagged Dsn1, a component of the Mtw1 complex. This assay revealed a direct physical interaction between the Okp1 and Mtw1 complexes.

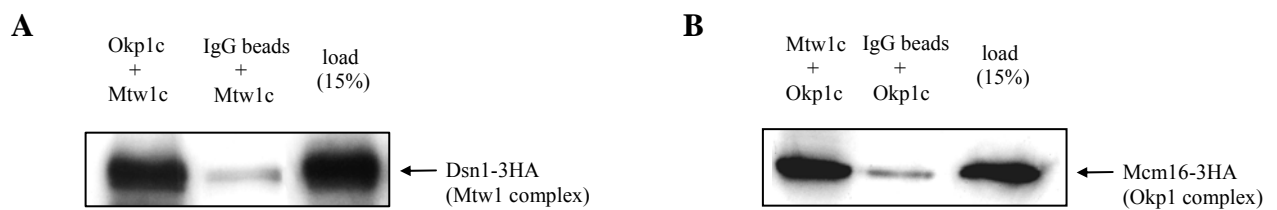


Figure 37. Physical link between Okp1 and Mtw1 kinetochore complexes.

- (A) *Binding of TEV-released Mtw1 complex to immobilized Okp1 complex.* The Okp1 complex and the Mtw1 complex were affinity-purified from 1500 OD of cells via a TAP-tag. The Mtw1 complex was released from the beads by addition of TEV protease and subsequently added to either immobilized Okp1 complex or empty IgG beads. Binding was performed for 1h at RT. After washing, proteins were acid eluted and analyzed by anti-HA immunoblotting.
- (B) *Binding of TEV-released Okp1 complex to immobilized Mtw1 complex.* Same conditions as in (A) but inverse experimental setup.

In order to verify this interaction a second binding assay was performed, but under inverse conditions (Figure 37B). This time the soluble Okp1 complex was added to immobilized Mtw1 complex. As shown in the corresponding immunoblot, HA-tagged Mcm16 was strongly retained by the Mtw1 complex.

These results confirm a biochemical interaction between the Okp1 and the Mtw1 complex, and thus support the preceding ChIP analyses.

2.2.2 Dephosphorylation of Okp1 and Mtw1 complexes has no influence on their interaction

The previous analysis revealed binding between the Okp1 and the Mtw1 complex (Figure 37). Since both complexes contain phosphorylated proteins (Westermann et al., 2003; Lechner lab, unpublished data), the question arises, if these modifications have an influence on the association of the two complexes. To analyze this, both complexes were immobilized on IgG beads and incubated with phosphatase. Dephosphorylation was exemplary verified for Ame1, a component of the Okp1 complex (Figure 38A). After phosphatase treatment, no phosphorylated forms of the protein could be detected. Binding was performed by addition of soluble Mtw1 complex to immobilized Okp1 complex. Complex formation was analyzed by immunoblotting against HA-tagged Dsn1 (Figure 38B).

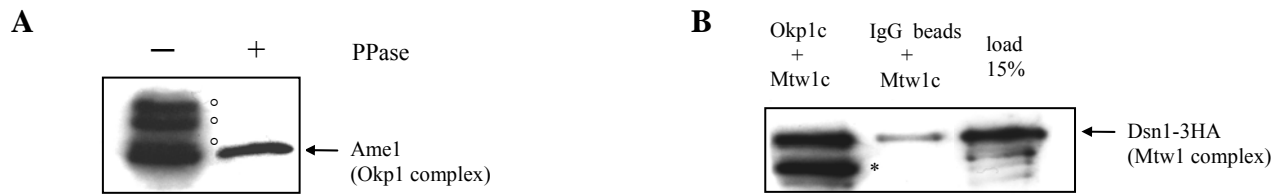


Figure 38. Dephosphorylation of the Okp1 and the Mtw1 complex does not abolish their interaction.

- (A) *Dephosphorylation of the Okp1 complex.* The Okp1 complex was affinity-purified from 3000 ODs of cells and bound to IgG beads. One half of the sample was incubated with 50 U of calf intestinal phosphatase for 1 h at 30°C, the other with buffer only. With 1/10 of each sample an anti-Ame1 immunoblot was performed. The remaining samples were used for the binding assay depicted in Figure (B). (Open circles indicate phosphorylated Ame1 species).
- (B) *Dephosphorylation of the Okp1 and Mtw1 complex does not abolish their interaction.* Okp1 and Mtw1 complexes were affinity-purified from 1500 ODs of cells, bound to IgG beads and dephosphorylated as in (A). The TEV-released Mtw1 complex was added to immobilized Okp1 complex and empty IgG beads. Binding was performed for 1 h at RT. After washing the beads, proteins were acid eluted and analyzed by anti-HA immunoblotting. (Asterisk denotes cross reacting Okp1-TAP).

Dephosphorylation of the Mtw1 and the Okp1 complexes does not interfere with their binding. Therefore, phosphorylation of these complexes may rather be implicating in the regulation of other processes.

2.2.3 Testing for further interaction partners of the Okp1 and Mtw1 complexes

The preceding assay revealed a physical interaction between the Okp1 and Mtw1 complexes. In order to identify further binding partners of both complexes, soluble Ndc80 or DDD complexes were added to immobilized Okp1 or Mtw1 complexes. As revealed by immunoblotting against HA-tagged Nuf2 (a component of the Ndc80 complex), no binding between the Okp1 and the Ndc80 complexes could be determined (Figure 39A). However, the performed binding assay revealed a slight interaction between the Ndc80 complex and the Mtw1 complex (Figure 39B).

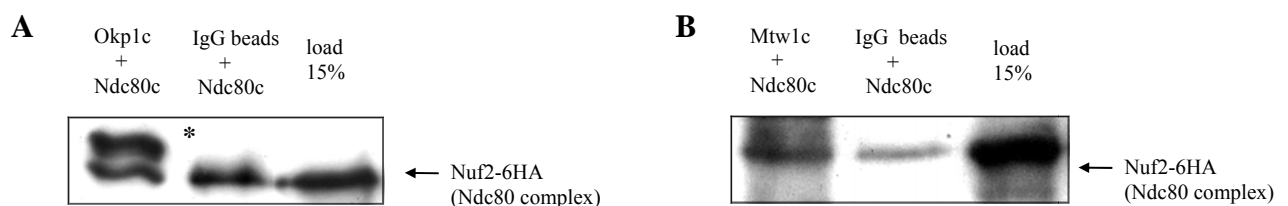


Figure 39. Testing for interactions of the Ndc80 complex with either the Okp1 or the Mtw1 complex.

- (A) *No binding of TEV-released Ndc80 complex to immobilized Okp1 complex could be observed.* The Okp1 and the Ndc80 complex were affinity-purified from 1500 OD of cells via a TAP-tag. The Ndc80 complex was released from beads by addition of prescission protease and subsequently added to either immobilized Okp1 complex or empty IgG beads. Binding was performed for 1 h at RT. After washing the beads, proteins were acid eluted and analyzed by anti-HA immunoblotting. (Asterisk indicates cross-reactivity of the secondary antibody with the protein A tag of Okp1).
- (B) *Only a minor binding of TEV-released Ndc80 complex to immobilized Mtw1 complex could be found.* Same experiment as in (A) but this time the TEV-released Ndc80 complex was added to immobilized Mtw1 complex.

Accordingly, under the given conditions neither the Okp1 nor the Mtw1 complexes clearly interact with the Ndc80 complex.

In order to establish a complete interaction-network, including kinetochore complexes from the central to the outer layer, also physical links to the microtubule associated DDD complex were analyzed. When soluble DDD complex was incubated with either immobilized Okp1 or Mtw1 complexes, no specific interaction of the DDD complex member Duo1 with the Okp1 or Mtw1 complex could be observed (Figure 40A and B).

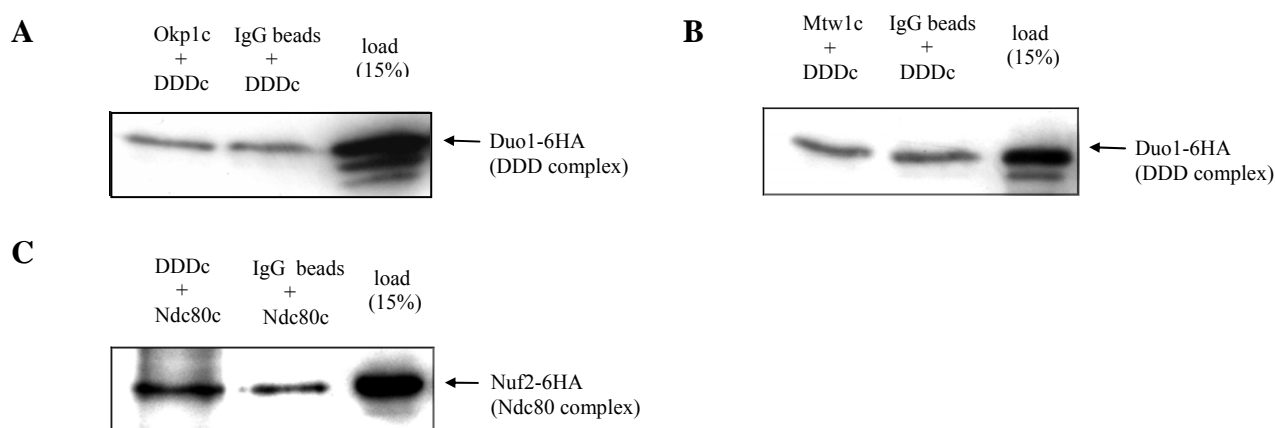


Figure 40. Testing for interactions of the DDD complex with the Okp1, Mtw1 and the Ndc80 complex.

- (A) *No binding of TEV-released DDD complex to immobilized Okp1 complex.* The Okp1 and the DDD complex were affinity-purified from 1500 OD of cells via a TAP-tag. The DDD complex was released from beads by addition of prescission protease and subsequently added to either immobilized Okp1 complex or empty IgG beads. Binding was performed for 1 h at RT. After washing the beads, proteins were acid eluted and analyzed by anti-HA immunoblotting.
- (B) *No binding of TEV-releases DDD complex to immobilized Mtw1 complex.* Same experiment as in (A) but this time TEV-cleaved DDD complex was incubated with immobilized Mtw1 complex.
- (C) *Slight interaction of the Ndc80 complex to the DDD complex.* Same experiment as in (A), but this time prescission-released Ndc80 complex was added to immobilized DDD complex.

Furthermore, also no stable interaction between DDD and Ndc80 complexes could be determined. Incubation of soluble Ndc80 complex with immobilized DDD complex revealed only a minor interaction of Ndc80 complex member Nuf2 with the DDD complex (Figure 40C).

2.2.4 Mtw1 and Ndc80 complexes interact with the Spc105 complex

Sequential co-purifications performed with components of the Mtw1, Ndc80 and Spc105 complexes indicated that all three complexes are closely associated (Nekrasov et al., 2003). Therefore, direct binding of these isolated complexes was tested next. Soluble Mtw1 or Ndc80 complexes were incubated with immobilized Spc105 complex (Figure 41A and B). As determined by immunoblotting against HA-tagged Dsn1 (Mtw1 complex member) or Nuf2 (Ndc80 complex member) the Spc105 complex interacts with both the Mtw1 and the Ndc80 complex. These interactions suggest a bridging function for the Spc105 complex between Mtw1 and Ndc80 complexes.

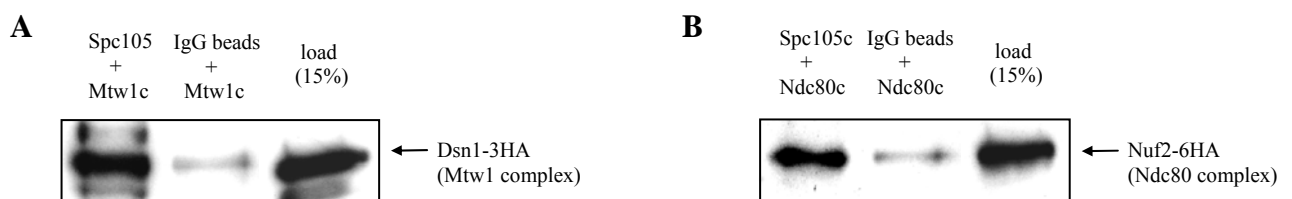


Figure 41. The Spc105 complex is physically linked to the Mtw1 and the Ndc80 complex.

- (A) *Binding of prescission-released Mtw1 complex to immobilized Spc105 complex.* The Spc105 and the Mtw1 complex were affinity-purified from 1500 OD of cells via a TAP-tag. The Mtw1 complex was released from beads by addition of prescission protease and subsequently added to either immobilized Spc105 complex or empty IgG beads. Binding was performed for 1 h at RT. After washing the beads, proteins were acid eluted and analyzed by anti-HA immunoblotting.
- (B) *Binding of prescission-released Ndc80 complex to immobilized Spc105 complex.* Same experiment as in (A), but this time a prescission-released Ndc80 complex was added to the immobilized Spc105 complex.

2.2.5 The Okp1, Mtw1 or Ndc80 complexes also do not interact with the DDD complex under dephosphorylating conditions

So far the DDD complex, which makes direct contact to microtubules, could not be linked to any kinetochore complex of the central layer. However, phosphorylation of individual complexes might have obstructed the identification of such interactions. Phosphorylation of the DDD complex is thought to weaken the interaction of kinetochores and microtubules by destabilizing its interaction with the Ndc80 complex (Shang et al., 2003). Therefore, dephosphorylation may favor interactions between the different complexes. To test for this possibility Okp1, Mtw1, Ndc80 and the DDD complexes were first dephosphorylated *in vitro* and thereafter subjected to binding assays (Figure 44). Dephosphorylated and soluble DDD complex was added to immobilized and likewise dephosphorylated Okp1 or Mtw1 complexes (Figure 42A). Subsequently, also the association of soluble and dephosphorylated Ndc80 complex with immobilized and dephosphorylated DDD complex was tested (Figure 42B). In neither case a specific interaction of a respective reporter protein was observed.

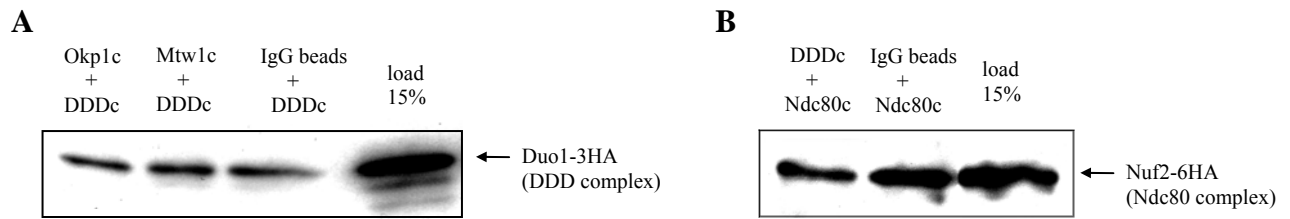


Figure 42. No stable association between the dephosphorylated DDD complex and dephosphorylated Okp1, Mtw1 or Ndc80 complexes was observed.

- (A) *No binding of dephosphorylated Okp1 or Mtw1 complex to dephosphorylated DDD complex.* Okp1, Mtw1 and DDD complexes were isolated from 1500 ODs by their TAP-tags, bound to IgG beads and incubated with 50 U of calf intestinal phosphatase for 1 h at 30°C. TEV-released DDD complex was added in parallel to the Okp1 and Mtw1 columns and also to empty IgG beads and incubated for 1 h at RT. After washing the beads, proteins were acid eluted and analyzed by an anti-HA immunoblot.
- (B) *No binding of dephosphorylated Ndc80 complex to immobilized and dephosphorylated DDD complex.* Same experimental setup as in (A), but this time pre-scission-released and dephosphorylated Ndc80 complex was added to dephosphorylated and immobilized DDD complex.

In summary, the *in vitro* binding experiments reported here uncovered interactions between the Okp1 and Mtw1 complex and furthermore between the Spc105 complex and Mtw1 or Ndc80 complexes. According to previous classifications (Wigge and Kilmartin, 2001; Janke et al., 2001; He et al., 2001; De Wulf et al., 2003) all of these interaction groups are located in the central layer of the kinetochore. In contrast, no stable associations with the microtubule binding DDD complex could be determined (neither under phosphorylated nor dephosphorylated conditions). These observations may indicate a cooperativity of the central layer complexes in the binding of the DDD complex.

3. DISCUSSION

3.1 Functional analysis of *ame1-2 ts* mutants

Aim of the present work is the functional characterization of the essential protein Ame1. Ame1 is a component of the Okp1 complex that is part of the *S. cerevisiae* kinetochore (Cheeseman et al., 2002b; Ortiz et al., 1999). This complex is located at the middle layer of the kinetochore structure together with the Mtw1 and the Ndc80 complexes, thus mediating between the DNA binding Cse4 and CBF3 complex on the one hand and the microtubule-associated DDD complex on the other.

Since Ame1 is an essential protein it was not possible to simply delete its gene and analyze the implications of a kinetochore built up in absence of Ame1 on cellular events. Instead, an *ame1* temperature sensitive (*ts*) mutant was constructed by error prone PCR. Located at the center of the kinetochore, the *ame1-2* mutant strongly influences the overall structure of this assembly. This in turn has dramatic effects on microtubule attachment, spindle morphology and cytokinesis.

3.1.1 The monopolar segregation defect in *ame1-2* is caused by breaking of one kinetochore-microtubule attachment

The monopolar chromosome segregation observed in *ame1-2* can result from two different effects: In the first case the two sister chromatids are attached to microtubules emanating from the same pole (syntelic attachment) and pulled to one side of the cell. In the other case bipolar attachment to microtubules emanating from opposing poles is achieved, but this interaction is not stable enough and unable to resist the tension applied on it. In consequence, one attachment breaks apart and both sisters follow the movement of one pole. The experimental data gained with *ame1-2* clearly favor the latter explanation.

Syntelic attachment is normally resolved by the activity of the Ipl1 kinase. Its activity is regulated by tension (Dewar et al., 2004). As long as tension is missing, Ipl1 is active. Defects in Ipl1 activity cause a monopolar distribution of chromosomes, preferentially into the daughter, since they predominantly associate with microtubules of the old spindle pole (Tanaka et al., 2002). This spindle pole is always distributed into the daughter (Pereira et al., 2001). Degradation kinetics of Pds1 in *ame1-2* are similar to cells with a spindle assembly checkpoint activated as a result of missing tension (Scc1 depletion, Biggins and Murray, 2001). Furthermore, the delay in Pds1 degradation corresponds to the delay in Esp1 activation. Therefore, spindle assembly checkpoint activation due to lack of tension apparently occurs in *ame1-2*. Accordingly, the strain should be able to activate the Ipl1

kinase. Therefore, the defect in resolving syntelic attachments should not be the cause of the monopolar distribution observed in *ame1-2*. This is also supported by the fact that there is no clear preference in the segregation of sister chromatids to either pole, because in 53% of the cells the *CEN5* signal is found in the mother and in 44% in the daughter. *ipl1* mutants most generally show a biased distribution in favour of the daughter (Tanaka et al., 2002; Scharfenberger et al., 2003).

ChIP analyses performed with *ame1-2* indicate that the mutation severely compromises the entire kinetochore structure thus arguing for a weakening of kinetochore-microtubule attachments. Localization of all analyzed components of the central kinetochore complexes (Okp1, Mtw1, Spc105, and Ndc80) is strongly reduced at the *ame1-2* kinetochore and the mutation also affects the association of the DDD complex.

In conclusion these findings favor a model according to which Amel is not needed for the establishment of kinetochore-microtubule attachments, since *ame1-2* is able to distribute the DNA masses between mother and daughter. Nevertheless, the *ame1-2* mutant induces a structural weakening of the kinetochore, which thereafter is unable to withstand the applied tension. This leads to a statistical breaking of one of the two microtubule attachments resulting in a monopolar distribution of sister chromatids. Amel is therefore implicated in the achievement and maintenance of bipolar kinetochore-microtubule attachments.

3.1.2 Amel and the spindle attachment checkpoint

The ame1-2 defect does not interfere with the induction of the occupancy checkpoint

Analyses of the occupancy checkpoint in presence of nocodazole indicated that the *ame1-2* mutant is able to sense loss of attachment at kinetochores, since cells maintained permanently high Pds1 levels and arrested with unreplicated DNA. A permanent arrest with a 2N DNA content requires functionality of both occupancy and spindle positioning checkpoint. Elimination of either checkpoint leads to a delay in mitotic exit and rereplication but not in a permanent arrest. Therefore, if *ame1-2* would cause a defect in the occupancy checkpoint then the cell cycle arrest with a 2N DNA content would not be permanent. Additional analyses performed in a Bub2 deletion strain (inactivation of the spindle positioning checkpoint) in presence of nocodazole also demonstrate functionality of the occupancy checkpoint in *ame1-2*. Abrogation of both checkpoints (*AME1Δmad2Δbub2*) results in mitotic exit timing indistinguishable from wild type cells untreated with nocodazole. Therefore, a defective occupancy checkpoint should cause a similar behavior of an *ame1-2Δbub2* double mutant and an *AME1Δmad2Δbub2* double mutant. However, this is not the case, since *Δbub2ame1-2* rather resembles a *MAD2Δbub2* strain in FACS analyses.

The *ame1-2* defect causes a delay in the inactivation of the spindle attachment checkpoint

The delay observed in the degradation of Pds1 in the *ame1-2* mutant can be due to an activation of the checkpoint by either loss of tension as a result of the braking of one kinetochore-microtubule attachment (see 3.1.1) or a few unattached kinetochores that would also lead to loss of tension. Loss of occupancy of all 32 kinetochores (addition of nocodazole) does normally lead to permanent inhibition of Pds1 degradation. However, it is not clear how a few unattached kinetochores influence the inactivation of the spindle attachment checkpoint. They may just lead to a partial induction of the checkpoint and therefore Pds1 degradation would only be delayed.

Arguing in favor of an induction of the spindle assembly checkpoint by missing tension is the similarity in the degradation kinetics of Pds1 observed in *ame1-2* and a wild type strain depleted of the cohesion Scc1. A secondary effect due to loss of tension should be a permanent activation of Ipl1. This should result in a constant untethering of microtubules from kinetochores and in consequence to retention of DNA in the mother. But this is not the case in *ame1-2*, since the mutant is able to distribute its DNA. Noteworthy, the tension checkpoint is not entirely stringent (see Scc1 depletion). Cells eventually overcome this arrest, proceed in the cell cycle and inactivate Ipl1. Another explanation could be that the short bipolar attachment achieved before the breaking of one attachment is sufficient for inactivation of Ipl1 at the particular kinetochore.

The temporal activation of the spindle assembly checkpoint (delay in Pds1 degradation) observed in the *ame1-2* mutant contrasts the permanent arrest of the strain with a 2N DNA content. As mentioned before, abrogation of either the spindle assembly checkpoint or the spindle positioning checkpoint should only delay mitotic exit and rereplication, but not cause a permanent cell cycle arrest. However, deletion of Bub2 (spindle positioning checkpoint) in *ame1-2* still leads to a permanent arrest with a 2N DNA content. Thus, the permanent arrest of *ame1-2* is not due to an activation of the spindle checkpoint. This is supported by the addition of nocodazole to the *ame1-2Abub2* double mutant, which results in the formation of a 4N peak. Nocodazole leads to the strongest spindle assembly activation known and prevents a segregation of DNA into mother and daughter cell. Therefore, the permanent arrest of *ame1-2* can more likely be attributed to an uneven distribution of DNA and the replication machinery due to the monopolar segregation defect of the mutant.

Taken together, the analyses of *ame1-2* indicate that checkpoint functions are not impaired in this mutant. The functionality of the spindle checkpoint is achieved despite a reduction in the kinetochore localization of all members of the Ndc80 complex implicated in checkpoint function (Janke et al., 2001; McClelland et al., 2003). In support of this notion, depletion of vertebrate Ndc80 by RNAi leads to a reduction of checkpoint protein Mad1 and Mad2. But even at 10% of their wild type levels, these proteins are still sufficient to induce a checkpoint arrest (Martin-Fluesma et al., 2002; DeLuca et al., 2003; McClelland et al., 2003).

Interestingly, another *ame1-4* allele analyzed by Pot et al. (2005) indicates a requirement of Ame1 for the maintenance of the checkpoint. The *ame1-4* strain initially arrests in G2/M phase, can escape this arrest leading to the formation of a 4N peak. These additional observations likely reflect a specificity of the mutant allele used for their studies.

3.1.3 The *ame1-2* defect interferes with the Cdc14 release from the nucleolus in early anaphase (FEAR)

The activation of the spindle attachment checkpoint in *ame1-2* should also lead to a delay in the activation of FEAR. However, *ame1-2* does not only show a delay in the induction of FEAR, but is rather unable to release Cdc14 from the nucleolus. This failure to induce FEAR can be attributed to an induction of the spindle assembly checkpoint, since deletion of checkpoint protein Mad2 allowed for an activation of FEAR. However, even though Esp1 is finally activated due to falling Pds1 levels, no nucleolar release of Cdc14 was observed. Accordingly, mere activation of Esp1 is not sufficient for FEAR induction, but may have to occur in a particular time-frame relative to other cellular events. This time limit may have elapsed, when Esp1 gets finally activated in *ame1-2*.

The failure in FEAR induction and the inability to segregate the nucleolus in *ame1-2* can be due to the monopolar distribution and spindle defect of the mutant. However, neither of these defects can explain the lack of FEAR in *ame1-2*, since a wild type strain depleted of Mad2 and treated with nocodazole also keeps its nucleolus in the mother and does not polymerize spindles, but retains the ability of FEAR induction.

3.1.4 *ame1-2* prevents the formation of a stable mitotic spindle

Failures in the achievement of bipolar attachment allow for spindle pole separation in the presence of an active spindle assembly checkpoint (low Esp1 activity). This together with a failure in FEAR induction (Cdc14 release) is known to interfere with spindle formation (Higuchi and Uhlmann, 2005). Since Pds1 degradation is delayed in *ame1-2* and Cdc14 is not released, one of the causes for the spindle defect can be a premature separation of spindle pole bodies in presence of low Esp1 and Cdc14 activity. However, this is unlikely the major reason for the spindle defect in *ame1-2*. Lack of Cdc14 as cause could be excluded due to the following observations:

1. Overexpression of Cdc14 could not rescue spindle formation in *ame1-2*. This experiment was performed in a strain background where sister chromatide separation can be achieved by an inducible protease. This way Pds1 levels and sister chromatid separation can be uncoupled. This strain is unable to form spindles if Pds1 levels are kept high. An overexpression of Cdc14 on the other hand rescues this phenotype (Higuchi and Uhlmann, 2005). Nevertheless,

Cdc14 overexpression did not allow for spindle formation, when the *ame1-2* allele was additionally integrated into this strain.

2. A constitutively non-phosphorylated variant of Sli15 (the only known substrate of Cdc14 involved in spindle stabilization) was introduced in the *ame1-2* strain. This construct should stabilize spindles independent of FEAR (Pereira and Schiebel, 2003). However, also in this strain background no rescue of the *ame1-2* spindle defect was observed.

Esp1 influences spindle stability either directly by translocation to the spindle or indirectly by activation of FEAR and the subsequent transient release of Cdc14 from the nucleolus (Jensen et al., 2001, Zeng et al., 1999; Sullivan et al., 2001; Pereira and Schiebel, 2003; Higuchi and Uhlmann, 2005). However, for the following reasons spindle pole body separation in presence of low Esp1 activity could also be excluded as major cause for the spindle defect in *ame1-2*:

1. Esp1 activity appears in *ame1-2* but is delayed as compared to wild type. This raises the question if the timing between spindle pole separation (due to the bipolar attachment defect) and Esp1 activation might be disturbed? However, the percentage of cells with spindle defects in presence of active Esp1 is considerably higher than the percentage of cells that separate the poles in absence of Esp1 activity.
2. Spindle defects were frequently observed at spindle poles distances that are characteristic of metaphase. At this stage of the cell cycle, Esp1 is normally inactive and therefore the activity of Esp1 should be irrelevant for the stability of metaphase spindles in *ame1-2*.
3. As mentioned above, Cdc14 overexpression is able to rescue spindle formation in cells that separate spindle poles in absence of Esp1 activity, but not in *ame1-2*.
4. Although previous reports showed that spindle formation in presence of high Pds1 levels can be rescued by Esp1 overexpression (Higuchi and Uhlmann, 2005), increasing the activity of Esp1 by either inactivating the spindle assembly checkpoint through deletion of Mad2 or overexpression allowed only for a partial rescue of the spindle defect in *ame1-2*. Therefore, the slight activation of the spindle assembly checkpoint in *ame1-2* plays only a subordinate role in the spindle defect of the mutant.

Besides a spindle pole separation in presence of low Esp1 and Cdc14 activity, the spindle defect in *ame1-2* may have other explanations: First, one could speculate that the spindle defect may result from an imbalance in the number of microtubules on one pole versus the other due to the connection of one kinetochore with two microtubules from the same pole (syntelic kinetochore attachment). Accordingly, the number of microtubules available for midzone overlap may be reduced or annulated. However, this is unlikely the case, since *ip11* mutants that are unable to resolve syntelic attachments and segregate their DNA in a very imbalanced manner still form stable spindles (Tanaka et al., 2002). Second, several kinetochore components also function as

spindle stabilizing proteins (Müller-Reichert et al., 2003; Bouck and Bloom 2005; Li et al., 2002; Janke et al., 2002). In contrast to these, Ame1 does not locate to the spindle at any given time.

Third, several proteins involved in spindle stabilization and regulation of microtubule dynamics are also found at the kinetochore. These include the Sli15-Ipl1 complex, Cin8, Slk19, Stu1 and Stu2 (He et al., 2001; Zeng et al., 1999; Sullivan et al., 2001; Yin et al., 2002; Pearson et al., 2003; Severin et al., 2001). All of them are known to translocate from the kinetochore to the spindle. However, it is unclear whether their kinetochore localization is a prerequisite for their function in spindle stabilization.

As already mentioned above, a defect in the spindle localization of Sli15 and accordingly of Ipl1 due to lack of Cdc14 activity in *ame1-2* could be excluded. Kinetochore localization of Slk19, Stu2 and Stu1 on the other hand seems to be impaired in *ame1-2*, as deduced from ChIP analyses. As far as Stu2 is concerned, a translocation to the plus end and stabilization of kinetochore microtubules upon lateral contact has been reported (Tanaka et al., 2005). Even though this effect applies primarily to kinetochore microtubules, it may also be a way to deliver Stu2 to polar microtubules upon their transient contact with kinetochores. Mutations in Cin8 and Stu1 on the other hand are known to cause metaphase defects (Saunders et al., 1997; Yin et al., 2002). Accordingly, a further investigation of all three factors may help to better understand the spindle defect of the *ame1-2* strain.

3.1.5 Establishment of bipolar attachments rescues the *ame1-2* spindle defect

When cells were arrested in metaphase by depletion of Cdc20 and subsequently shifted to the restrictive temperature intact metaphase and after the release from the arrest also intact anaphase spindles were formed. Accordingly, a preformed metaphase spindle is no longer prone to the *ame1-2* defect. This was further confirmed by the analyses of spindle formation in nocodazole arrested and subsequently released *ame1-2* cells. Under these conditions no spindles were polymerized indicating that the establishment of bipolar attachments prior to the induction of the *ame1-2* mutation is the reason for spindle rescue. Thus, the *ame1-2* mutation may interfere with an irreversible step in spindle stabilization prior to or during the establishment of bipolar kinetochore-microtubule attachments.

One explanation could be an inactivation of the spindle checkpoint after the establishment of a metaphase spindle (Palframan et al., 2006). This is unlikely however, since *ame1-2* cells released from the Cdc20 arrest are able to activate the spindle assembly checkpoint as seen by the delay in the degradation of Pds1.

Another explanation for the spindle rescue is that the induction of the *ame1-2* mutation after the establishment of bipolar attachment might cause a less severe kinetochore defect than *ame1-2* induced before. Similar has previously been reported for kinetochore protein Nsl1 (Scharfenberger et al., 2003). Indeed, ChIP analyses performed with *ame1-2* cells arrested in metaphase by Cdc20 depletion prior to the induction of the mutation indicated that the kinetochore localization of all analyzed kinetochore components was increased as compared to cells incubated at 37°C without a previous metaphase arrest. Components of the Mtw1 complex in particular almost reached wild type levels. Since kinetochore localization of the Mtw1 complex correlates with the ability of *ame1-2* cells to form stable spindles, one may thus speculate that this complex may have a major role in the generation of spindle stabilizing factors. Additionally, the reduced kinetochore defect may maintain a kinetochore structure that is required for an unknown spindle stabilizing effect.

3.1.6 Cytokinesis is impaired in the *ame1-2* mutant

FACS analyses performed with *ame1-2* mutant cells indicate that the strain is defective in cytokinesis. Unlike wild type, *ame1-2* cells arrested with a 2N DNA content even four hours after the wild type had reached G1. A permanent activation of the spindle assembly checkpoint can be excluded as cause for this effect, since the *ame1-2* strain is only delayed in Pds1 degradation. The cytokinesis defect in *ame1-2* can also not be attributed to an activation of the spindle positioning checkpoint or failure in MEN (mitotic exit). Analysis of the nucleolar release of Cdc14 in *ame1-2* showed that MEN is functional in the mutant.

Alternatively, the cytokinesis defect of the *ame1-2* mutant may be attributed to missing anaphase spindles. It is known that in animals cells spindle midzone defects interfere with proper cytokinesis (Glotzer et al., 2005; Guertin et al., 2002; McCollume, 2004). A connection between spindle midzone and cytokinesis has recently also been reported for yeast (Norden et al., 2006). Spindle midzone recruitment of the Ipl1/Sli15 heterodimer abolishes an inhibition of cytokinesis. The relocation of these factors involves active Cdc14. Thus, Cdc14 and microtubule mediated accumulation of proteins at the spindle midzone might be necessary for the execution of cytokinesis. Since MEN is functional in *ame1-2*, the cytokinesis defect of this mutant can more likely be attributed to the absence of an anaphase spindle. This is also supported by the finding that treatment of an *AME1Δbub2* strain with nocodazole also interferes with cytokinesis, although this strain rereplicates its DNA and thus activates MEN. Nocodazole leads to a depolymerization of microtubules, which are required for the abscission of mother and daughter cells. Thus, the spindle defect in *ame1-2* also has a direct influence on cytokinesis in the mutant.

3.1 7. A comprehensive model of Ame1 kinetochore functions

Finally, it can be concluded that the *ame1-2* mutation has profound effects on several aspects of mitosis. It not only compromises the kinetochore structure and abolishes stable bipolar attachments, but also interferes with the induction of FEAR, spindle morphology, and cytokinesis (Figure 45). The most interesting defect of the *ame1-2* strain is its inability to form stable metaphase and anaphase spindles. Most likely at least two different factors contribute to this phenotype: First, spindle pole separation due to failures in bipolar attachment occur in absence of Esp1 (activation of the spindle checkpoint) and Cdc14 (FEAR) activity. Second, an unknown pathway involved in spindle formation is compromised by the *ame1-2* kinetochore. The latter may directly interfere with the activation or repositioning of spindle stabilizing and/or polymerizing factors.

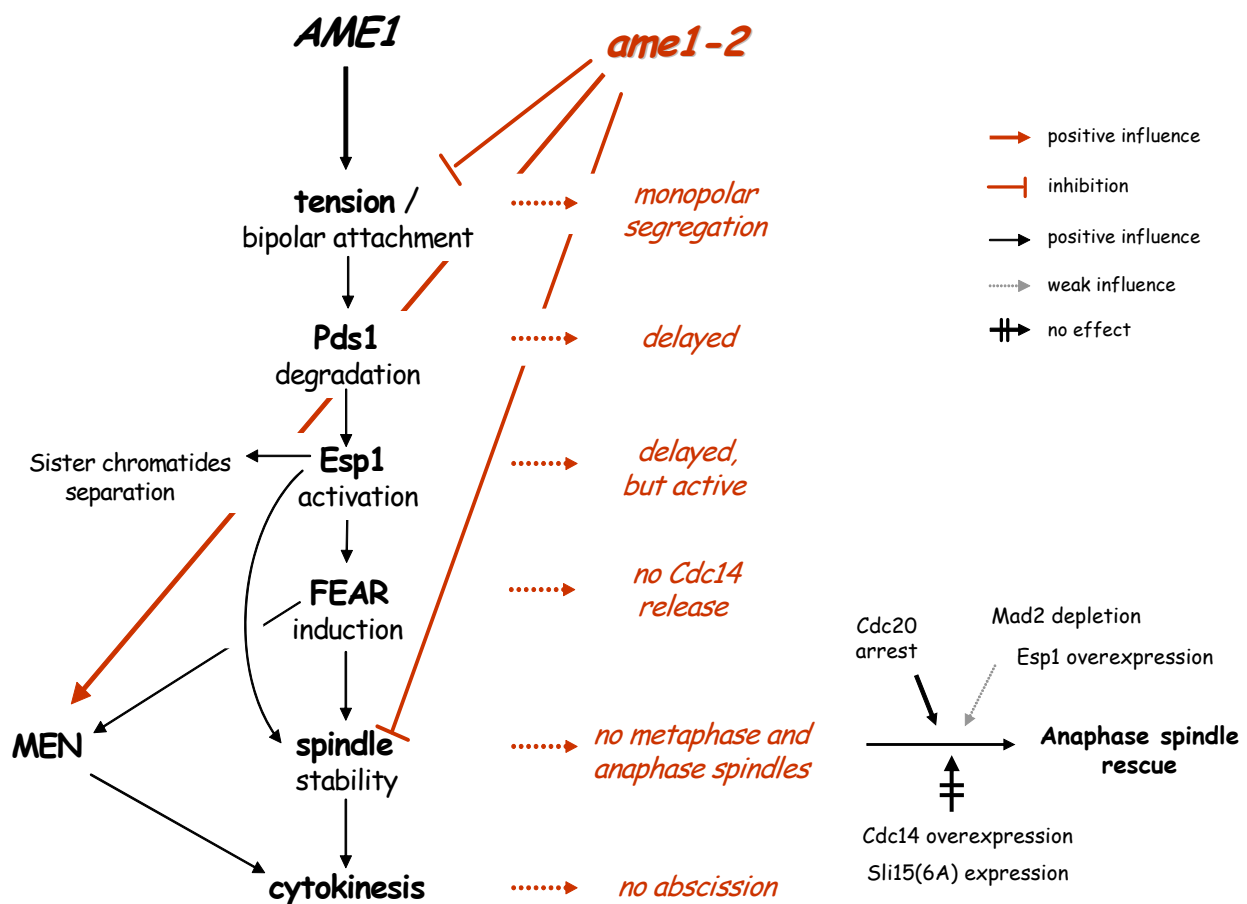


Figure 43. Influence of the *ame1-2* allele on various aspects of mitosis. *ame1-2* interferes with the establishment of a bipolar spindle attachment and spindle formation. Additionally, also a FEAR independent influence on spindle stability was uncovered.

Noteworthy, *ame1-2* is a particular kinetochore mutant. Whereas the anaphase spindle defects of other kinetochore mutants (e.g. *ns11*, *ask1* or *dam1*) can be rescued by depletion of checkpoint protein Mad2 (Scharfenberger et al., 2003; Li et al., 2002; Cheeseman et al., 2001), only a partial rescue of spindle formation was this way achieved in *ame1-2*. Moreover, the *ame1-2* allele has a stronger influence on the overall organization of the kinetochore than the *ns11* mutant for example (Scharfenberger et al., 2003). Accordingly, the mutant phenotype of *ame1-2* appears to be broader and in direct comparison more severe.

3.2 Refined structural model of the *S. cerevisiae* kintochore

The *S. cerevisiae* kinetochore is a complex structural unit comprising more than 60 different proteins (McAinsh et al., 2003). These factors are organized in a distinct number of complexes. Even though a concept of their hierarchical organization starts to emerge and a lot of genetical relations have been identified, not many biochemical evidences for their interactions have been shown so far. In the present work two alternative approaches were used to determine interrelations between the different complexes: chromatin immunoprecipitation (ChIP) and a biochemical binding assay performed with individually purified complexes.

Previous reports have established a certain, albeit limited concept of the organization of the yeast kinetochore. It describes a number of kinetochore complexes and groups them into an inner, central and outer layer depending on their localization in respect to microtubules ore DNA. However, the interaction network of the different kinetochore complexes is far from being understood. Convincing experimental evidence documents a direct association of the CBF3 complex with centromeric DNA (Lechner and Carbon, 1991). CBF3 thus represents the inner kinetochore layer and all other kinetochore complexes are recruited in dependency of CBF3 (Ortiz et al., 1999; Janke et al., 2001; Goshima and Yanagida, 2000). Mutations in this complex lead to a complete loss of kinetochore-microtubule attachment both *in vitro* and *in vivo* (He et al., 2001; Sorger et al., 1994; Goh and Kilmarti, 1993). As revealed by copurification analysis, the central kinetochore layer comprises four different complexes, which are all linked to each other. The Mtw1 complex has been shown to copurify components of the Ndc80 and Okp1 complexes, and the reciprocal is also true (Westermann et al., 2003; De Wulf et al., 2003; Nekrasov et al., 2003). Moreover, the Ndc80 and the Mtw1 complexes have also been linked to the Spc105 complex (Nekrasov et al., 2003).

The current thesis now provides first hand evidence for direct interactions amongst the central kinetochore complexes. These data were derived from biochemical binding experiments with isolated single complexes. The Okp1 complex directly interacts with the Mtw1 complex, which in turn associates with the Spc105 complex. The latter one additionally connects to the Ndc80

complex. Thus, Spc105 has a bridging function between Ndc80 and Mtw1 complexes. This interaction pattern places all four complexes in a straight consecutive order: Okp1 complex - Mtw1 complex – Spc105 complex – Ndc80 complex. Although no stable cross-connections could be detected they may have been missed due to limitations of the assay and can therefore not be excluded. Also no physical interaction between the central kinetochore layer and the outer DDD complex could be reconstituted. However, kinetochore association of the DDD complex may require cooperativity between central layer members and may thus be inaccessible to the described binding assay. So far it is known that the localization of the DDD complex is CBF3 and Ndc80 complex dependent (Li et al., 2002; Cheesman et al., 2002b; Janke et al., 2002; Jones et al., 2001).

Previous analyses on the organization of the kinetochore revealed that neither the Mtw1 nor the Okp1 complex depend on the Ndc80 complex for centromere association. Similarly, DNA binding by the Okp1 complex is independent of the Mtw1 complex (De Wulf et al., 2003; Westermann et al., 2003). *Vice versa*, also kinetochore association of the Mtw1 complex was believed to not involve the Okp1 complex. However, this assumption has to be revised due to the finding that centromeric binding of Nsl1, a component of the Mtw1 complex, is strongly reduced in mutants of the Okp1 protein (Scharfenberger et al., 2003). The present work serves to support this observation, but additionally reveals that the kinetochore association of all central layer complexes requires the presence of the Okp1 complex. Mutations in Ame1, another member of the Okp1 complex, abolish centromeric binding of exemplary Mtw1, Ndc80, Spc105, and DDD complex members. Noteworthy, the reduced amounts of the DDD complex at the mutant kinetochore may also be a secondary effect and attributed to the mislocalization of the Ndc80 complex (Li et al., 2002; Cheesman et al., 2002b; Janke et al., 2002; Jones et al., 2001). However, kinetochore localization of the DDD complex is less reduced than that of the other complexes (Mtw1, Ndc80, and Spc105). This may reflect direct interaction of the DDD complex with microtubules (Li et al., 2002; Janke et al., 2002). Additionally, kinetochore localization of the DDD complex might also be partially independent of the central kinetochore layer and require the interaction with the kinetochore core (Cse4 and CBF3 complex).

These findings indicate that the localization of all complexes of the central layer is dependent on the Okp1 complex. However, when bipolar attachment was achieved prior to the induction of the *ame1-2* mutation, localization of Mtw1 complex members became independent of Ame1 and accordingly of the Okp1 complex. This indicates that tension leads to a stable incorporation of the Mtw1 complex into the kinetochore structure although the localization of the Okp1 complex can still be influenced by the shift to the restrictive temperature.

The only kinetochore proteins whose DNA association was not altered by *ame1-2* were Ndc10 and Cse4, indicating that the inner kinetochore structure is not disturbed by the mutation. These

findings are consistent with published data that show a dependency of all kinetochore proteins on the presence of an intact CBF3 complex (Ortiz et al., 1999; Janke et al., 2001; Goshima and Yanagida, 2000).

On basis of the data presented in the current work, the structural model of the *S. cerevisiae* kinetochore can be refined as follows (Figure 46): The Okp1 complex apparently occupies a central position in the yeast kinetochore and is located in direct vicinity to the DNA associated CBF3 complex. This makes the Okp1 complex to another indispensable requirement for the kinetochore recruitment of all other central layer complexes: Mtw1, Spc105, and Ndc80. Newly identified interactions between all four complexes together with ChIP data are in line with copurification experiments and provide strong evidence for their mutual occurrence in the central kinetochore layer.

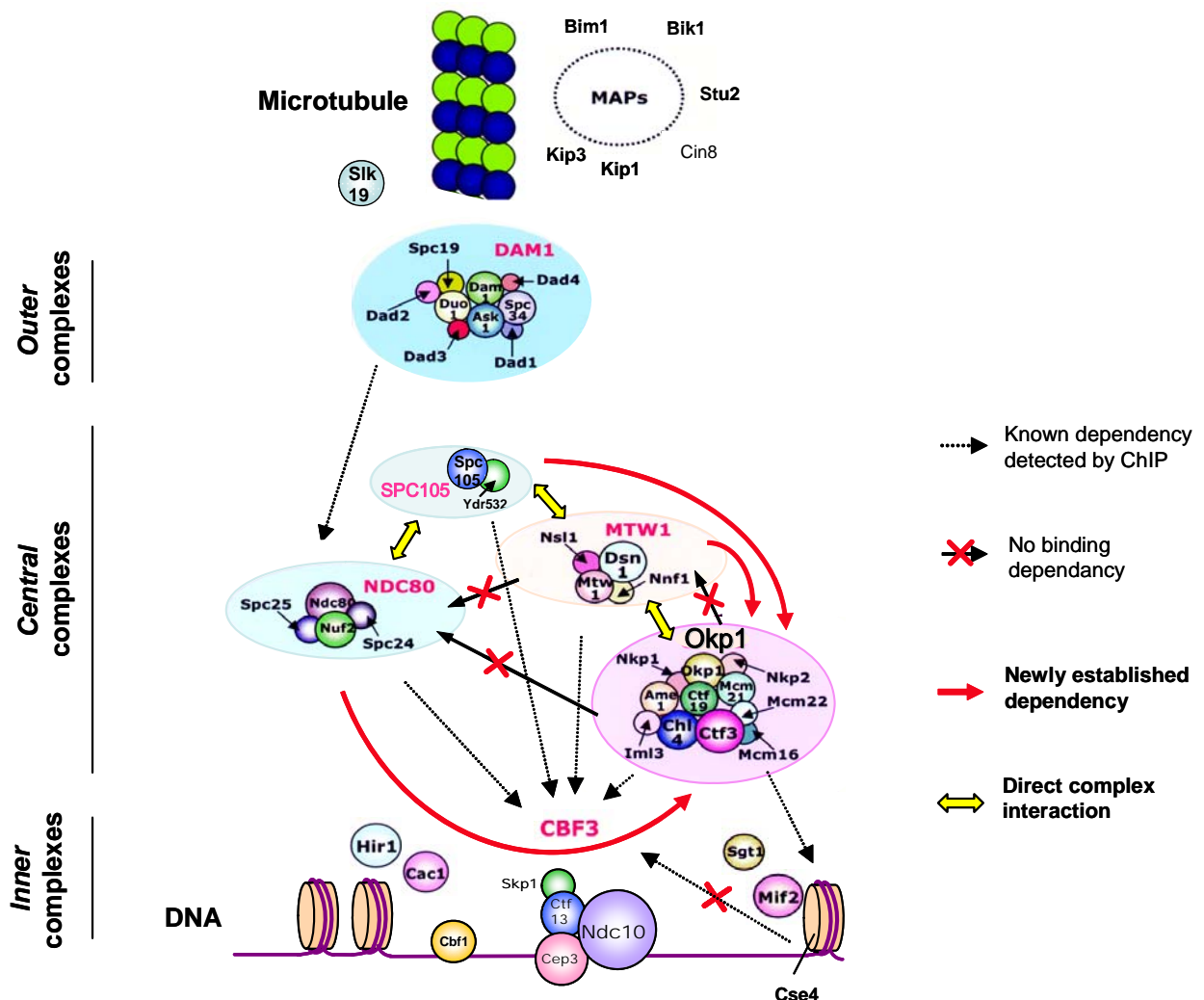


Figure 44. Refined model of the *S. cerevisiae* kinetochore (modified from Tan et al., 2005).

Depicted are newly identified physical interactions (yellow arrows) and binding dependencies as uncovered by ChIP (red arrows). Previously established connections are indicated with dashed lines.

4. METHODS

4.1 Culturing conditions

4.1.1 *E. coli*

E. coli strains were grown in LB/amp liquid medium or on LB/amp plates at 37°C.

LB:	10 g/l Tryptone	SOB:	20 g/l Tryptone
	5 g/l Yeast extract		5 g/l Yeast extract
	10 g/l NaCl		0.5 g/l NaCl
	pH 7.0		pH 7.0
			25 mM KCl
			10 mM MgCl ₂

Plates contained 2% agar.

Ampicillin was added to a final concentration of 100 µg/ml.

4.1.2 *S. cerevisiae*

Yeast strains were grown at 30°C for wild type strains or at 23°C for *ts* strains. For the induction of the *ame1-2* mutation cultures were shifted to 37°C.

All plates used contained 2% (w/v) agar.

YPD:	10 g/l Yeast extract	YPG:	10 g/l Yeast extract
	20 g/l Peptone from casein		20 g/l Peptone from casein
	20 g/l Glucose		20 g/l Galactose
YPR:	10 g/l Yeast extract	YPGR:	10 g/l Yeast extract
	20 g/l Peptone from casein		20 g/l Peptone from casein
	20 g/l Raffinose		20 g/l Galactose
			20 g/l Raffinose

SD (synthetic dropout):	6.7 g/l Yeast Nitrogen Base w/o amino acids
	20 g/l Glucose
	0.8 g/l Complete Supplement Mixture –Ade/His/Trp/Leu/Ura

Amino acids supplement ¹	final concentration
Adenine	30 mg/l
Histidine	20 mg/l
Leucine	20 mg/l
Tryptophan	30 mg/l
Uracil	20 mg/l

¹omit the respective amino acid for SD-Trp, SD-His, SD-Leu ...

FOA plates: SD plates containing all amino acids and 0.1% 5'-FOA.

YPD plates with kanamycin: YPD plates with the addition of 200 mg/l G418.

Media for microscopy contained 0.01% adenine and were filter sterilized instead of autoclaving.

4.2 Molecular biology techniques

4.2.1 Standard methods

DNA recombinant work was performed essentially as described (Sambrook et al., 2001).

4.2.1.1 PCR Amplifications

For gene deletion and genomic tagging of yeast genes expand long template Taq polymerase was used.

A 50 µl reaction contained:	program: initial denaturing 3 min 94°C
1 x PCR buffer	denaturing: 94°C 20 sec
0.5 mM dNTPs	annealing: 54°C 45 sec
1 µM primers	extension: 68°C 2.5 min
1.5 U polymerase	denaturing: 94°C 20 sec
1 µg plasmid or genomic DNA	annealing: 54°C 45 sec
	extension: 68°C 2.5 min +20 sec/cycle
	final extension: 7 min 68°C

} 10 cycles

} 20 cycles

For colony PCR the following set-up was used:

A 25 µl reaction contained:	program: initial denaturing 3 min 94°C
1 x PCR buffer	denaturing: 94°C 45 sec
200 µM dNTPs	annealing: T _m 45 sec
1 µM primers	extension: 72°C 1 min/kb
3 U Taq	final extension: 7 in 68°C
0.5 µl extract	

} 35 cycles

4.2.1.2 Cloning of PCR products

PCR products were first precipitated with NH₄Ac/Isopropanol in order to remove dNTPs and oligonucleotides, treated with T4 polymerase for the removal of A overhangs, and finally run on a agarose gel and gel extracted. 5' ends were phosphorylated in a polynucleotide kinase reaction with 1.5 mM ATP.

4.2.1.3 Restriction analysis

Restriction analyses were performed as described in the data sheets of the respective enzyme. Usually 1-5 µg plasmid was digested with about 5-20 U enzyme in a 10-30 µl reaction and incubated for 1 h at 37°C. Fragments were analyzed on agarose gels.

4.2.1.4 Agarose gel electrophoreses

To all samples 6x loading dye was added and fragments were run on 1-2% agarose gels in 1x TAE buffer.

TAE buffer:	242 g/l Tris	6x loading dye:	0.25% Bromphenol blue
	57.1 ml/l Glacial acid		0.25% Xylene cyanol
	100 ml/l 0.5 M EDTA		30% Glycerol
	pH 7.2		

4.2.1.5 Isolation of DNA from agarose gels

All DNA fragments were isolated from agarose gels by the QIAEX II gel extraction kit from Qiagen.

4.2.1.6 Klenow reaction

Klenow polymerase was used for the removal of 3' protruding ends. The reaction was performed in the presence of 200 µM dNTPs in klenow buffer with 10 U/µg DNA. After incubation at 37°C for 10 min the enzyme was heat inactivated for 10 min at 70°C.

4.2.1.7 T4 polymerase reaction

T4 polymerase was used for the removal of 5' protruding ends. The reaction was performed in the presence of 0.5 mM dNTPs in polymerase buffer with 4 U/µg DNA. After incubation at 11°C for 20 min the enzyme was heat inactivated for 10 min at 75°C.

4.2.1.8 CIAP

In order to prevent religation, vectors were treated with calf intestinal alkaline phosphatase. 10 U CIAP were added to 5 µg DNA in a 50 µl reaction and incubated for 2 h at 37°C.

4.2.1.9 Phenol/Chloroform extraction

In order to remove proteins from DNA, the sample was mixed with 1 volume of pre-equilibrated phenol (phenol:chloroform:isoamylalcohol 25:24:1), vortexed for 1 min and centrifuged for 5 min at 14 krpm. The aqueous phase was removed, re-extracted with 1 volume of chloroform and EtOH precipitated.

4.2.1.10 DNA precipitation

LiCl/EtOH

1/10 volume of 10 M LiCl and 2.5 volumes of EtOH were added to the sample, incubated for 30 min at -20°C and centrifuged for 30 min at 4°C and 14 krpm. The pellet was washed with 70% EtOH, dried and resuspended in TE.

NH₄Ac/Isopropanol

This precipitation was used for the removal of oligonucleotides from PCR reactions. 1/10 volume of 10 M NH₄Ac and 1 volume of isopropanol were added to the sample, incubated for 30 min at RT and centrifuged for 30 min at RT and 14 krpm. The pellet was washed with 70% EtOH, dried and resuspended in TE.

4.2.1.11 Ligation

Ligations were performed with 75 ng of vector DNA and 2 Weiss units ligase in a 10 μl reaction. The molar ratio of vector to insert was 1:3 for sticky-end ligations and 1:2 for blunt-end ligations. The reaction was incubated o/n at RT and transformed the next day.

4.2.1.12 Transformations of *E. coli*

Chemical competent cells (according to Hanahan, 1983)

DH5 α cell were inoculated in 50 ml SOB/10 mM MgCl₂ from an o/n culture. The culture was incubated at 37°C and harvested at an OD₅₇₈ of 0.5 (10 min, 4 krpm, and 4°C). The pellet was resuspended in 15 ml cold Tbf1 and incubated on ice for 10 min. After another centrifugation step the pellet was carefully resuspended in 1.8 ml cold Tbf2 and 200 μl aliquots were frozen in liquid nitrogen. Competent cells were stored at -80°C .

Tbf1: 30 mM KAc
50 mM MgCl₂
100 mM KCl
15% Glycerol
pH 5.8

Tbf2: 10 mM MOPS/NaOH, pH 7.0
75 mM CaCl₂
10 mM KCl
15% Glycerol

Transformation by heat shock

5 μl ligation reaction (out of 10 μl) were added to 50 μl competent cells and incubated for 30 min on ice. The cells were heat shocked for 90 sec at 37°C and 800 μl SOC were added. The transformation reaction was incubated for 1 h at 37°C while shaking. 150 μl were plated on LB/amp plates and incubated o/n at 37°C .

SOB: 5 g/l Yeast extract
20 g/l Tryptone
0.5 g/l NaCl
10 ml/l 250 mM KCl
5 ml/L MgCl₂
pH 7.5

SOC: SOB with 4% Glucose

Electro-competent cells

DH5 α cell were inoculated in 500 ml SOB/10 mM MgCl₂ with 5 ml of an o/n culture. The culture was incubated at 37°C till an OD₅₇₈ of 0.5 was reached, cooled on ice for 30 min and harvested at 4 krpm and 4°C for 10 min. The cells were washed with 500 ml, 300 ml and 15 ml cold water respectively and finally with 10 ml 15% glycerol. The pellet was carefully resuspended in 1.5 ml 10% glycerol and 50 μl aliquots were frozen in liquid nitrogen. Competent cells were stored at -80°C .

Electroporation

To the competent cells 5 μl DNA was added and incubated for 5 min on ice. The electroporation was performed in cuvettes with a Gene Pulser (BioRad) at 25 μF , 2.5 kV and 200 Ω . 1 ml SOC was immediately added and the suspension was shaken for 1 h at 37°C . The transformation was plated on LB/amp plates and incubated o/n at 37°C .

4.2.1.13 *E. coli* colony PCR

One clone was resuspended in 20 μl H₂O and heated for 5 min at 95°C . 5 μl were used as template in a 25 μl PCR reaction.

4.2.1.14 Isolation of plasmids from *E. coli*

Plasmid DNA for restriction analysis, cloning and transformation of *S. cerevisiae* was isolated by the alkaline lysis method of Birnboim and Doly (1979). 3 ml o/n culture in LB/amp was centrifuged for 1 min at 14 krpm. Lysis was performed with 100 µl cold solution I for 5 min at RT and 200 µl solution II for 5 min on ice. Precipitation of genomic DNA was achieved with 150 µl solution III and centrifugation for 5 min at 14 krpm. The supernatant was precipitated with 800 µl EtOH for 5 min on ice, centrifuged for 5 min, washed with 70% EtOH, dried and resuspended in 25 µl TE.

Solution I:	50 mM Glucose 10 mM EDTA 25 mM Tris-HCl 100 µg/ml pH 8.0	Solution II:	0.2 N NaOH 1% SDS
Solution III:	60 ml 5 M KCl 11.5 ml glacial acid 28.5 ml H ₂ O	TE:	10 mM Tris-HCl pH 8.0 1 mM EDTA pH 8.0

4.2.2 Working with yeast (general techniques)

4.2.2.1 Yeast transformation (adapted from Schiestl and Gietz, 1989)

50 ng plasmid DNA or 1-2 µg of PCR fragments were used for transformation of yeast cells. 50 ml of a logarithmically growing culture were harvested at 3 krpm for 5 min and 4°C, washed first with 1 volume of water and then with 1 ml of LiSorb. The pellet was resuspended in LiSorb at 10 µl/OD. To 100 µl of competent cells the DNA, 100 µg single stranded carrier DNA and 600 µl LiPEG were added. After shaking for 30 min at RT and the addition of 70 µl DMSO the cells were heat shocked for 15 min at 37°C, washed with water and plated on selective plates. For GFP taggings, galactose promoter integration and transformation on kanamycin plates, cells were recovered for 6 h at 25°C in YPD or YPG medium before plating on selective plates. Correct integration or tagging was verified by colony PCR, Western blotting or microscopy.

LiSorb:	100 mM LiAc 10 mM Tris/HCl pH 8.0 1 mM EDTA pH 8.0 1 M Sorbitol	LiPEG:	100 mM LiAc 10 mM Tris/HCl pH 8.0 1 mM EDTA pH 8.0 40% PEG 3350
---------	--	--------	--

4.2.2.2 Isolation of genomic DNA

100 OD of a logarithmically growing culture were harvested for 10 min at 3 krpm and the pellet was resuspended in 1 ml NTES buffer supplemented with 1 mg RNase. The sample was transferred to 4 1.5 ml cups and glass beads were added to the meniscus. Cells were lysed for 30 min at 4°C and 1800 rpm. After a phenol/chloroform extraction the aqueous phase was EtOH precipitated. The dried pellet was resuspended in 50 µl TE. The genomic DNA was either XhoI or NotI digested and analyzed on an agarose gel.

NTES:	10 mM Tris/HCl pH 8.0 100 mM NaCl 1 mM EDTA pH 8.0
-------	--

4.2.2.3 Yeast colony PCR

One clone was resuspended in 25 µl NTES and glass beads were added to the meniscus. The sample was shaken for 30 min at 1800 rpm and 4°C and phenol extracted. 0.5 µl of the aqueous phase was used as template for the PCR.

4.2.2.4 Mating

An α and an a mating strain were freshly streaked out on YPD-plates and the same amount of both was mixed. After 6 h zygote formation could be observed.

4.2.2.5 Sporulation, tetrad dissection

For sporulation diploid strains were inoculated in 10 ml of sporulation medium and incubated for 4 to 6 days at 25°C. For tetrad dissection 1 ml was harvested and resuspended in 50 µl sorbitol buffer with 10 U zymolyase for 20-35 min at 30°C. The reaction was stopped by the addition of 1 ml cold sorbitol buffer. 20 µl were spotted on a selective plate and tetrads were dissected with a micromanipulator.

Sorbitol buffer:	1 M Sorbitol 10 mM Tris/HCl pH 7.5	Zymolyase:	500 U/ml H ₂ O
------------------	---------------------------------------	------------	---------------------------

4.3 Biochemical techniques (general methods)

4.3.1 Yeast protein extracts

About 10-20 OD₅₇₈ were harvested for 5 min at 3 krpm and 4°C and washed with 1 ml ESB buffer. The pellet was resuspended in ESB at a concentration of 2 µl/OD, heated for 3 min at 95°C and frozen in liquid nitrogen. In order to lyse the cells glass beads were added to the meniscus and shaken for 30 min at 4°C and 1800 rpm. After lysis, the tube was punctuated with a hot needle and placed on top of a 15 ml tube and a centrifugation for 3 min at 2.5 krpm and 4°C followed. The lysate was transferred to a new tube and clarified for 30 min at 14 krpm and 4°C. The protein concentration of the supernatant was determined according to 5.3.2.

ESB buffer: 80 mM Tris/HCl pH6.8
2% SDS
10% Glycerol
1.5% DTT

4.3.2 Bradford

Protein concentration was determined after the method of Bradford (1976). To 1 µl sample and 99 µl of water 900 µl of Bradford solution was added and incubated for 5 min at RT. The absorption of the sample was measured at 595 nm. To determine the concentration of the sample a standard curve with rabbit IgG ranging from 0 – 40 mg/ml was used.

5 x Bradford solution: 500 mg/l Coomassies Brilliant Blue G250
250 ml/l EtOH
500 ml/l H₃PO₄

4.3.3 SDS-PAGE

Separation of proteins by SDS polyacrylamide gel electrophoreses was performed after the method of Leammli and King (1970). 8-15% SDS-acrylamide gels were used.

Running buffer: 3 g/l Tris Base
14.2 g/l Glycin
1 g/l SDS

4.3.4 Western blotting

Proteins that have been separated on a SDS polyacrylgel were transfered onto a PVDF membrane with a blotting apparatus from BioRad. The semi dry method of Kyshe-Andersen (1984) was used. The transference took place at 15 V for 1 h. The membrane was blocked for 1 h at RT with blocking buffer and incubated 1 h with the primary antibody. After 3 washes with blocking buffer for 10 min the secondary antibody was applied for another hour. The membrane was washed again 3 x 10 min with blocking buffer and 2 x 5 min with assay buffer. For the visualization of the formed antibody complexes the reaction of the alkaline phosphatase with the substrate CDP-Star was used. After 5 min incubation with CDP-Star the chemiluminescence could be detected on a film.

primary antibodies:	anti HA	1:1000	secondary antibodies:	anti mouse	1:5000
(in blocking buffer)	anti myc	1: 500	(in blocking buffer)	anti rat	1:5000
	anti FLAG	1:1000		anti rabbit	1:5000
	anti ProteinA	1:2500			
Blotting buffer:	5.8 g/l Tris Base		5 x PBS:	51.5 g/l Na ₂ HPO ₄ x 2H ₂ O	
	2.9 g/l Glycin			11.75 g/l NaH ₂ PO ₄ x H ₂ O	
	0.38 g/l SDS			20 g/l NaCl	
				pH 7.4	
Blocking buffer:	0.2% Casein		Assay buffer:	0.1 M Diethanolamin	
	0.1% Tween-20			1 mM MgCl ₂	
	in 1 x PBS			pH 10	

4.4 Special methods

4.4.1 Construction of *ame1 ts* mutants (adapted from Janke et al., 2001)

4.4.1.1 Cloning of a temperature sensitive *ame1* parental strain

Construction of a AME1 shuffle strain

Since *AME1* is an essential gene a shuffle strain had to be constructed for its analysis. To this end the *AME1* gene was disrupted in the diploid strain YPH501 by genomic integration of the PCR product of primers AME1-S2 and AME1-9/KAN-1 with pYM12 as template. The disruption was verified by colony PCR (AME1-5 and KAN-HIS) and the strain transformed with plasmid pAW885, carrying a wild type copy of *AME1* in a pRS416 (URA3) backbone. The diploid strain was sporulated and tetrads dissected on YPD + G418 plates. The *AME1* shuffle strain YAW418 was obtained this way.

Mutagenesis of AME1 by error prone PCR

AME1 was isolated by PCR from yeast genomic DNA using primers AME1-7 and AME1-8 and blunt-end ligated with an XhoI/XbaI-linearized pBSISK plasmid. The 1.6 kb *AME1* fragment was subcloned with XhoI and XbaI into pRS416. The resulting plasmid, pAW885 was used as template (80ng) for the error prone PCR with primers AME1-4 and M2 in a 100 µl reaction. In order to introduce mutations in *AME1* standard PCR conditions had to be changed: Primer concentration was reduced from 0.5 pmol to 0.3 pmol, instead of 2.5 mM MgCl₂ a mixture of 1.5 mM MgCl₂ and 1 mM MnCl₂ added and the amount of Gold Star Taq-Polymerase was increased from 2.3 U to 5 U. Finally an imbalance of dNTPs was added (200µM for dATP and dGTP vs. 400 µM for dCTP and dTTP). The PCR reaction was initially denatured for 3 min at 95°C, followed by 35 reaction-cycles with 30 sec at 94°C / 45 sec at 53°C / 1min 45 sec at 72°C, and a final extension step of 7 min at 72°C. The mutagenized PCR product was cut with DpnI (to remove the non-mutagenized plasmid used as template), EtOH- precipitated and used for yeast transformation.

Transformation and ligation of ame1 ts alleles

pJO882 containing a wild type copy of *AME1* in pRS415 was cut with BamHI and SpeI. 75 ng of this vector together with 5 µl of the mutagenized PCR product were transformed into the *AME1* shuffle strain (YAW418) without prior ligation. Cells were resuspended in 1 ml medium without leucine, plated on 10 leu- plates and incubated for 3 days at 23°C. Transformants were replica plated twice on FOA plates, to shuffle out the *AME1* wild type copy. Clones were tested for *ts* growth at 37°C.

Isolation of ts plasmids from yeast

The DNA of the *ts* clones was isolated and transformed into electro-competent *E. coli* cells. Plasmids were prepared and digested with ApaI in order to distinguish between the URA3 wild type plasmid and pRS415 plasmid. pAW891 was obtained this way.

Integration of the ame1 ts alleles in yeast

In order to transform the *ts* alleles into yeast, pAW891 was cut with XbaI and XhoI and sticky-end ligated into the integration vector pRS305 resulting into pAW896. The plasmid was cut in the LEU2-marker with Eco91I and transformed into shuffle strain YAW418. After 2 rounds of counter selection on FOA the temperature sensitivity was verified. One clone, YAW457 contained the *ame1-2 ts* allele used for further investigation.

Bar1 disruption in the ame1-2 ts strain

In order to make yeast cells more sensitive to alpha factor, the *BAR1* gene was disrupted by integration of PvuII-linearized pMS746, using the recyclable *HIS3* marker. Transformants were verified for their sensitivity against 250 ng/ml alpha factor. The *HIS3* marker was recycled by a method adapted from Güldener et al. (1996). The strain was transformed with plasmid pSH47 containing the Cre-recombinase under the control of a galactose inducible promoter. Transformants were grown o/n in medium containing raffinose. At an OD₅₇₈ of 0.5 2% galactose was added and the incubation continued for another 24 h. Finally transformants were plated on FOA containing plates. After 2 rounds of counter selection on FOA the clones were tested for no growth on his- and ura- plates. The resulting YAW481 strain was used for all subsequent manipulations.

4.4.1.2 Construction of *ame1-2* strains for functional analysis

Spindle labeling with GFP-tubulin

Plasmid pASF125 was cut with StuI and *TUB1-GFP* was integrated into the *URA3* locus. Clones with a strong fluorescent signal were chosen for analysis.

CEN5 labeling with GFP

For fluorescence labeling of centromere 5, plasmid pCJ092 containing the GFP labeled tet-repressor was cut with StuI and integrated into the *ADE2* locus. In a second step a tet-operator sequence was introduced close to the centromeric region of chromosome V.

Galactose inducible genes

For construction of a repressible *CDC20* strain, the PCR product of ON R3-CDC20 and F4-CDC20 with pFA6a-HIS3MX6-GAL-3HA as template was integrated into yeast. Clones were verified by no growth on glucose.

Depletion of Mad2

In order to deplete for the Mad2 protein, a galactose inducible promoter followed by ubiquitine and a single arginine residue was introduced in front of the gene. Cells were grown o/n in galactose-containing medium and shifted for 12 h to glucose-containing medium. The depletion was verified by immunoblotting.

4.4.2 Epitopal tagging of genes

For epitopal tagging of endogenous genes and for gene deletions, the PCR based method of Knop et al., (1999) was used. Integration cassettes were amplified by PCR with oligonucleotides containing an additional 50 bp adapter sequence required for genomic integration. Most of the tags used in this work were introduced at the C-terminus of the respective gene. PCR reactions and yeast transformations were performed as previously described. Integrations were verified by colony PCR or immunoblotting.

4.4.3 Cell synchronization

Alpha factor arrest

All strains synchronized by alpha factor contained a disrupted *BAR1* gene. 250 ng/ml alpha factor was added to a logarithmically growing culture at an OD₅₇₈ of 0.3-0.5. After 2.5-3 h incubation, more than 90% of the cells were arrested in G1 with a so-called shmoo. Cells were released from the arrest by washing and resuspension in fresh medium and shifted to the restrictive temperature for subsequent analysis.

Alpha factor: 1 mg/ml in 0.1 M NaAc pH 5.6

Metaphase arrest in the absence of spindles (Nocodazole arrest)

To a logarithmically growing culture 15 µg/ml nocodazole was added at an OD₅₇₈ of 0.3-0.5. After 3 h incubation, more than 90% of the cells were arrested in G2 with large buds. Cells were released from the arrest by washing and resuspension in fresh medium and shifted to the restrictive temperature for subsequent analysis.

Nocodazole: 10 mg/ml in DMSO

Metaphase arrest in the presence of spindles (Cdc20 depletion)

In order to repress *CDC20* gene expression a galactose inducible promoter was integrated in front of its ORF. In order to deplete for Cdc20, a logarithmically growing culture was shifted from YPG to YPD medium. After 3 h incubation at 23 or 37°C, cells were large budded and arrested in metaphase. Cells could be released from the block by washing and resuspension in YPGR.

Protein overexpression (Esp1, Cdc14)

Strains with ESP1 or CDC14 under the control of a galactose inducible promoter were grown o/n in medium containing raffinose. Overexpression was induced at an OD₅₇₈ of 0.3-0.5 with 3% galactose for indicated periods of time.

4.4.4 Microscopy

All microscopy samples were analyzed on a Carl Zeiss LSM confocal laser scanning microscope equipped with a 488 nm excitation filter and an argon ion laser.

Imaging of fixed GFP- tagged strains

1 ml of yeast culture was harvested, fixed with 3.7 % formaldehyde for 5 min at RT, washed twice with water and kept on ice until the microscopical evaluation. For a 3 dimensional resolution of spindles, 5 z stacks were acquired and maximal intensity projection calculated.

Live time imaging of GPP-tagged strains

200 µl of cells growing in microscopy medium at an OD₅₇₈ of 0.55 were spotted on a glass bottom culture dish preincubated for 10 min with 6% concavalin A. After 30 – 60 min incubation at 37°C, the rich medium was changed against 3 ml of SD medium and the plate was set up in a temperature controlled chamber on the microscope. Time-lapse sequences were recorded in 60 sec intervals by scanning through 5 z stacks. For all pictures maximal intensity projections were calculated.

4.4.5 Quantification of Pds1-levels

About 5 OD₅₇₈ of a strain with myc-tagged Pds1 were harvested at different time points, lysed and the protein concentration determined. For each time point 40 µg total protein extract were analyzed by SDS-PAGE and immunoblotting. Chemoluminescence was detected with a Fluor-STM-Multi Imager (BioRad) and the software Quantity One.

4.4.6 FACS analysis

For each time point about 2 OD₅₇₈ of cells were harvested and fixed o/n with 10 ml of 70% EtOH. Cells were washed with 50 mM Tris buffer pH 7.5, resuspended in 1 ml Tris buffer supplemented with 2 mg RNase and shaken for 4 h at 37 °C. The buffer was exchanged for 500 µl pepsin solution and the incubation continued for another 30 min. For DNA staining the sample was washed with 1 ml staining buffer and resuspended in 400 µl propidium iodide solution. The sample was diluted 1:50, so that 300 counts/min were achieved and analyzed with a FACS Calibur (Becton Dickinson). For a measurement 10 000 events were counted at low flow rate. Data were evaluated with the CellQuestPro software.

10 x RNase:	10 mg/ml in 10 mM Tris/HCl pH 7.5 15 mM NaCl heat 15 min at 100°C slowly cool down to RT	Pepsin solution:	50 mg Pepsin 550 µl 1 N HCl in 9.5 ml H ₂ O
Staining solution:	180 mM Tris/HCl pH 7.5 180 mM NaCl 70 mM MgCl ₂	Propidium iodide:	5 mg/ml (100 x) in staining solution

4.4.7 Chromatin immunoprecipitation - ChIP (adapted from Hecht et al., 1998)

At an OD₅₇₈ of 0.5 50 ml o/n culture was shifted for 3.5 h to 37°C. Cells were harvested at 3 krpm and 37°C for 5 min, washed with 1 volume of water and fixed in 45 ml H₂O with 1.25 ml 37% formaldehyde. After shaking for 45 min at RT cells were washed twice with 1 volume of PBS, resuspended in 1 ml PBS and transferred to a 2 ml cup. After one further centrifugation step, the pellet was resuspended in 200 µl lysis buffer, glass beads added to the meniscus and lysis performed for 30 min at 4°C and 1800 rpm. The efficiency of the lysis was controlled by light microscopy, the tube punctuated with a hot needle and set on top of a 15 ml tube. Glass beads were removed by centrifugation for 2 min at 1 krpm and 4°C and the lysate was sonified (90 sec, 50 %, interval, 60 % output) in an ice/water bad. After transfer into a 1.5 ml tube the sample was centrifuged for 30 min at 14 krpm and 4°C. 20 µl of the supernatant representing the input were stored o/n at 4°C. The rest was added to 10 µl of Protein A Sepharose CL-4B matrix and incubated o/n at 4°C with the respective antibody. The next day, beads were washed 3x with 200 µl lysis buffer, 2x with 200 µl WI and WII buffers respectively and once with 200 µl TE. In between each washing step the beads were precipitated by centrifugation for 1 min at 1 krpm. Elution was performed with 130 µl elution buffer for 10 min at 65°C. Beads were pelleted for 2 min at 14 krpm and 120 µl of the supernatant decrosslinked for 6 h at 65°C. 100 µl elution buffer was added to the input from the previous day and also incubated for 6 h at 65°C. Proteins were digested in 120 µl TE with 15 µl proteinase K and 1 µg carrier DNA. After phenol extraction of peptides, the DNA was precipitated with 25 µl 5 M LiCl in 50 mM Tris/HCl pH 8 and 600 µl EtOH. The pellet was dried and resuspended in TE at a ratio of 1 OD/µl for the input and 0.2 OD/µl for the IP. 5 µl of a 1:40 dilution of the input and a 1:5 dilution of the IP were used as template for a triplex PCR with 3 different primer sets: ChrIII-1/2 (4 kb from CEN, 213 bp product), CEN3-12/13 (at the centromere, 243 bp product) and ChrIII-3/4 (1.9 kb from CEN, 321 bp product). dNTPs were added at a concentration of 200 µM and the ratio of the primers varied from 0.3 µM to 1.2 µM, so that an equimolar amplification of all 3 products was achieved. 1.5 U polymerase (peqLab) was used for a 50 µl reaction. PCR products were run on an 8% acrylamide gel with 0.5 x TBE as running buffer.

PBS:	140 mM NaCl 2.5 mM KCl 8.1 mM Na ₂ HPO ₄ x 2H ₂ O 1.5 mM KH ₂ PO ₄	Lysis buffer:	50 mM Hepes/KOH pH 7.5 140 mM NaCl 1 mM EDTA pH 8.0 1% Triton X100 0.1% NaDOC
Wash I (WI):	50 mM Hepes/KOH pH 7.5 500 mM NaCl 1 mM EDTA pH 8.0 1% Triton X100 0.1% NaDOC	Wash II (WII):	10 mM Tris/HCl pH 8.0 250 mM LiCl 1 mM EDTA pH 8.0 0.5% NaDOC 0.5% NP-40
TE:	10 mM Tris-HCl pH 8.0 1 mM EDTA pH 8.0	Elution buffer:	1% SDS in TE

Proteinase K: 10 mg/ml in
1 mM CaCl₂
5 mM Tris/HCl pH 8.0

TBE (5 x): 54 g/l Tris Base
27.5 g/l Boric acid
10 mM EDTA pH 8.0

4.4.8 Quantifications of ChIP-experiments by real-time PCR

The amount of *CEN3* in the input and the IP fractions of a ChIP was quantified by real-time PCR using the TagMan method (Heid et al., 1996). A 20 µl PCR reaction with 4 µl template was set up. Dilution factors varied from 1:50 to 1:200 in case of the input and from 1:10 to 1:150 in case of the IP. Primers were used at a concentration of 0.9 µM and the TaqMan probe (5'FAM/3'TAMRA) at a concentration of 0.25 µM. The reaction also contained 10 µl Roxmix (AB-1139/Abgen) and 2 mM MgCl₂. Samples were pipetted in a 96 well plate (AB-1100/Abgene) and sealed afterwards (AB-1170/Abgene). Thermal cycling and detection of fluorescent signals were performed with an ABI Prism 7700 Sequence Detection System (PE Biosystems).

For each batch of samples a standard curve with 0.02 to 0.32 attomol of DNA was measured. Samples were analyzed as duplicates in at least two independent runs. The maximally tolerated deviation in the final DNA content was 15%. DNA contents were normalized for the difference in the input sample of the mutant and the wild type. The relative amount of *CEN3* DNA recovered from *ame1-2* was determined in comparison to wild type. The recovery from wild type was set to 1.

4.4.9 TAP purification (adapted from Puig et al., 1999)

For isolation of kinetochore complexes the tandem affinity purification method was used. The TAP tag contained a Prot A and a CBP domain separated by either a TEV or a PreScission protease cleavage site.

For one TAP purification, 1-3 l of yeast culture (OD₅₈₇ of 2) were harvested for 15 min at 5 krpm and 4°C. The pellet was washed with 50 ml of cold water and 25 ml of lysis buffer. At this step the pellet could be frozen in liquid nitrogen and stored at -80°C. The next day, the pellet was thawed in a 37°C water bath and resuspended in lysis buffer with inhibitors at an concentration of 100 OD/ml. Cells were lysed with glass beads for 30 min at 4°C and 1800 rpm (IKA Vibrax VXR shaker). The lysate was clarified at 17 krpm and 4°C for 30 min and preequilibrated huIgG beads were added (10 µl of 50% slurry to 100 OD). After a 3 h to o/n rotation at 4°C, the beads were collected in a chromatography column (BioRad) and washed with 10 ml of WI, WII and TEV cleavage buffer, respectively. At this step the complex was either eluted with acetic acid or cleaved off the beads by TEV or PreScission protease. For acid elution 2 x 0.5 ml 0.5 M NH₄Ac/HAc, pH 3.4 were used. The sample was vacuum dried, resuspended in loading buffer and analysed by SDS-PAGE. The TEV cleavage reaction (2.5 U TEV/1000 ODs) was performed in a Mobicol column in 200 µl buffer supplemented with 0.5 mM DTT for 4 h at 16°C on a turning wheel. PreScission cleavage (2 U/1000 OD) was performed under the same conditions but at 4°C. Samples were eluted with a syringe into a new cup and glycerol added to a final concentration of 20%. Samples were frozen in liquid nitrogen and stored at -80°C.

Lysis buffer: 50 mM Tris/HCl pH 8.0
(Okp1-complex) 140 mM KCl
5 mM MgCl₂
10% glycerol
1% Triton X-100
0.05% NaDOC

Protease inhibitors: E-64 10 µM
(final concentration) Phenantroline 1 mM
Pepstatin 10 µg/ml
Leupeptin 10 µM

Wash I (WI): lysis buffer with 1mM PMSF

TEV buffer: 50 mM Tris/HCl pH 7.5
10 mM NaCl
1.5 mM MgCl₂
0.15% NP-40

Lysis buffer: 50 mM Tris/HCl pH 8
(other complexes) 140 mM NaCl
1 mM EDTA pH 8
1% Triton X-100
0.05% NaDOC

Wash II (WII): 10 mM Tris/HCl pH 8
250 mM LiCl
1 mM EDTA
0.5% NP-40
0.5% NaDOC
1 mM PMSF

4.4.10 Complex binding assays

In order to test for the interaction between two kinetochore complexes, they were individually affinity-purified from 1500 ODs of yeast cells by a TAP-tag and bound to IgG beads (75 µl IgG beads, 50% slurry). One complex was released from the beads by TEV or prescission protease cleavage. It was subsequently added in parallel to either the immobilized first complex or empty IgG beads and incubated for 1h at RT. Beads were washed with 5 ml TEV buffer and eluted with 2 x 250 µl 0.5 M NH₄Ac/HAc, pH 3.4. The eluate was lyophilized, resuspended in SDS sample buffer and analyzed by immunoblotting.

5. MATERIALS

5.1 Plasmids, strains and oligonucleotides

5.1.1 Plasmids

Plasmid	Gene	primers/ enzymes	Reference
pJO879	<i>AME1</i> (P-ORF-Term)		this study
pJO882	<i>AME1</i> (P-ORF-Term); <i>LEU2</i>		this study
pAW885	<i>AME1</i> (P-ORF-Term); <i>URA3</i>		this study
pAW891	<i>ame1-2</i> (P-ORF-Term); <i>LEU2</i>		this study
pAW896	<i>ame1-2</i> (P-ORF-Term); <i>LEU2</i>	BstEII	this study
pAW914	TAP-tag with prescission cleavage site; <i>klURA3</i>		this study
pAW1035	<i>ame1-2</i> (ORF) - <i>ADE2</i> (P-ORF-Term) - terminator region <i>AME1</i>	PstI/XhoI	this study
pAW1010	<i>GAL-Flag-ESP1</i> (protease active); <i>ADE2</i>	BamHI/EcoRV	this study
pASF125	<i>TUB1-GFP</i> ; <i>URA3</i>	StuI	Straight et al., 1997
pBL927	<i>bub2::TRP1</i>	PstI	this study, B. Lang
pBS1539	TAP-tag (CBP-TEV-ProtA); <i>klURA3</i>	TAP-fw/rev	Puig et al., 2001
pCJ092	<i>tetR-GFP</i> ; <i>ADE2</i>	StuI	Janke et al., 2002
pCJ141	<i>TUB1-CFP</i> ; <i>TRP1</i>	SnaBI	
pFA6A-13Myc-HIS3MX6	<i>MYCx13</i> ; <i>HIS3</i>	F2/R1	Longtine et al., 1998
pFA6a-GFP(S65T)-HIS3MX6	<i>GFP(S65T)-HIS3MX6</i>	F2/R2	Longtine et al., 1998
pFA6a-HIS3MX6-GAL-3HA	<i>HIS3MX6-GAL-3HA</i>	R3/F4	Longtine et al., 1998
pFA6a-TRP1-GAL-3HA	<i>TRP1-GAL-3HA</i>	R3/F4	Longtine et al., 1998
pFA6a-kanMX6-GAL-3HA	<i>kanMX6-GAL-3HA</i>	R3/F4	Longtine et al., 1998
pGP199-1	<i>3xGFP-klTRP1</i>	S2/S3	
pGP250-1	<i>sli15</i> (S335A S427A 373A S462A S437A T474A)- <i>GFP-kanMX6</i>	StuI	Pereira and Schiebel, 2003
pJO608	<i>mad2::TRP1</i>	BamHI/KpnI	constructed by J. Ortiz
pJO719	<i>klTRP1-GAL-Ubi-R</i>		Scharfenberger et al., 2003
pMS746	<i>bar1::loxP-HIS3-loxP</i>	ClaI/PvuII	constructed by M. Scharfenberger
pSH47	<i>GAL-CRE</i> ; <i>ARS</i> ; <i>CEN</i> ; <i>URA3</i>		Güldener et al., 1996
pSM1023	<i>3xGFP-kanMX6</i>	S2/S3	
pXH136	<i>ChrV-tetO2x112-URA3-ChrV</i> , integration close to <i>CEN5</i>	BamHI	He et al., 2000
pYM2	<i>HAX3-HIS3MX6</i>	S2/S3	Knop et al., 1999
pYM3	<i>HAX6-klTRP1</i>	S2/S3	Knop et al., 1999
pYM6	<i>MYC9-klTRP1</i>	S2/S3	Knop et al., 1999
pYM7	<i>ProtA-kanMX6</i>	S2/S3	Knop et al., 1999
pYM10	<i>TEV-ProtA-7xHIS-HIS3MX6</i>	S2/S3	Knop et al., 1999
pYM12	<i>EGFP-kanMX4</i>	S2/S3	Knop et al., 1999
pYM28	<i>EGFP-HIS3MX6</i>	S2/S3	Knop et al., 1999
pYM29	<i>EGFP-klTRP1</i>	S2/S3	Knop et al., 1999
pYM-N34	<i>kanMX4-MET25</i>	S1/S4	Knop et al., 1999

5.1.2 *S. cerevisiae* strains

All *S. cerevisiae* strains used in this work either were derived from YPH501 (diploid strain), YPH499 (haploid strain) or W303.

Strains	Genotype	Reference
Wild type and <i>ame1-2</i> strains		
YMS231	<i>MATa sst1::loxP</i>	Scharfenberger et al., 2003
YAW481	<i>MATa sst1::loxP ame1::kanMX6 leu2::ame1-2::LEU2</i>	this study
Strains with GFP-tagged spindles		
YNG307	<i>MATa sst1::loxP ura3::TUB1-GFP::URA3</i>	
YAW498	<i>MATa sst1::loxP ura3::TUB1-GFP::URA3 ame1::kanMX6 leu2::ame1-2::LEU2</i>	this study
YAW641	<i>MATa sst1::loxP cdc20::kanMX6::pGAL1-3HA-CDC2 cdc15-1 ura3::TUB1-GFP::URA3</i>	this study
YAW642	<i>MATa sst1::loxP cdc20::TRP1::pGAL1-3HA-CDC20 cdc15-1 ura3::TUB1-GFP::URA3 ame1::kanMX6 leu2::ame1-2::LEU2</i>	this study
YAW592	<i>MATa sst1::loxP bub2::TRP1 ura3::TUB1-GFP::URA3 leu2::LEU2</i>	this study
YAW593	<i>MATa sst1::loxP bub2::TRP1 ura3::Tub1-GFP::URA3 ame1::kanMX6 leu2::ame1-2::LEU2</i>	this study
YAW1005	<i>MATa sst1::loxP mad2::pGAL1-UbiR-MAD2::klTRP1 ura3::TUB1-GFP::URA3</i>	this study
YAW1006	<i>MATa sst1::loxP mad2::pGAL1-UbiR-MAD2::klTRP1 ura3::TUB1-GFP::URA3 ame1::kanMX6 leu2::ame1-2::LEU2</i>	this study
YAW972	<i>MATa sst1::loxP lys2::pGal-Flag-ESP::LYS2 kan::pMET-CDC20::kanMX4 ura3::TUB1-GFP</i>	this study
YAW916	<i>MATa sst1::loxP lys2::pGal-Flag-ESP::LYS2 ura3::Tub1-GFP::URA3 ame1::kanMX6 leu2::ame1-2::LEU2</i>	this study
Y 1539	<i>MATa scc1(TEV268)-3HA::LEU Gal-NLS-myc9-TEVprotease-NSL2::TRP1(x10) MET-HA3-CDC20::TRP GAL-CDC14-pk::URA his3::TUB1p-yEGFP-TUB1::HIS3</i>	Higuchi and Uhlmann, 2005
YAW988	<i>MATa scc1(TEV268)-3HA::LEU Gal-NLS-myc9-TEVprotease-NSL2::TRP1(x10) MET-HA3-CDC20::TRP GAL-CDC14-pk::URA his3::TUB1p-yEGFP-TUB1::HIS3 AME1::ame1-2::ADE2</i>	this study, derived from, Y1539
YAW983	<i>MATa sst1::loxP ade2::Sli15(6A)-GPF-kanMX6::ADE2 ura3::TUB1-GFP::URA3</i>	this study
YAW985	<i>MATa sst1::loxP ade2::Sli15(6A)-GPF-kanMX6::ADE2 ura3::TUB1-GFP::URA3 ame1::kanMX6 leu2::ame1-2::LEU2</i>	this study
YAW646	<i>MATa sst1::loxP ndc80-1 ame1::kanMX6 leu2::ame1-2::LEU2 ura3::GFP-Tub-URA3</i>	this study
Strains with tagged <i>CEN5</i>		
YMS331	<i>MATa sst1::loxP ade2::tetR-GFP::ADE2 ura3::CEN5-tetO2x112::URA3 leu2::LEU2</i>	Scharfenberger et al., 2003
YAW574	<i>MATa sst1::loxP ade2::tetR-GFP::ADE2 ura3::CEN5-tetO2x112::URA3 ame1::kanMX6 leu2::ame1-2::LEU2</i>	this study
YAW603	<i>MATa sst1::loxP ade2::tetR-GFP::ADE2 ura3::CEN5-tetO2x112::URA3 cdc20::TRP1::pGAL-CDC20 ame1::kanMX6 leu2::ame1-2::LEU2</i>	this study
Strains with tagged <i>Pds1/Slk19</i>		
YMS299	<i>MATa sst1::loxP PDS1-9myc::klTRP1</i>	Scharfenberger et al., 2003
YAW522	<i>MATa sst1::loxP PDS1-9myc::klTRP1 ame1::kanMX6 leu2::ame1-2::LEU2</i>	this study
YAW840	<i>MATa sst1::loxP PDS1-9MYC::klTRP1 scc1::pGAL1-3HA-SCC1::HIS3</i>	this study
YAW932	<i>MATa sst1::loxP PDS1-13myc::HIS3MX6 cdc20::pGAL1-3HA-CDC20::TRP1</i>	this study
YAW933	<i>MATa sst1::loxP PDS1-13myc::HIS3MX6 cdc20::pGAL1-3HA-CDC20::TRP1 ame1::kanMX6 leu2::ame1-2::LEU2 ura3::TUB1-GFP::URA3</i>	this study
YAW964	<i>MATa sst1::loxP SLK19-13myc::HIS3MX6 ura3::TUB1-GFP</i>	this study
YAW965	<i>MATa sst1::loxP SLK19-13myc::HIS3MX6 ura3::Tub1-GFP-URA3 ame1::kanMX6 leu2::ame1-2::LEU2</i>	this study
Strains with GFP-tagged <i>CDC14</i>		
YAW666	<i>MATa sst1::loxP CDC14-GFP::HIS3MX6 cdc15-1</i>	this study
YAW667	<i>MATa sst1::loxP CDC14-GFP::HIS3MX6 cdc15-1 ame1::kanMX6 leu2::ame1-2::LEU2</i>	this study
YMS707	<i>MATa sst1::loxP CDC14-GFP::HIS3MX6 cdc15-1 mad2::TRP1</i>	this study

YAW921	<i>MATa sst1::loxP CDC14-GFP::HIS3MX6 cdc15-1 trp1::pGAL-SCC1::TRP1</i>	this study
YAW889	<i>MATa sst1::loxP CDC14-GFP::HIS3MX6 cdc15-1 cdc20::GAL-3HA-CDC20::kan trp1::TRP1</i>	this study
YAW890	<i>MATa sst1::loxP CDC14-GFP::HIS3MX6 cdc15-1 cdc20::GAL1-3HA-CDC20::TRP1</i> <i>ame1::kanMX6 leu2::ame1-2::LEU2</i>	this study
YAW1026	<i>MATa sst1::loxP CDC14-GFP::HIS3MX6 ame1::kanMX6 leu2::ame1-2::LEU2</i>	this study

Strains with GFP-tagged genes

YMS679	<i>MATa sst1::loxP AME1-3GFP::kanMX6 TUB1-CFP::TRP1</i>	this study
YAW649	<i>MATa sst1::loxP SLK19-GFP::HIS3MX6</i>	this study
YAW676	<i>MATa sst1::loxP SLK19-GFP::HIS3MX6 ame1::kanMX6 leu2::ame1-2::LEU2</i>	this study
YAW685	<i>MATa sst1::loxP SPC19-GFP::klTRP1</i>	this study
YAW687	<i>MATa sst1::loxP SPC19-GFP::klTRP1 ame1::kanMX6 leu2::ame1-2::LEU2</i>	this study
YMS696	<i>MATa sst1::loxP STU1-GFP::HIS3MX6</i>	this study
YAW698	<i>MATa sst1::loxP STU1-GFP::HIS3MX6 ame1::kanMX6 leu2::ame1-2::LEU2</i>	this study
YMS699	<i>MATa sst1::loxP BUB1-GFP::HIS3MX6</i>	this study
YAW711	<i>MATa sst1::loxP BUB1-GFP::HIS3MX6 ame1::kanMX6 leu2::ame1-2::LEU2</i>	this study
YAW724	<i>MATa sst1::loxP NDC80-GFP::HIS3MX6</i>	this study
YAW726	<i>MATa sst1::loxP NDC80-GFP::HIS3MX6 ame1::kanMX6 leu2::ame1-2::LEU2</i>	this study
YAW725	<i>MATa sst1::loxP SPC24-GFP::HIS3MX6</i>	this study
YAW727	<i>MATa sst1::loxP SPC24-GFP::HIS3MX6 ame1::kanMX6 leu2::ame1-2::LEU2</i>	this study
YMS739	<i>MATa sst1::loxP MAD2-3GFP::TRP1</i>	this study
YAW740	<i>MATa sst1::loxP MAD2-3GFP::TRP1 ame1::kanMX6 leu2::ame1-2::LEU2</i>	this study
YJO759	<i>MATa sst1::loxP SPC34-GFP::HIS3MX6</i>	this study
YAW734	<i>MATa sst1::loxP SPC34-GFP::HIS3MX6 ame1::kanMX6 leu2::ame1-2::LEU2</i>	this study
YJO757	<i>MATa sst1::loxP NUF2-GFP::HIS3MX6</i>	this study
YAW733	<i>MATa sst1::loxP NUF2-GFP::HIS3MX6 ame1::kanMX6 leu2::ame1-2::LEU2</i>	this study
YJO799	<i>MATa sst1::loxP SPC25-GFP::HIS3MX6</i>	this study
YAW782	<i>MATa sst1::loxP SPC25-GFP::HIS3MX6 ame1::kanMX6 leu2::ame1-2::LEU2</i>	this study
YMS849	<i>MATa sst1::loxP STU2-GFP::HIS3MX6</i>	this study
YAW850	<i>MATa sst1::loxP STU2-GFP::HIS3MX6 ame1::kanMX6 leu2::ame1-2::LEU2</i>	this study
YAW872	<i>MATa sst1::loxP DUO1-GFP::HIS3MX6</i>	this study
YAW873	<i>MATa sst1::loxP DUO1-GFP::HIS3MX6 ame1::kanMX6 leu2::ame1-2::LEU2</i>	this study
YAW881	<i>MATa sst1::loxP SPC105-GFP::HIS3MX6</i>	this study
YAW882	<i>MATa sst1::loxP SPC105-GFP::HIS3MX6 ame1::kanMX6 leu2::ame1-2::LEU2</i>	this study
YJO968	<i>MATa sst1::loxP MCM16-GFP::HIS3MX6</i>	this study
YAW963	<i>MATa sst1::loxP MCM16-GFP::HIS3MX6 ame1::kanMX6 leu2::ame1-2::LEU2</i>	this study

TAP-tagged strains

YJO359	<i>MATa sst1::loxP SPC105-ProtA::HIS3MX6</i>	
YAW427	<i>MATa sst1::loxP SPC25-TAP::URA3 NUF2-6HA::klTRP1</i>	this study
YAW453	<i>MATa OKP1-ProtA::kanMX6</i>	this study
YAW480	<i>MATa DAD1-STag-TEV-ZZ::kanMX6 DUO1-6HA::klTRP1</i>	this study
YAW512	<i>MATa sst1::loxP SPC25-TAP(prescission):: URA3 NUF2-6HA::klTRP1</i>	this study
YAW513	<i>MATa MTW1-TAP(prescission)::URA3 DSN1-3HA::kanMX6</i>	this study
YAW514	<i>MATa sst1::loxP OKP1-TAP(prescission)::URA3</i>	this study
YAW527	<i>MATa OKP1-TAP::URA3 MCM16-6HA::klTRP1</i>	this study

5.1.3 Oligonucleotides

All sequences are given in 5' to 3' direction. Adapter sequences are followed by a 50 bp sequence of the gene subjected to be modified.

Oligo.	Sequence
AME1-S2-1	TATATATATATATATATATATATATACATCTTTTGAACCAATTCCATCGATGAATTCGAGCTCG
AME1-9/KAN-1	TGTCTTGACTATTTGCGTGTTTCATTTAAAGAAAAACCTCAGTCCAGCGACATGGAGGCCCA
AME1-4	CACAACCTTCCTTAGTATGGAA
AME1-5	GCGGGATCCGGAGTGATGAAGGTGCGAAAC
AME1-7	TCCGCTCGAGCACATCTACTGGACGCCACGGAT
AME1-8	TGCTCTAGAGCAGGTGCGAACTGCTTGCTTGACTAAG
M2	TTGTGTGGAATTGTGAGCG
KAN-HIS	TGGGCCTCCATGTCGCTGG
MAD2-fUbiR	ATGTTAAATACTCGTACAAGAGTATTGAAAACCACTTCAAAGGGGGCCCAATAGCAGCGCGCGTAATACGACTCAC
MAD2-rUbiR	ACTCGAAAAATTCTGTAAGTGTCTTGTGAACCTTTAGTGATATTGATTGTGAGGATCCGTGCCTACCACCT

Adapter sequences

S1	CGTACGCTGCAGGTCGAC
S2	ATCGATGAATTCGAGCTCG
S3	CGTACGCTGCAGGTCGAC
S4	CATCGATGAATTCTCTGTCG
F2	CGGATCCCCGGGTAAATTAA
R1	GAATTCGAGCTCGTTTAAAC
R3	GCACTGAGCAGCGTAATCTG
F4	GAATTCGAGCTCGTTTAAAC
TAP-fw	TCCATGGAAAAGAGAAG
TAP-rev	TACGACTCACTATAGGG

ChIP primers

CH1-1	ACTTTGGCTTTCCGCTCGTG
CH1-2	GAAAGTCTTCTAGAGTTACAGG
CH1-3	GACCAGCATGTAGGAAGGTG
CH1-4	ACATTGATAAATTGCTCTCACCA
CEN3-12	GATCAGCGCCAAACAATATGG
CEN3-13	AACTTCCACCAGTAAACGTTTC

Real time PCR primers

CEN3-probe	TTAACTTTCGGAAATCAAATACACTAATATTTTA (5'-FAM; 3'-AMRA)
CEN3-fw	AGTCACATGATGATATTTGATTTTAT
CEN3-rev	ATTCAATGAAATATATATTTCTTACTATTT

5.2 Chemicals and enzymes

If not indicated differently, all chemicals were obtained from Applichem (Darmstadt). Materials of general use were provided by Greiner (Solingen), Sarstedt (Nümbrecht) or Neolab (Heidelberg).

Abgene (Hamburg)

Roxmix for RT-PCR, plates and sealing

Amersham (Freiburg)

Protein A Sepharose CL4-B, ECL detection system

Bio-Rad (Hercules)

PolyPrep chromatography columns, protein standards

Braun (Melsungen)

Glass beads (\varnothing 0.45-0.5 mm)

Calbiochem (La Jolla)

Alpha factor, G418 sulfate

Difco (Detroit)

Yeast extract, Tryptone, YNB

Fluca (Buchs)

Diethanolamine, Lithiumacetate, TEMED, Formaldehyde

ICN (Mannheim)

Zymolyase

Invitrogen (Karlsruhe)

TEV and Prescission protease, 4-12% Nupage gradient gels, anti-GFP

Kodak (New Haven)

x-ray films

MBI (St.Leon Roth)

Restriction enzymes, DNA ladders, dNTPs, λ phosphatase

Millipore (Bedford)

PVDF blotting membranes, sterile filtering devices

MWG-Biotech (Ebersberg)

Oligonucleotides, sequencing

NEB (Beverly)

Restriction enzymes

Pall (Dreieich)

Centricons

Pineda (Berlin)

Custom-ordered antibodies: anti-Ame1, anti-Cse4, anti-Dam1, anti-Mcm21, anti-Ndc10, anti-Ndc80, anti-Nsl1 and anti-Okp1

Qiagen (Hilden)

QiaexII glass milk for DNA isolation from agarose gels

Roche (Mannheim)

Anti-Myc, anti-HA, Expand long template PCR system kit, CDP-Star

Roth (Karlsruhe)

Colloidal Coomassie, EDTA, Glycine, Phenol, Tris

Santa Cruz (Heidelberg)

Anti-Mad2

Serva (Heidelberg)

Coomassie Brilliant blue R250 and G250, PEG 8000, Raffinose, SDS, Tween

Sigma (Deisenhofen)

Anti-rabbit, anti-mouse, anti-rat (all alkaline phosphatase labeled), human IgG agarose, Propidium iodide

Thermo (Ulm)

Oligonucleotides

5.3 Instruments

Agarose gel electrophoresis system	Pharmacia
ABI Prism 7700 Sequence Detection System	PE Biosystems
Blotting apparatus, Trans blot SD	Bio-Rad
Centrifuges	DuPont, Sorvall
Confocal scanning microscope, LSM510 meta	Zeiss
FACS Callibur	Becton Dickinson
Fluorescence microscope	Zeiss
FluorS-Multi Imager	Bio-Rad
Freezer -20°C	Liebherr
Freezer -80°C	Thermo Electron
Gel dryer	Bio-Rad
Heating blocks	Eppendorf
Incubators	Heraeus, Infors
Laminar flow	Enviroco
Light microscope	Zeiss
Micromanipulator for tetrad dissection	Singer Instruments
PCR mashines	Techne
Photometer	Thermo Electron
Power supplies, P25	Biometra
Rocker WT17	Biometra
SDS-PAGE apparatus	Bio-Rad
Sonifier B15	Branson
Table top centrifuges	Eppendorf
Ultrasound waterbath	Merck
Waterbath	Lauda
Water deionising facility, MilliQPlus	Millipore

7. REFERENCES

- Adames, N. R. and Cooper, J. A. (2000). Microtubule interactions with the cell cortex causing nuclear movements in *Saccharomyces cerevisiae*. *J Cell Biol* **149**, 863-74.
- Adames, N. R., Oberle, J. R. and Cooper, J. A. (2001). The surveillance mechanism of the spindle position checkpoint in yeast. *J Cell Biol* **153**, 159-68.
- Akhmanova, A. and Hoogenraad, C. C. (2005). Microtubule plus-end-tracking proteins: mechanisms and functions. *Curr Opin Cell Biol* **17**, 47-54.
- Asakawa, K., Yoshida, S., Otake, F. and Toh-e, A. (2001). A novel functional domain of Cdc15 kinase is required for its interaction with Tem1 GTPase in *Saccharomyces cerevisiae*. *Genetics* **157**, 1437-50.
- Baker, R. E., Fitzgerald-Hayes, M. and O'Brien, T. C. (1989). Purification of the yeast centromere binding protein CP1 and a mutational analysis of its binding site. *J Biol Chem* **264**, 10843-50.
- Baker, R. E. and Masison, D. C. (1990). Isolation of the gene encoding the *Saccharomyces cerevisiae* centromere-binding protein CP1. *Mol Cell Biol* **10**, 2458-67.
- Bardin, A. J. and Amon, A. (2001). Men and sin: what's the difference? *Nat Rev Mol Cell Biol* **2**, 815-26.
- Bardin, A. J., Visintin, R. and Amon, A. (2000). A mechanism for coupling exit from mitosis to partitioning of the nucleus. *Cell* **102**, 21-31.
- Bell, S. P. and Dutta, A. (2002). DNA replication in eukaryotic cells. *Annu Rev Biochem* **71**, 333-74.
- Biggins, S. and Murray, A. W. (2001). The budding yeast protein kinase Ipl1/Aurora allows the absence of tension to activate the spindle checkpoint. *Genes Dev* **15**, 3118-29.
- Biggins, S., Severin, F. F., Bhalla, N., Sassoon, I., Hyman, A. A. and Murray, A. W. (1999). The conserved protein kinase Ipl1 regulates microtubule binding to kinetochores in budding yeast. *Genes Dev* **13**, 532-44.
- Biggins, S. and Walczak, C. E. (2003). Captivating capture: how microtubules attach to kinetochores. *Curr Biol* **13**, R449-60.
- Bloecher, A., Venturi, G. M. and Tatchell, K. (2000). Anaphase spindle position is monitored by the BUB2 checkpoint. *Nat Cell Biol* **2**, 556-8.
- Blow, J. J. and Dutta, A. (2005). Preventing re-replication of chromosomal DNA. *Nat Rev Mol Cell Biol* **6**, 476-86.
- Bouck, D. and Bloom, K. (2005a). The role of centromere-binding factor 3 (CBF3) in spindle stability, cytokinesis, and kinetochore attachment. *Biochem Cell Biol* **83**, 696-702.
- Bouck, D. C. and Bloom, K. S. (2005b). The kinetochore protein Ndc10p is required for spindle stability and cytokinesis in yeast. *Proc Natl Acad Sci U S A* **102**, 5408-13.
- Bram, R. J. and Kornberg, R. D. (1987). Isolation of a *Saccharomyces cerevisiae* centromere DNA-binding protein, its human homolog, and its possible role as a transcription factor. *Mol Cell Biol* **7**, 403-9.
- Buonomo, S. B., Rabitsch, K. P., Fuchs, J., Gruber, S., Sullivan, M., Uhlmann, F., Petronczki, M., Toth, A. and Nasmyth, K. (2003). Division of the nucleolus and its release of CDC14 during anaphase of meiosis I depends on separase, SPO12, and SLK19. *Dev Cell* **4**, 727-39.
- Buvelot, S., Tatsutani, S. Y., Vermaak, D. and Biggins, S. (2003). The budding yeast Ipl1/Aurora protein kinase regulates mitotic spindle disassembly. *J Cell Biol* **160**, 329-39.
- Byers, B. and Goetsch, L. (1974). Duplication of spindle plaques and integration of the yeast cell cycle. *Cold Spring Harb Symp Quant Biol* **38**, 123-31.
- Byers, B. and Goetsch, L. (1975). Behavior of spindles and spindle plaques in the cell cycle and conjugation of *Saccharomyces cerevisiae*. *J Bacteriol* **124**, 511-23.
- Cahill, D. P., Kinzler, K. W., Vogelstein, B. and Lengauer, C. (1999). Genetic instability and darwinian selection in tumours. *Trends Cell Biol* **9**, M57-60.
- Cai, M. and Davis, R. W. (1990). Yeast centromere binding protein CBF1, of the helix-loop-helix protein family, is required for chromosome stability and methionine prototrophy. *Cell* **61**, 437-46.
- Carminati, J. L. and Stearns, T. (1997). Microtubules orient the mitotic spindle in yeast through dynein-dependent interactions with the cell cortex. *J Cell Biol* **138**, 629-41.
- Cerutti, L. and Simanis, V. (1999). Asymmetry of the spindle pole bodies and spg1p GAP segregation during mitosis in fission yeast. *J Cell Sci* **112** (Pt 14), 2313-21.
-

- Chan, G. K., Jablonski, S. A., Sudakin, V., Hittle, J. C. and Yen, T. J. (1999). Human BUBR1 is a mitotic checkpoint kinase that monitors CENP-E functions at kinetochores and binds the cyclosome/APC. *J Cell Biol* **146**, 941-54.
- Cheeseman, I. M., Anderson, S., Jwa, M., Green, E. M., Kang, J., Yates, J. R., 3rd, Chan, C. S., Drubin, D. G. and Barnes, G. (2002a). Phospho-regulation of kinetochore-microtubule attachments by the Aurora kinase Ipl1p. *Cell* **111**, 163-72.
- Cheeseman, I. M., Brew, C., Wolyniak, M., Desai, A., Anderson, S., Muster, N., Yates, J. R., Huffaker, T. C., Drubin, D. G. and Barnes, G. (2001). Implication of a novel multiprotein Dam1p complex in outer kinetochore function. *J Cell Biol* **155**, 1137-45.
- Cheeseman, I. M., Drubin, D. G. and Barnes, G. (2002b). Simple centromere, complex kinetochore: linking spindle microtubules and centromeric DNA in budding yeast. *J Cell Biol* **157**, 199-203.
- Chen, R. H., Brady, D. M., Smith, D., Murray, A. W. and Hardwick, K. G. (1999). The spindle checkpoint of budding yeast depends on a tight complex between the Mad1 and Mad2 proteins. *Mol Biol Cell* **10**, 2607-18.
- Chen, R. H., Shevchenko, A., Mann, M. and Murray, A. W. (1998). Spindle checkpoint protein Xmad1 recruits Xmad2 to unattached kinetochores. *J Cell Biol* **143**, 283-95.
- Chen, R. H., Waters, J. C., Salmon, E. D. and Murray, A. W. (1996). Association of spindle assembly checkpoint component XMAP2 with unattached kinetochores. *Science* **274**, 242-6.
- Clarke, L. and Carbon, J. (1980). Isolation of a yeast centromere and construction of functional small circular chromosomes. *Nature* **287**, 504-9.
- Cleveland, D. W., Mao, Y. and Sullivan, K. F. (2003). Centromeres and kinetochores: from epigenetics to mitotic checkpoint signaling. *Cell* **112**, 407-21.
- Cohen-Fix, O., Peters, J. M., Kirschner, M. W. and Koshland, D. (1996). Anaphase initiation in *Saccharomyces cerevisiae* is controlled by the APC-dependent degradation of the anaphase inhibitor Pds1p. *Genes Dev* **10**, 3081-93.
- Connelly, C. and Hieter, P. (1996). Budding yeast SKP1 encodes an evolutionarily conserved kinetochore protein required for cell cycle progression. *Cell* **86**, 275-85.
- Cottingham, F. R. and Hoyt, M. A. (1997). Mitotic spindle positioning in *Saccharomyces cerevisiae* is accomplished by antagonistically acting microtubule motor proteins. *J Cell Biol* **138**, 1041-53.
- D'Amours, D., Stegmeier, F. and Amon, A. (2004). Cdc14 and condensin control the dissolution of cohesin-independent chromosome linkages at repeated DNA. *Cell* **117**, 455-69.
- De Antoni, A., Pearson, C. G., Cimini, D., Canman, J. C., Sala, V., Nezi, L., Mapelli, M., Sironi, L., Faretta, M., Salmon, E. D. et al. (2005). The Mad1/Mad2 complex as a template for Mad2 activation in the spindle assembly checkpoint. *Curr Biol* **15**, 214-25.
- De Wulf, P., McAinsh, A. D. and Sorger, P. K. (2003). Hierarchical assembly of the budding yeast kinetochore from multiple subcomplexes. *Genes Dev* **17**, 2902-21.
- DeLuca, J. G., Howell, B. J., Canman, J. C., Hickey, J. M., Fang, G. and Salmon, E. D. (2003). Nuf2 and Hec1 are required for retention of the checkpoint proteins Mad1 and Mad2 to kinetochores. *Curr Biol* **13**, 2103-9.
- Desai, A. and Mitchison, T. J. (1997). Microtubule polymerization dynamics. *Annu Rev Cell Dev Biol* **13**, 83-117.
- Desai, A., Verma, S., Mitchison, T. J. and Walczak, C. E. (1999). Kin I kinesins are microtubule-destabilizing enzymes. *Cell* **96**, 69-78.
- Dewar, H., Tanaka, K., Nasmyth, K. and Tanaka, T. U. (2004). Tension between two kinetochores suffices for their bi-orientation on the mitotic spindle. *Nature* **428**, 93-7.
- DeZwaan, T. M., Ellingson, E., Pellman, D. and Roof, D. M. (1997). Kinesin-related KIP3 of *Saccharomyces cerevisiae* is required for a distinct step in nuclear migration. *J Cell Biol* **138**, 1023-40.
- Diffley, J. F. (2004). Regulation of early events in chromosome replication. *Curr Biol* **14**, R778-86.
- Doheny, K. F., Sorger, P. K., Hyman, A. A., Tugendreich, S., Spencer, F. and Hieter, P. (1993). Identification of essential components of the *S. cerevisiae* kinetochore. *Cell* **73**, 761-74.
- Enquist-Newman, M., Cheeseman, I. M., Van Goor, D., Drubin, D. G., Meluh, P. B. and Barnes, G. (2001). Dad1p, third component of the Duo1p/Dam1p complex involved in kinetochore function and mitotic spindle integrity. *Mol Biol Cell* **12**, 2601-13.
- Erickson, H. P. and O'Brien, E. T. (1992). Microtubule dynamic instability and GTP hydrolysis. *Annu Rev Biophys Biomol Struct* **21**, 145-66.
- Espelin, C. W., Kaplan, K. B. and Sorger, P. K. (1997). Probing the architecture of a simple kinetochore using DNA-protein crosslinking. *J Cell Biol* **139**, 1383-96.

- Espelin, C. W., Simons, K. T., Harrison, S. C. and Sorger, P. K. (2003). Binding of the essential *Saccharomyces cerevisiae* kinetochore protein Ndc10p to CDEII. *Mol Biol Cell* **14**, 4557-68.
- Euskirchen, G. M. (2002). Nnf1p, Dsn1p, Mtw1p, and Nsl1p: a new group of proteins important for chromosome segregation in *Saccharomyces cerevisiae*. *Eukaryot Cell* **1**, 229-40.
- Fang, G., Yu, H. and Kirschner, M. W. (1998a). The checkpoint protein MAD2 and the mitotic regulator CDC20 form a ternary complex with the anaphase-promoting complex to control anaphase initiation. *Genes Dev* **12**, 1871-83.
- Fang, G., Yu, H. and Kirschner, M. W. (1998b). Direct binding of CDC20 protein family members activates the anaphase-promoting complex in mitosis and G1. *Mol Cell* **2**, 163-71.
- Fitch, I., Dahmann, C., Surana, U., Amon, A., Nasmyth, K., Goetsch, L., Byers, B. and Futcher, B. (1992). Characterization of four B-type cyclin genes of the budding yeast *Saccharomyces cerevisiae*. *Mol Biol Cell* **3**, 805-18.
- Fitzgerald-Hayes, M., Clarke, L. and Carbon, J. (1982). Nucleotide sequence comparisons and functional analysis of yeast centromere DNAs. *Cell* **29**, 235-44.
- Fraschini, R., Formenti, E., Lucchini, G. and Piatti, S. (1999). Budding yeast Bub2 is localized at spindle pole bodies and activates the mitotic checkpoint via a different pathway from Mad2. *J Cell Biol* **145**, 979-91.
- Frenz, L. M., Lee, S. E., Fesquet, D. and Johnston, L. H. (2000). The budding yeast Dbf2 protein kinase localises to the centrosome and moves to the bud neck in late mitosis. *J Cell Sci* **113 Pt 19**, 3399-408.
- Fujiwara, T., Tanaka, K., Inoue, E., Kikyo, M. and Takai, Y. (1999). Bni1p regulates microtubule-dependent nuclear migration through the actin cytoskeleton in *Saccharomyces cerevisiae*. *Mol Cell Biol* **19**, 8016-27.
- Furge, K. A., Wong, K., Armstrong, J., Balasubramanian, M. and Albright, C. F. (1998). Byr4 and Cdc16 form a two-component GTPase-activating protein for the Spg1 GTPase that controls septation in fission yeast. *Curr Biol* **8**, 947-54.
- Gardner, M. K., Pearson, C. G., Sprague, B. L., Zarzar, T. R., Bloom, K., Salmon, E. D. and Odde, D. J. (2005). Tension-dependent regulation of microtubule dynamics at kinetochores can explain metaphase congression in yeast. *Mol Biol Cell* **16**, 3764-75.
- Gardner, R. D., Poddar, A., Yellman, C., Tavormina, P. A., Monteagudo, M. C. and Burke, D. J. (2001). The spindle checkpoint of the yeast *Saccharomyces cerevisiae* requires kinetochore function and maps to the CBF3 domain. *Genetics* **157**, 1493-502.
- Geymonat, M., Spanos, A., Smith, S. J., Wheatley, E., Rittinger, K., Johnston, L. H. and Sedgwick, S. G. (2002). Control of mitotic exit in budding yeast. In vitro regulation of Tem1 GTPase by Bub2 and Bfa1. *J Biol Chem* **277**, 28439-45.
- Geymonat, M., Spanos, A., Walker, P. A., Johnston, L. H. and Sedgwick, S. G. (2003). In vitro regulation of budding yeast Bfa1/Bub2 GAP activity by Cdc5. *J Biol Chem* **278**, 14591-4.
- Ghosh, S. K., Poddar, A., Hajra, S., Sanyal, K. and Sinha, P. (2001). The IML3/MCM19 gene of *Saccharomyces cerevisiae* is required for a kinetochore-related process during chromosome segregation. *Mol Genet Genomics* **265**, 249-57.
- Glotzer, M. (2005). The molecular requirements for cytokinesis. *Science* **307**, 1735-9.
- Goh, P. Y. and Kilmartin, J. V. (1993). NDC10: a gene involved in chromosome segregation in *Saccharomyces cerevisiae*. *J Cell Biol* **121**, 503-12.
- Gorbsky, G. J. and Ricketts, W. A. (1993). Differential expression of a phosphoepitope at the kinetochores of moving chromosomes. *J Cell Biol* **122**, 1311-21.
- Goshima, G. and Yanagida, M. (2000). Establishing biorientation occurs with precocious separation of the sister kinetochores, but not the arms, in the early spindle of budding yeast. *Cell* **100**, 619-33.
- Gould, K. L., Moreno, S., Owen, D. J., Sazer, S. and Nurse, P. (1991). Phosphorylation at Thr167 is required for *Schizosaccharomyces pombe* p34cdc2 function. *Embo J* **10**, 3297-309.
- Granot, D. and Snyder, M. (1991). Segregation of the nucleolus during mitosis in budding and fission yeast. *Cell Motil Cytoskeleton* **20**, 47-54.
- Gruneberg, U., Campbell, K., Simpson, C., Grindlay, J. and Schiebel, E. (2000). Nud1p links astral microtubule organization and the control of exit from mitosis. *Embo J* **19**, 6475-88.
- Guacci, V., Koshland, D. and Strunnikov, A. (1997). A direct link between sister chromatid cohesion and chromosome condensation revealed through the analysis of MCD1 in *S. cerevisiae*. *Cell* **91**, 47-57.
- Guertin, D. A., Trautmann, S. and McCollum, D. (2002). Cytokinesis in eukaryotes. *Microbiol Mol Biol Rev* **66**, 155-78.

-
- Güldener, U., Heck, S., Fiedler, T., Beinhauer, J. and Hegemann, J. (1996). A new efficient gene disruption cassette for repeated use in budding yeast. *Nucleic Acids Res* **24**, 2519-2524.
- Gunawardane, R. N., Lizarraga, S. B., Wiese, C., Wilde, A. and Zheng, Y. (2000). gamma-Tubulin complexes and their role in microtubule nucleation. *Curr Top Dev Biol* **49**, 55-73.
- Hanahan, D. (1983). Studies on transformation of *Escherichia coli* with plasmids. *J Mol Biol* **166**, 557-80.
- Hartwell, L. H. (1971). Genetic control of the cell division cycle in yeast. II. Genes controlling DNA replication and its initiation. *J Mol Biol* **59**, 183-94.
- Hartwell, L. H., Culotti, J., Pringle, J. R. and Reid, B. J. (1974). Genetic control of the cell division cycle in yeast. *Science* **183**, 46-51.
- Hartwell, L. H., Culotti, J. and Reid, B. (1970). Genetic control of the cell-division cycle in yeast. I. Detection of mutants. *Proc Natl Acad Sci U S A* **66**, 352-9.
- Hassold, T. and Hunt, P. (2001). To err (meiotically) is human: the genesis of human aneuploidy. *Nat Rev Genet* **2**, 280-91.
- He, X., Asthana, S. and Sorger, P. K. (2000). Transient sister chromatid separation and elastic deformation of chromosomes during mitosis in budding yeast. *Cell* **101**, 763-75.
- He, X., Rines, D. R., Espelin, C. W. and Sorger, P. K. (2001). Molecular analysis of kinetochore-microtubule attachment in budding yeast. *Cell* **106**, 195-206.
- Hecht, A. and Grunstein, M. (1999). Mapping DNA interaction sites of chromosomal proteins using immunoprecipitation and polymerase chain reaction. *Methods Enzymol* **304**, 399-414.
- Heid, C. A., Stevens, J., Livak, K. J. and Williams, P. M. (1996). Real time quantitative PCR. *Genome Res* **6**, 986-94.
- Hieter, P., Pridmore, D., Hegemann, J. H., Thomas, M., Davis, R. W. and Philippsen, P. (1985). Functional selection and analysis of yeast centromeric DNA. *Cell* **42**, 913-21.
- Higuchi, T. and Uhlmann, F. (2005). Stabilization of microtubule dynamics at anaphase onset promotes chromosome segregation. *Nature* **433**, 171-6.
- Hildebrandt, E. R. and Hoyt, M. A. (2000). Mitotic motors in *Saccharomyces cerevisiae*. *Biochim Biophys Acta* **1496**, 99-116.
- Howell, B. J., Hoffman, D. B., Fang, G., Murray, A. W. and Salmon, E. D. (2000). Visualization of Mad2 dynamics at kinetochores, along spindle fibers, and at spindle poles in living cells. *J Cell Biol* **150**, 1233-50.
- Hoyt, M. A., Totis, L. and Roberts, B. T. (1991). *S. cerevisiae* genes required for cell cycle arrest in response to loss of microtubule function. *Cell* **66**, 507-17.
- Hoyt, M. A., He, L., Loo, K. K. and Saunders, W. S. (1992). Two *Saccharomyces cerevisiae* kinesin-related gene products required for mitotic spindle assembly. *J Cell Biol* **118**, 109-20.
- Hu, F. and Elledge, S. J. (2002). Bub2 is a cell cycle regulated phospho-protein controlled by multiple checkpoints. *Cell Cycle* **1**, 351-5.
- Hu, F., Wang, Y., Liu, D., Li, Y., Qin, J. and Elledge, S. J. (2001). Regulation of the Bub2/Bfa1 GAP complex by Cdc5 and cell cycle checkpoints. *Cell* **107**, 655-65.
- Hunter, A. W. and Wordeman, L. (2000). How motor proteins influence microtubule polymerization dynamics. *J Cell Sci* **113 Pt 24**, 4379-89.
- Hwang, L. H., Lau, L. F., Smith, D. L., Mistrot, C. A., Hardwick, K. G., Hwang, E. S., Amon, A. and Murray, A. W. (1998). Budding yeast Cdc20: a target of the spindle checkpoint. *Science* **279**, 1041-4.
- Ito, T., Chiba, T., Ozawa, R., Yoshida, M., Hattori, M. and Sakaki, Y. (2001). A comprehensive two-hybrid analysis to explore the yeast protein interactome. *Proc Natl Acad Sci U S A* **98**, 4569-74.
- Jacobs, C. W., Adams, A. E., Szaniszló, P. J. and Pringle, J. R. (1988). Functions of microtubules in the *Saccharomyces cerevisiae* cell cycle. *J Cell Biol* **107**, 1409-26.
- Janke, C., Ortiz, J., Lechner, J., Shevchenko, A., Shevchenko, A., Magiera, M. M., Schramm, C. and Schiebel, E. (2001). The budding yeast proteins Spc24p and Spc25p interact with Ndc80p and Nuf2p at the kinetochore and are important for kinetochore clustering and checkpoint control. *Embo J* **20**, 777-91.
- Janke, C., Ortiz, J., Tanaka, T. U., Lechner, J. and Schiebel, E. (2002). Four new subunits of the Dam1-Duo1 complex reveal novel functions in sister kinetochore biorientation. *Embo J* **21**, 181-93.
- Jaspersen, S. L., Charles, J. F., Tinker-Kulberg, R. L. and Morgan, D. O. (1998). A late mitotic regulatory network controlling cyclin destruction in *Saccharomyces cerevisiae*. *Mol Biol Cell* **9**, 2803-17.
-

- Jaspersen, S. L., Huneycutt, B. J., Giddings, T. H., Jr., Resing, K. A., Ahn, N. G. and Winey, M. (2004). Cdc28/Cdk1 regulates spindle pole body duplication through phosphorylation of Spc42 and Mps1. *Dev Cell* **7**, 263-74.
- Jaspersen, S. L. and Morgan, D. O. (2000). Cdc14 activates cdc15 to promote mitotic exit in budding yeast. *Curr Biol* **10**, 615-8.
- Jaspersen, S. L. and Winey, M. (2004). The budding yeast spindle pole body: structure, duplication, and function. *Annu Rev Cell Dev Biol* **20**, 1-28.
- Jensen, S., Geymonat, M., Johnson, A. L., Segal, M. and Johnston, L. H. (2002). Spatial regulation of the guanine nucleotide exchange factor Lte1 in *Saccharomyces cerevisiae*. *J Cell Sci* **115**, 4977-91.
- Jensen, S., Segal, M., Clarke, D. J. and Reed, S. I. (2001). A novel role of the budding yeast separin Esp1 in anaphase spindle elongation: Evidence that proper spindle association of Esp1 is regulated by Pds1. *J Cell Biol* **152**, 27-40.
- Jiang, W. D. and Philippsen, P. (1989). Purification of a protein binding to the CDEI subregion of *Saccharomyces cerevisiae* centromere DNA. *Mol Cell Biol* **9**, 5585-93.
- Jones, M. H., He, X., Giddings, T. H. and Winey, M. (2001). Yeast Dam1p has a role at the kinetochore in assembly of the mitotic spindle. *Proc Natl Acad Sci U S A* **98**, 13675-80.
- Juang, Y. L., Huang, J., Peters, J. M., McLaughlin, M. E., Tai, C. Y. and Pellman, D. (1997). APC-mediated proteolysis of Ase1 and the morphogenesis of the mitotic spindle. *Science* **275**, 1311-4.
- Khodjakov, A. and Rieder, C. L. (1999). The sudden recruitment of gamma-tubulin to the centrosome at the onset of mitosis and its dynamic exchange throughout the cell cycle, do not require microtubules. *J Cell Biol* **146**, 585-96.
- Kinoshita, K., Habermann, B. and Hyman, A. A. (2002). XMAP215: a key component of the dynamic microtubule cytoskeleton. *Trends Cell Biol* **12**, 267-73.
- Kinzler, K. W. and Vogelstein, B. (1996). Lessons from hereditary colorectal cancer. *Cell* **87**, 159-70.
- Kitagawa, K. and Hieter, P. (2001). Evolutionary conservation between budding yeast and human kinetochores. *Nat Rev Mol Cell Biol* **2**, 678-87.
- Kitagawa, K., Abdulle, R., Bansal, P. K., Cagney, G., Fields, S. and Hieter, P. (2003). Requirement of Skp1-Bub1 interaction for kinetochore-mediated activation of the spindle checkpoint. *Mol Cell* **11**, 1201-13.
- Knop, M., Siegers, K., Pereira, G., Zachariae, W., Winsor, B., Nasmyth, K. and Schiebel, E. (1999). Epitope tagging of yeast genes using a PCR-based strategy: more tags and improved practical routines. *Yeast* **15**, 963-72.
- Kosco, K. A., Pearson, C. G., Maddox, P. S., Wang, P. J., Adams, I. R., Salmon, E. D., Bloom, K. and Huffaker, T. C. (2001). Control of microtubule dynamics by Stu2p is essential for spindle orientation and metaphase chromosome alignment in yeast. *Mol Biol Cell* **12**, 2870-80.
- Lechner, J. and Carbon, J. (1991). A 240 kd multisubunit protein complex, CBF3, is a major component of the budding yeast centromere. *Cell* **64**, 717-25.
- Lee, L., Klee, S. K., Evangelista, M., Boone, C. and Pellman, D. (1999). Control of mitotic spindle position by the *Saccharomyces cerevisiae* formin Bni1p. *J Cell Biol* **144**, 947-61.
- Lee, S. E., Frenz, L. M., Wells, N. J., Johnson, A. L. and Johnston, L. H. (2001). Order of function of the budding-yeast mitotic exit-network proteins Tem1, Cdc15, Mob1, Dbf2, and Cdc5. *Curr Biol* **11**, 784-8.
- Lengauer, C., Kinzler, K. W. and Vogelstein, B. (1997). Genetic instability in colorectal cancers. *Nature* **386**, 623-7.
- Lengauer, C., Kinzler, K. W. and Vogelstein, B. (1998). Genetic instabilities in human cancers. *Nature* **396**, 643-9.
- Li, R. and Murray, A. W. (1991). Feedback control of mitosis in budding yeast. *Cell* **66**, 519-31.
- Li, X. and Nicklas, R. B. (1995). Mitotic forces control a cell-cycle checkpoint. *Nature* **373**, 630-2.
- Li, Y., Bachant, J., Alcasabas, A. A., Wang, Y., Qin, J. and Elledge, S. J. (2002). The mitotic spindle is required for loading of the DASH complex onto the kinetochore. *Genes Dev* **16**, 183-97.
- Li, Y. and Benezra, R. (1996). Identification of a human mitotic checkpoint gene: hsMAD2. *Science* **274**, 246-8.
- Liakopoulos, D., Kusch, J., Grava, S., Vogel, J. and Barral, Y. (2003). Asymmetric loading of Kar9 onto spindle poles and microtubules ensures proper spindle alignment. *Cell* **112**, 561-74.
- Longtine, M. S., McKenzie, A., 3rd, Demarini, D. J., Shah, N. G., Wach, A., Brachat, A., Philippsen, P. and Pringle, J. R. (1998). Additional modules for versatile and economical PCR-based gene deletion and modification in *Saccharomyces cerevisiae*. *Yeast* **14**, 953-61.
- Luca, F. C., Mody, M., Kurischko, C., Roof, D. M., Giddings, T. H. and Winey, M. (2001). *Saccharomyces cerevisiae* Mob1p is required for cytokinesis and mitotic exit. *Mol Cell Biol* **21**, 6972-83.

- Maekawa, H., Usui, T., Knop, M. and Schiebel, E.** (2003). Yeast Cdk1 translocates to the plus end of cytoplasmic microtubules to regulate bud cortex interactions. *Embo J* **22**, 438-49.
- Mah, A. S., Jang, J. and Deshaies, R. J.** (2001). Protein kinase Cdc15 activates the Dbf2-Mob1 kinase complex. *Proc Natl Acad Sci U S A* **98**, 7325-30.
- Mailand, N. and Diffley, J. F.** (2005). CDKs promote DNA replication origin licensing in human cells by protecting Cdc6 from APC/C-dependent proteolysis. *Cell* **122**, 915-26.
- Martin-Lluesma, S., Stucke, V. M. and Nigg, E. A.** (2002). Role of Hec1 in spindle checkpoint signaling and kinetochore recruitment of Mad1/Mad2. *Science* **297**, 2267-70.
- Martinez-Exposito, M. J., Kaplan, K. B., Copeland, J. and Sorger, P. K.** (1999). Retention of the BUB3 checkpoint protein on lagging chromosomes. *Proc Natl Acad Sci U S A* **96**, 8493-8.
- Mathias, N., Johnson, S. L., Winey, M., Adams, A. E., Goetsch, L., Pringle, J. R., Byers, B. and Goebel, M. G.** (1996). Cdc53p acts in concert with Cdc4p and Cdc34p to control the G1-to-S-phase transition and identifies a conserved family of proteins. *Mol Cell Biol* **16**, 6634-43.
- McAinsh, A. D., Tytell, J. D. and Sorger, P. K.** (2003). Structure, function, and regulation of budding yeast kinetochores. *Annu Rev Cell Dev Biol* **19**, 519-39.
- McClelland, M. L., Gardner, R. D., Kallio, M. J., Daum, J. R., Gorbsky, G. J., Burke, D. J. and Stukenberg, P. T.** (2003). The highly conserved Ndc80 complex is required for kinetochore assembly, chromosome congression, and spindle checkpoint activity. *Genes Dev* **17**, 101-14.
- McCollum, D.** (2004). Cytokinesis: the central spindle takes center stage. *Curr Biol* **14**, R953-5.
- McEwen, B. F., Heagle, A. B., Cassels, G. O., Buttle, K. F. and Rieder, C. L.** (1997). Kinetochore fiber maturation in PtK1 cells and its implications for the mechanisms of chromosome congression and anaphase onset. *J Cell Biol* **137**, 1567-80.
- McGrew, J., Diehl, B. and Fitzgerald-Hayes, M.** (1986). Single base-pair mutations in centromere element III cause aberrant chromosome segregation in *Saccharomyces cerevisiae*. *Mol Cell Biol* **6**, 530-8.
- McIntosh, J. R.** (1991). Structural and mechanical control of mitotic progression. *Cold Spring Harb Symp Quant Biol* **56**, 613-9.
- McIntosh, J. R., Grishchuk, E. L. and West, R. R.** (2002). Chromosome-microtubule interactions during mitosis. *Annu Rev Cell Dev Biol* **18**, 193-219.
- Measday, V., Hailey, D. W., Pot, I., Givan, S. A., Hyland, K. M., Cagney, G., Fields, S., Davis, T. N. and Hieter, P.** (2002). Ctf3p, the Mis6 budding yeast homolog, interacts with Mcm22p and Mcm16p at the yeast outer kinetochore. *Genes Dev* **16**, 101-13.
- Meluh, P. B. and Koshland, D.** (1995). Evidence that the MIF2 gene of *Saccharomyces cerevisiae* encodes a centromere protein with homology to the mammalian centromere protein CENP-C. *Mol Biol Cell* **6**, 793-807.
- Meluh, P. B. and Koshland, D.** (1997). Budding yeast centromere composition and assembly as revealed by in vivo cross-linking. *Genes Dev* **11**, 3401-12.
- Meluh, P. B., Yang, P., Glowczewski, L., Koshland, D. and Smith, M. M.** (1998). Cse4p is a component of the core centromere of *Saccharomyces cerevisiae*. *Cell* **94**, 607-13.
- Menssen, R., Neutznier, A. and Seufert, W.** (2001). Asymmetric spindle pole localization of yeast Cdc15 kinase links mitotic exit and cytokinesis. *Curr Biol* **11**, 345-50.
- Michaelis, C., Ciosk, R. and Nasmyth, K.** (1997). Cohesins: chromosomal proteins that prevent premature separation of sister chromatids. *Cell* **91**, 35-45.
- Miller, R. K., Matheos, D. and Rose, M. D.** (1999). The cortical localization of the microtubule orientation protein, Kar9p, is dependent upon actin and proteins required for polarization. *J Cell Biol* **144**, 963-75.
- Miller, R. K. and Rose, M. D.** (1998). Kar9p is a novel cortical protein required for cytoplasmic microtubule orientation in yeast. *J Cell Biol* **140**, 377-90.
- Moll, T., Tebb, G., Surana, U., Robitsch, H. and Nasmyth, K.** (1991). The role of phosphorylation and the CDC28 protein kinase in cell cycle-regulated nuclear import of the *S. cerevisiae* transcription factor SWI5. *Cell* **66**, 743-58.
- Moore, A. and Wordeman, L.** (2004). The mechanism, function and regulation of depolymerizing kinesins during mitosis. *Trends Cell Biol* **14**, 537-46.
- Müller-Reichert, T., Sassoon, I., O'Toole, E., Romao, M., Ashford, A. J., Hyman, A. A. and Antony, C.** (2003). Analysis of the distribution of the kinetochore protein Ndc10p in *Saccharomyces cerevisiae* using 3-D modeling of mitotic spindles. *Chromosoma* **111**, 417-28.

- Murray, A.** (1995). Cyclin ubiquitination: the destructive end of mitosis. *Cell* **81**, 149-52.
- Nasmyth, K.** (1993). Control of the yeast cell cycle by the Cdc28 protein kinase. *Curr Opin Cell Biol* **5**, 166-79.
- Nasmyth, K.** (2002). Segregating sister genomes: the molecular biology of chromosome separation. *Science* **297**, 559-65.
- Nekrasov, V. S., Smith, M. A., Peak-Chew, S. and Kilmartin, J. V.** (2003). Interactions between centromere complexes in *Saccharomyces cerevisiae*. *Mol Biol Cell* **14**, 4931-46.
- Ng, R. and Carbon, J.** (1987). Mutational and in vitro protein-binding studies on centromere DNA from *Saccharomyces cerevisiae*. *Mol Cell Biol* **7**, 4522-34.
- Nicklas, R. B., Ward, S. C. and Gorbsky, G. J.** (1995). Kinetochore chemistry is sensitive to tension and may link mitotic forces to a cell cycle checkpoint. *J Cell Biol* **130**, 929-39.
- Norden, C., Mendoza, M., Dobbelaere, J., Kotwaliwale, C. V., Biggins, S. and Barral, Y.** (2006). The NoCut pathway links completion of cytokinesis to spindle midzone function to prevent chromosome breakage. *Cell* **125**, 85-98.
- Ortiz, J., Stemmann, O., Rank, S. and Lechner, J.** (1999). A putative protein complex consisting of Ctf19, Mcm21, and Okp1 represents a missing link in the budding yeast kinetochore. *Genes Dev* **13**, 1140-55.
- Palframan, W. J., Meehl, J. B., Jaspersen, S. L., Winey, M. and Murray, A. W.** (2006). Anaphase Inactivation of the Spindle Checkpoint. *Science*.
- Palmer, R. E., Sullivan, D. S., Huffaker, T. and Koshland, D.** (1992). Role of astral microtubules and actin in spindle orientation and migration in the budding yeast, *Saccharomyces cerevisiae*. *J Cell Biol* **119**, 583-93.
- Pasqualone, D. and Huffaker, T. C.** (1994). STU1, a suppressor of a beta-tubulin mutation, encodes a novel and essential component of the yeast mitotic spindle. *J Cell Biol* **127**, 1973-84.
- Pearson, C. G., Maddox, P. S., Zarzar, T. R., Salmon, E. D. and Bloom, K.** (2003). Yeast kinetochores do not stabilize Stu2p-dependent spindle microtubule dynamics. *Mol Biol Cell* **14**, 4181-95.
- Pearson, C. G. and Bloom, K.** (2004). Dynamic microtubules lead the way for spindle positioning. *Nat Rev Mol Cell Biol* **5**, 481-92.
- Pellman, D., Bagget, M., Tu, Y. H., Fink, G. R. and Tu, H.** (1995). Two microtubule-associated proteins required for anaphase spindle movement in *Saccharomyces cerevisiae*. *J Cell Biol* **130**, 1373-85.
- Pereira, G., Hofken, T., Grindlay, J., Manson, C. and Schiebel, E.** (2000). The Bub2p spindle checkpoint links nuclear migration with mitotic exit. *Mol Cell* **6**, 1-10.
- Pereira, G., Manson, C., Grindlay, J. and Schiebel, E.** (2002). Regulation of the Bfa1p-Bub2p complex at spindle pole bodies by the cell cycle phosphatase Cdc14p. *J Cell Biol* **157**, 367-79.
- Pereira, G. and Schiebel, E.** (2003). Separase regulates INCENP-Aurora B anaphase spindle function through Cdc14. *Science* **302**, 2120-4.
- Pereira, G., Tanaka, T. U., Nasmyth, K. and Schiebel, E.** (2001). Modes of spindle pole body inheritance and segregation of the Bfa1p-Bub2p checkpoint protein complex. *Embo J* **20**, 6359-70.
- Pinsky, B. A., Kung, C., Shokat, K. M. and Biggins, S.** (2006). The Ipl1-Aurora protein kinase activates the spindle checkpoint by creating unattached kinetochores. *Nat Cell Biol* **8**, 78-83.
- Pinsky, B. A., Tatsutani, S. Y., Collins, K. A. and Biggins, S.** (2003). An Mtw1 complex promotes kinetochore biorientation that is monitored by the Ipl1/Aurora protein kinase. *Dev Cell* **5**, 735-45.
- Pot, I., Knockleby, J., Aneliunas, V., Nguyen, T., Ah-Kye, S., Liszt, G., Snyder, M., Hieter, P. and Vogel, J.** (2005). Spindle checkpoint maintenance requires Ame1 and Okp1. *Cell Cycle* **4**, 1448-56.
- Puig, O., Caspary, F., Rigaut, G., Rutz, B., Bouveret, E., Bragado-Nilsson, E., Wilm, M. and Seraphin, B.** (2001). The tandem affinity purification (TAP) method: a general procedure of protein complex purification. *Methods* **24**, 218-29.
- Rieder, C. L., Cole, R. W., Khodjakov, A. and Sluder, G.** (1995). The checkpoint delaying anaphase in response to chromosome monoorientation is mediated by an inhibitory signal produced by unattached kinetochores. *J Cell Biol* **130**, 941-8.
- Rieder, C. L. and Salmon, E. D.** (1998). The vertebrate cell kinetochore and its roles during mitosis. *Trends Cell Biol* **8**, 310-8.
- Rieder, C. L., Schultz, A., Cole, R. and Sluder, G.** (1994). Anaphase onset in vertebrate somatic cells is controlled by a checkpoint that monitors sister kinetochore attachment to the spindle. *J Cell Biol* **127**, 1301-10.
- Roof, D. M., Meluh, P. B. and Rose, M. D.** (1992). Kinesin-related proteins required for assembly of the mitotic spindle. *J Cell Biol* **118**, 95-108.
- Ross, K. E. and Cohen-Fix, O.** (2004). A role for the FEAR pathway in nuclear positioning during anaphase. *Dev Cell* **6**, 729-35.

- Roy, N., Poddar, A., Lohia, A. and Sinha, P. (1997). The mcm17 mutation of yeast shows a size-dependent segregational defect of a mini-chromosome. *Curr Genet* **32**, 182-9.
- Russell, P. and Nurse, P. (1986). cdc25+ functions as an inducer in the mitotic control of fission yeast. *Cell* **45**, 145-53.
- Russell, P. and Nurse, P. (1987). Negative regulation of mitosis by wee1+, a gene encoding a protein kinase homolog. *Cell* **49**, 559-67.
- Sambrook, J., Fritsch, E. F. and Maniatis, T. (2001). Molecular cloning - A laboratory manual (3rd edition). *Cold Spring Harbor Laboratory Press, Cold Spring Harbor, New York*.
- Saunders, W. S. and Hoyt, M. A. (1992). Kinesin-related proteins required for structural integrity of the mitotic spindle. *Cell* **70**, 451-8.
- Saunders, W., Lengyel, V. and Hoyt, M. A. (1997). Mitotic spindle function in *Saccharomyces cerevisiae* requires a balance between different types of kinesin-related motors. *Mol Biol Cell* **8**, 1025-33.
- Scharfenberger, M., Ortiz, J., Grau, N., Janke, C., Schiebel, E. and Lechner, J. (2003). Nsl1p is essential for the establishment of bipolarity and the localization of the Dam-Duo complex. *Embo J* **22**, 6584-97.
- Schiebel, E. (2000). gamma-tubulin complexes: binding to the centrosome, regulation and microtubule nucleation. *Curr Opin Cell Biol* **12**, 113-8.
- Schiestl, R. H. and Gietz, R. D. (1989). High efficiency transformation of intact yeast cells using single stranded nucleic acids as a carrier. *Curr Genet* **16**, 339-46.
- Scholey, J. M., Brust-Mascher, I. and Mogilner, A. (2003). Cell division. *Nature* **422**, 746-52.
- Schuyler, S. C. and Pellman, D. (2001a). Microtubule "plus-end-tracking proteins": The end is just the beginning. *Cell* **105**, 421-4.
- Schuyler, S. C. and Pellman, D. (2001b). Search, capture and signal: games microtubules and centrosomes play. *J Cell Sci* **114**, 247-55.
- Segal, M. and Bloom, K. (2001). Control of spindle polarity and orientation in *Saccharomyces cerevisiae*. *Trends Cell Biol* **11**, 160-6.
- Seshan, A., Bardin, A. J. and Amon, A. (2002). Control of Lte1 localization by cell polarity determinants and Cdc14. *Curr Biol* **12**, 2098-110.
- Severin, F., Habermann, B., Huffaker, T. and Hyman, T. (2001). Stu2 promotes mitotic spindle elongation in anaphase. *J Cell Biol* **153**, 435-42.
- Shah, J. V., Botvinick, E., Bonday, Z., Furnari, F., Berns, M. and Cleveland, D. W. (2004). Dynamics of centromere and kinetochore proteins; implications for checkpoint signaling and silencing. *Curr Biol* **14**, 942-52.
- Shang, C., Hazbun, T. R., Cheeseman, I. M., Aranda, J., Fields, S., Drubin, D. G. and Barnes, G. (2003). Kinetochore protein interactions and their regulation by the Aurora kinase Ipl1p. *Mol Biol Cell* **14**, 3342-55.
- Shaw, S. L., Yeh, E., Maddox, P., Salmon, E. D. and Bloom, K. (1997). Astral microtubule dynamics in yeast: a microtubule-based searching mechanism for spindle orientation and nuclear migration into the bud. *J Cell Biol* **139**, 985-94.
- Shirayama, M., Matsui, Y., Tanaka, K. and Toh-e, A. (1994a). Isolation of a CDC25 family gene, MSI2/LTE1, as a multicopy suppressor of ira1. *Yeast* **10**, 451-61.
- Shirayama, M., Matsui, Y. and Toh, E. A. (1994b). The yeast TEM1 gene, which encodes a GTP-binding protein, is involved in termination of M phase. *Mol Cell Biol* **14**, 7476-82.
- Shou, W., Azzam, R., Chen, S. L., Huddleston, M. J., Baskerville, C., Charbonneau, H., Annan, R. S., Carr, S. A. and Deshaies, R. J. (2002). Cdc5 influences phosphorylation of Net1 and disassembly of the RENT complex. *BMC Mol Biol* **3**, 3.
- Shou, W., Seol, J. H., Shevchenko, A., Baskerville, C., Moazed, D., Chen, Z. W., Jang, J., Shevchenko, A., Charbonneau, H. and Deshaies, R. J. (1999). Exit from mitosis is triggered by Tem1-dependent release of the protein phosphatase Cdc14 from nucleolar RENT complex. *Cell* **97**, 233-44.
- Sironi, L., Melixetian, M., Faretta, M., Prosperini, E., Helin, K. and Musacchio, A. (2001). Mad2 binding to Mad1 and Cdc20, rather than oligomerization, is required for the spindle checkpoint. *Embo J* **20**, 6371-82.
- Song, S., Grenfell, T. Z., Garfield, S., Erikson, R. L. and Lee, K. S. (2000). Essential function of the polo box of Cdc5 in subcellular localization and induction of cytokinetic structures. *Mol Cell Biol* **20**, 286-98.
- Song, S. and Lee, K. S. (2001). A novel function of *Saccharomyces cerevisiae* CDC5 in cytokinesis. *J Cell Biol* **152**, 451-69.
- Sorger, P. K., Severin, F. F. and Hyman, A. A. (1994). Factors required for the binding of reassembled yeast kinetochores to microtubules in vitro. *J Cell Biol* **127**, 995-1008.

- Stearns, T.** (1997). Motoring to the finish: kinesin and dynein work together to orient the yeast mitotic spindle. *J Cell Biol* **138**, 957-60.
- Stegmeier, F., Huang, J., Rahal, R., Zmolik, J., Moazed, D. and Amon, A.** (2004). The replication fork block protein Fob1 functions as a negative regulator of the FEAR network. *Curr Biol* **14**, 467-80.
- Stegmeier, F., Visintin, R. and Amon, A.** (2002). Separase, polo kinase, the kinetochore protein Slk19, and Spo12 function in a network that controls Cdc14 localization during early anaphase. *Cell* **108**, 207-20.
- Stemmann, O. and Lechner, J.** (1996). The *Saccharomyces cerevisiae* kinetochore contains a cyclin-CDK complexing homologue, as identified by in vitro reconstitution. *Embo J* **15**, 3611-20.
- Stern, B. M. and Murray, A. W.** (2001). Lack of tension at kinetochores activates the spindle checkpoint in budding yeast. *Curr Biol* **11**, 1462-7.
- Stoler, S., Keith, K. C., Curnick, K. E. and Fitzgerald-Hayes, M.** (1995). A mutation in CSE4, an essential gene encoding a novel chromatin-associated protein in yeast, causes chromosome nondisjunction and cell cycle arrest at mitosis. *Genes Dev* **9**, 573-86.
- Straight, A. F., Marshall, W. F., Sedat, J. W. and Murray, A. W.** (1997). Mitosis in living budding yeast: anaphase A but no metaphase plate. *Science* **277**, 574-8.
- Strunnikov, A. V., Kingsbury, J. and Koshland, D.** (1995). CEP3 encodes a centromere protein of *Saccharomyces cerevisiae*. *J Cell Biol* **128**, 749-60.
- Sullivan, M., Higuchi, T., Katis, V. L. and Uhlmann, F.** (2004). Cdc14 phosphatase induces rDNA condensation and resolves cohesin-independent cohesion during budding yeast anaphase. *Cell* **117**, 471-82.
- Sullivan, M., Lehane, C. and Uhlmann, F.** (2001). Orchestrating anaphase and mitotic exit: separase cleavage and localization of Slk19. *Nat Cell Biol* **3**, 771-7.
- Sullivan, M. and Uhlmann, F.** (2003). A non-proteolytic function of separase links the onset of anaphase to mitotic exit. *Nat Cell Biol* **5**, 249-54.
- Tan, A. L., Rida, P. C. and Surana, U.** (2005). Essential tension and constructive destruction: the spindle checkpoint and its regulatory links with mitotic exit. *Biochem J* **386**, 1-13.
- Tanaka, K., Mukae, N., Dewar, H., van Breugel, M., James, E. K., Prescott, A. R., Antony, C. and Tanaka, T. U.** (2005). Molecular mechanisms of kinetochore capture by spindle microtubules. *Nature* **434**, 987-94.
- Tanaka, T. U., Rachidi, N., Janke, C., Pereira, G., Galova, M., Schiebel, E., Stark, M. J. and Nasmyth, K.** (2002). Evidence that the Ipl1-Sli15 (Aurora kinase-INCENP) complex promotes chromosome bi-orientation by altering kinetochore-spindle pole connections. *Cell* **108**, 317-29.
- Taylor, S. S., Ha, E. and McKeon, F.** (1998). The human homologue of Bub3 is required for kinetochore localization of Bub1 and a Mad3/Bub1-related protein kinase. *J Cell Biol* **142**, 1-11.
- Tirnauer, J. S., O'Toole, E., Berrueta, L., Bierer, B. E. and Pellman, D.** (1999). Yeast Bim1p promotes the G1-specific dynamics of microtubules. *J Cell Biol* **145**, 993-1007.
- Townsley, F. M. and Ruderman, J. V.** (1998). Proteolytic ratchets that control progression through mitosis. *Trends Cell Biol* **8**, 238-44.
- Toyn, J. H., Johnson, A. L., Donovan, J. D., Toone, W. M. and Johnston, L. H.** (1997). The Swi5 transcription factor of *Saccharomyces cerevisiae* has a role in exit from mitosis through induction of the cdk-inhibitor Sic1 in telophase. *Genetics* **145**, 85-96.
- Tytell, J. D. and Sorger, P. K.** (2006). Analysis of kinesin motor function at budding yeast kinetochores. *J Cell Biol* **172**, 861-74.
- Uetz, P., Giot, L., Cagney, G., Mansfield, T. A., Judson, R. S., Knight, J. R., Lockshon, D., Narayan, V., Srinivasan, M., Pochart, P. et al.** (2000). A comprehensive analysis of protein-protein interactions in *Saccharomyces cerevisiae*. *Nature* **403**, 623-7.
- Uhlmann, F., Lottspeich, F. and Nasmyth, K.** (1999). Sister-chromatid separation at anaphase onset is promoted by cleavage of the cohesin subunit Scc1. *Nature* **400**, 37-42.
- Uhlmann, F. and Nasmyth, K.** (1998). Cohesion between sister chromatids must be established during DNA replication. *Curr Biol* **8**, 1095-101.
- Uhlmann, F., Wernic, D., Poupart, M. A., Koonin, E. V. and Nasmyth, K.** (2000). Cleavage of cohesin by the CD clan protease separin triggers anaphase in yeast. *Cell* **103**, 375-86.
- Vallen, E. A., Scherson, T. Y., Roberts, T., van Zee, K. and Rose, M. D.** (1992). Asymmetric mitotic segregation of the yeast spindle pole body. *Cell* **69**, 505-15.

- van Breugel, M., Drechsel, D. and Hyman, A. (2003). Stu2p, the budding yeast member of the conserved Dis1/XMAP215 family of microtubule-associated proteins is a plus end-binding microtubule destabilizer. *J Cell Biol* **161**, 359-69.
- Verma, R., Annan, R. S., Huddleston, M. J., Carr, S. A., Reynard, G. and Deshaies, R. J. (1997). Phosphorylation of Sic1p by G1 Cdk required for its degradation and entry into S phase. *Science* **278**, 455-60.
- Vinh, D. B., Kern, J. W., Hancock, W. O., Howard, J. and Davis, T. N. (2002). Reconstitution and characterization of budding yeast gamma-tubulin complex. *Mol Biol Cell* **13**, 1144-57.
- Visintin, R. and Amon, A. (2001). Regulation of the mitotic exit protein kinases Cdc15 and Dbf2. *Mol Biol Cell* **12**, 2961-74.
- Visintin, R., Craig, K., Hwang, E. S., Prinz, S., Tyers, M. and Amon, A. (1998). The phosphatase Cdc14 triggers mitotic exit by reversal of Cdk-dependent phosphorylation. *Mol Cell* **2**, 709-18.
- Visintin, R., Hwang, E. S. and Amon, A. (1999). Cfi1 prevents premature exit from mitosis by anchoring Cdc14 phosphatase in the nucleolus. *Nature* **398**, 818-23.
- Visintin, R., Prinz, S. and Amon, A. (1997). CDC20 and CDH1: a family of substrate-specific activators of APC-dependent proteolysis. *Science* **278**, 460-3.
- Visintin, R., Stegmeier, F. and Amon, A. (2003). The role of the polo kinase Cdc5 in controlling Cdc14 localization. *Mol Biol Cell* **14**, 4486-98.
- Wang, W. Q., Bembenek, J., Gee, K. R., Yu, H., Charbonneau, H. and Zhang, Z. Y. (2004). Kinetic and mechanistic studies of a cell cycle protein phosphatase Cdc14. *J Biol Chem* **279**, 30459-68.
- Weiss, E. and Winey, M. (1996). The *Saccharomyces cerevisiae* spindle pole body duplication gene MPS1 is part of a mitotic checkpoint. *J Cell Biol* **132**, 111-23.
- Westermann, S., Cheeseman, I. M., Anderson, S., Yates, J. R., 3rd, Drubin, D. G. and Barnes, G. (2003). Architecture of the budding yeast kinetochore reveals a conserved molecular core. *J Cell Biol* **163**, 215-22.
- Wigge, P. A. and Kilmartin, J. V. (2001). The Ndc80p complex from *Saccharomyces cerevisiae* contains conserved centromere components and has a function in chromosome segregation. *J Cell Biol* **152**, 349-60.
- Winey, M. and O'Toole, E. T. (2001). The spindle cycle in budding yeast. *Nat Cell Biol* **3**, E23-7.
- Xu, S., Huang, H. K., Kaiser, P., Latterich, M. and Hunter, T. (2000). Phosphorylation and spindle pole body localization of the Cdc15p mitotic regulatory protein kinase in budding yeast. *Curr Biol* **10**, 329-32.
- Yeh, E., Skibbens, R. V., Cheng, J. W., Salmon, E. D. and Bloom, K. (1995). Spindle dynamics and cell cycle regulation of dynein in the budding yeast, *Saccharomyces cerevisiae*. *J Cell Biol* **130**, 687-700.
- Yin, H., Pruyne, D., Huffaker, T. C. and Bretscher, A. (2000). Myosin V orientates the mitotic spindle in yeast. *Nature* **406**, 1013-5.
- Yin, H., You, L., Pasqualone, D., Kopski, K. M. and Huffaker, T. C. (2002). Stu1p is physically associated with beta-tubulin and is required for structural integrity of the mitotic spindle. *Mol Biol Cell* **13**, 1881-92.
- Yoshida, S., Asakawa, K. and Toh-e, A. (2002). Mitotic exit network controls the localization of Cdc14 to the spindle pole body in *Saccharomyces cerevisiae*. *Curr Biol* **12**, 944-50.
- Yoshida, S. and Toh-e, A. (2001). Regulation of the localization of Dbf2 and mob1 during cell division of *saccharomyces cerevisiae*. *Genes Genet Syst* **76**, 141-7.
- Yoshida, S. and Toh-e, A. (2002). Budding yeast Cdc5 phosphorylates Net1 and assists Cdc14 release from the nucleolus. *Biochem Biophys Res Commun* **294**, 687-91.
- Zachariae, W. and Nasmyth, K. (1999). Whose end is destruction: cell division and the anaphase-promoting complex. *Genes Dev* **13**, 2039-58.
- Zachariae, W., Schwab, M., Nasmyth, K. and Seufert, W. (1998a). Control of cyclin ubiquitination by CDK-regulated binding of Hct1 to the anaphase promoting complex. *Science* **282**, 1721-4.
- Zachariae, W., Shevchenko, A., Andrews, P. D., Ciosk, R., Galova, M., Stark, M. J., Mann, M. and Nasmyth, K. (1998b). Mass spectrometric analysis of the anaphase-promoting complex from yeast: identification of a subunit related to cullins. *Science* **279**, 1216-9.
- Zeng, X., Kahana, J. A., Silver, P. A., Morphew, M. K., McIntosh, J. R., Fitch, I. T., Carbon, J. and Saunders, W. S. (1999). Slk19p is a centromere protein that functions to stabilize mitotic spindles. *J Cell Biol* **146**, 415-25.

The present work was conducted under supervision of PD Dr. Johannes Lechner at the Department of Biochemistry of the University of Heidelberg (BZH).

ACKNOWLEDGMENTS

I would like to acknowledge the following people for their kind support in the accomplishment of the present work:

Johannes Lechner for the opportunity to work on such an exciting topic, for numerous experimental suggestions, exciting scientific discussions and for his permanent support;

Felix Wieland for being my first referee;

Elmar Schiebel (ZMBH, Heidelberg), Frank Uhlmann (Imperial Cancer Research Fund, London), and David Drubin (University of California, Berkeley) for kind provision of strains and plasmids;

Jennifer Ortiz de Lechner for experimental advise during the initial stages of my PhD thesis, her intensive collaboration and support;

Maren Scharfenberger for experimental support and discussion;

Stefan Kemmler for stimulating discussions and advice;

Barbara Lang and Eileen Dietzel for technical support.

Finally I am very thankful to my family Gertrud, Irene, Beatrice, Uschi and Roland who have supported and motivated me during these years. I am especially grateful to my husband Thorsten, who has encouraged and supported my all the time.